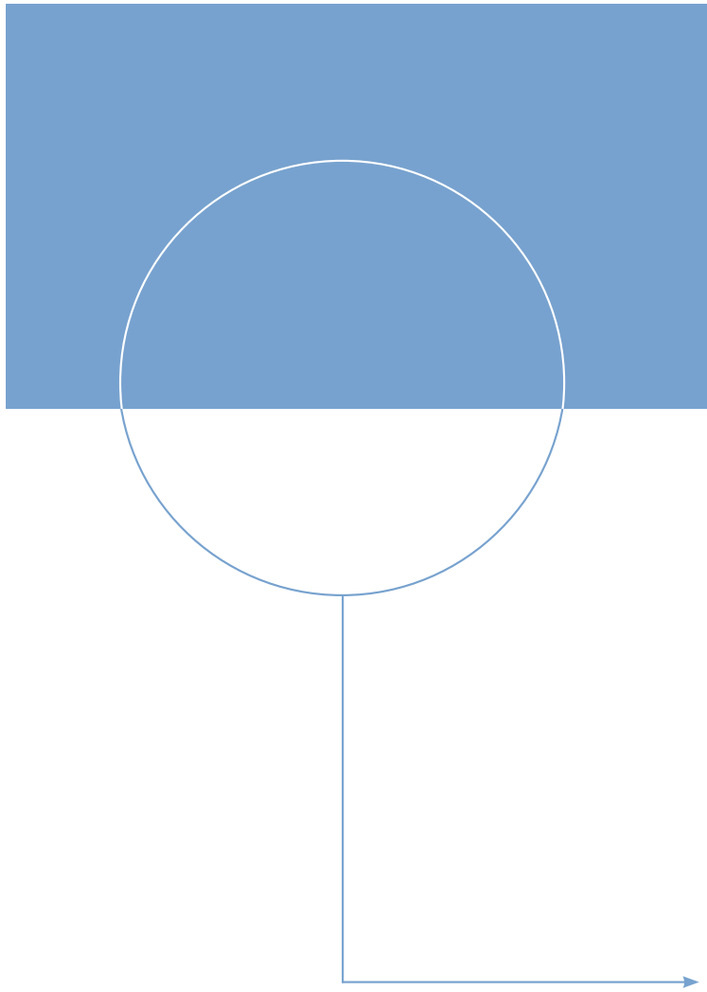

Master's thesis

2021

Andreas Tveita Nesje

NTNU
Norwegian University of
Science and Technology
Faculty of Information Technology and Electrical
Engineering
Department of Engineering Cybernetics

Andreas Tveita Nesje

Model Based Parameter Estimations of Heat Pumps and Heat Dynamics of a Household

June 2021

NTNU
Norwegian University of
Science and Technology

NTNU
Norwegian University of
Science and Technology

NTNU

Norwegian University of
Science and Technology

Model Based Parameter Estimations of Heat Pumps and Heat Dynamics of a Household

Andreas Tveita Nesje

Industrial Cybernetics
Submission date: June 2021
Supervisor: Professor Sebastien Gros

Norwegian University of Science and Technology
Department of Engineering Cybernetics

Preface

This master thesis is written in the course *TTK 4900 Engineering Cybernetics* in the spring of 2021 by Andreas Tveita Nesje. It is the finishing course of the two-year Master of Science in Engineering programme *Industrial Cybernetics*. The course is led by the Faculty of Information and Electrical Engineering and the Department of Engineering Cybernetics at the Norwegian University of Science and Technology(NTNU) in Trondheim. The programme is for students with a bachelor's degree in technology, and Nesje has a bachelor's degree in Renewable Energy from NTNU in Trondheim.

The purpose of the thesis is to develop models that can be used in a spot price based Model Predictive Controller that control the reference temperature of a heat pump system in a household. The project is led by Professor Sebastien Gros, who also is the supervisor of this project.

I am grateful for excellent supervising, aid and support received during the past months. First of all, Prof. Gros has been handing me lots of valuable data and has been available around the clock giving me with advice. I would also thank my co-students for good discussions and general support.

Abstract

Studies show that the society needs to adapt to the transition related to increased electrification and renewable energy into the energy mix. The combination of more electricity consumption and non-dispatchable energy sources will cause higher electricity price volatility. Consumer flexibility exploiting the volatility will benefit both the consumers and the society by reduced costs related to the electricity bill and power grid strains. This thesis investigates and develops models that can be used in a Model Predictive Controller (MPC) controlling a heat pump system based on the spot price, hence providing consumer flexibility.

The system that is investigated is part of a household in Trondheim, Norway. It consists of four rooms with one heat pump in each room. The goal of the model is to estimate the power consumption of the heat pumps and the heat dynamics of the rooms. The development of the models is done in four stages. First, the power saturation levels of the indoor and outdoor units of the system are identified. Secondly, the power models is developed and analyzed, one by one, building on each other. Then, the same is done for the temperature models. The last stage is a predictive capability test of the power and temperature models combined, where a simulation on a new data set is performed in order to discover strengths and weaknesses of the models.

Each proposed model contains parameters that is unknown. In order to find the parameters that are best suitable for the system, a model based-parameter estimation with Python and CasADi is performed. The least-square method is applied where the difference between the model estimates and measurements is minimized.

The heat pump power models are replicating the internal controller of the heat pumps. The first model is of a standard proportional(P)-controller. The second model is a P-controller where a bias term is added. The third power model is also a P-controller with a bias term, where the relation between the heat pump performance and the outdoor temperature is investigated. The final heat pump power model is replicating a proportional-integrator controller.

The temperature models are estimating the temperature in each room. The first model

calculates the room temperature based on the heat transfer from the heat pump and outdoor air. The second and third temperature model have added a new state representing the heat inertia of the walls of each room. The difference between the two models is that the third neglects the heat transfer from the wall to the outdoor air.

A simulation on two combinations of the most consistent heat pump power and temperature models was performed to test the predictive capabilities. The results showed that the models were able to replicate the most significant trends of the system behavior. However, more testing should be done before implementing them in an MPC.

Sammendrag

Studier viser at samfunnet må tilpasse seg overgangen knyttet til økt elektrifisering og fornybar energi til energimiksen. Kombinasjonen av høyere strømforbruk og ikke-regulerbare energikilder vil føre til høyere variasjon i strømprisen. Forbrukerfleksibilitet som utnytter variasjon i strømprisen, vil være til fordel for både forbrukerne og samfunnet ved reduserte kostnader knyttet til strømregningen og nettbelastningen. Denne masteroppgaven undersøker og utvikler modeller som kan brukes i en *Model Predictive Controller* (MPC) som styrer en varmepumpe basert på spotprisen, noe som bidrar til økt forbrukerfleksibilitet.

Systemet som undersøkes er en del av en husstand i Trondheim. Den består av fire rom med en varmepump i hvert rom. Målet med modellen er å estimere energiforbruket til varmepumpene og varmedynamikken til rommene. Utviklingen av modellene ble gjort i fire trinn. Først ble effektmetningsnivåene til varmepumpene identifisert. Deretter ble varmepumpemodellene og temperaturmodellene utviklet og analysert. Til slutt ble det utført en prediktiv kapabilitetstest av de kombinerte varmepumpe- og temperaturmodellene, hvor det ble gjort en simulering på et nytt datasett for å avdekke styrker og svakheter ved modellene.

Hver modell inneholdt parametere som er ukjente. For å finne parametrene som er best egnet for systemet, ble det utført det en modellbasert parameterestimering i Python og CasADi. Den minste kvadratiske metode ble benyttet der differansen mellom modellanslag og målinger ble minimert.

Varmepumpemodellene representerer de interne kontrollerne til varmepumpene. Den første modellen er av en standard proporsjonal (P)-kontroller. Den andre modellen er en P-kontroller hvor det ble lagt til en parameter som utgjevner skjevheter i systemet. Den tredje varmepumpemodellen er også en P-kontroller med en skjevhetsparameter, hvor sammenhengen mellom varmepumpens ytelse og utetemperaturen ble undersøkt. Den fjerde og siste varmepumpemodellen replikerer en proporsjonal-integratorkontroller.

Temperaturmodellene estimerer temperaturen i hvert rom. Den første modellen beregner romtemperaturen basert på varmeoverføringen fra varmepumpen og uteluften. Den andre

og tredje temperaturmodellen har lagt til en ny tilstand som representerer varmetregheten til veggene i hvert rom. Forskjellen mellom de to siste modellene er at den tredje neglisjerer varmeoverføringen fra veggen til uteluften.

Det ble gjort en simulering på to kombinasjoner av de mest konsistente varmepumpe- og temperaturmodellene for å teste prediktive evner. Resultatene viste at modellene klarte å replikere de viktigste trendene i systemadferden. Flere tester bør imidlertig gjøres før de implementeres i en MPC.

Table of Contents

List of Figures

List of Tables

Abbreviations

All abbreviations and acronyms used in the thesis are explained in the text.

Nomenclature

All nomenclature is described in the text.

1 Introduction

While starting writing this Master's thesis, Norway set two new power consumption records. Between 8 and 9 AM January 15th a consumption of 24,536 MWh was measured, and at the same hours on February 4th a consumption of 25,146 MWh was measured. According to Statnett, which is the system operator of the Norwegian power system, the reason for the new records was due to cold weather and increased electrification of the society. In times of high electricity demand, more user flexibility would benefit both Transmission System Operators and consumers.[1,2]

1.1 Background

Analyses of the power market in Europe from the present until 2040, carried out by Statnett, predict a stable average spot price, but higher price volatility. Two reasons for this are more electrification of the society and more renewable energy in the energy mix. Ways to lower the average spot price and its volatility can be through more flexibility of consumers and households. [3]

1.1.1 Electrification

In order to lower the CO_2 emissions in Norway, it is planned to replace fossil energy with electrical energy. This transformation is called electrification and is happening is in several sectors such as industry, transport and energy production. In a scenario by Norwegian Water and Energy Directorate (NVE) it is predicted that the electrical energy consumption will be 23 TWh larger in 2040 than the present due to electrification. Even though the energy production is also expected to increase, the price of electricity will be about 7 and 10 øre/KWh higher in 2030 and 2040 respectively, than if the electrification measures were not implemented.[4]

1.1.2 More Renewable Energy in The Energy Mix

In order to succeed in the electrification transition, it is necessary to increase the renewable energy production. Due to lowered prices on wind and solar plants, it is expected that they will be the main energy source in the energy mix in Europe. In the model EU11 by Statnett it is predicted that wind and solar energy will go from 19 % in 2020 to 46, 67 and 86 % in 2030, 2040 and 2050, respectively.[3]

Wind and solar power are non-dispatchable energy sources, which means that the energy produced can not be controlled adjusted to the demand. The power plants are dependent on wind and sun radiation. With a high portion of non-dispatchable energy sources, the power prices will be much more volatile. In times of power deficit the prices will go up and in times with power surplus the prices will fall. There have been examples when the power price is negative, and this scenario is more likely to happen more often as more non-dispatchable energy sources is in the power system.[3]

The power price volatility in Norway has been low during the past few years because of the hydroelectric power plants ability to balance the power price. In Denmark, the price volatility is higher because of impacts caused of the big portion of wind power in their energy mix. With more transmission lines to Europe, increased power consumption and increased portion of non-dispatchable energy sources, the price volatility is expected to increase, see figure 1.1.[5]

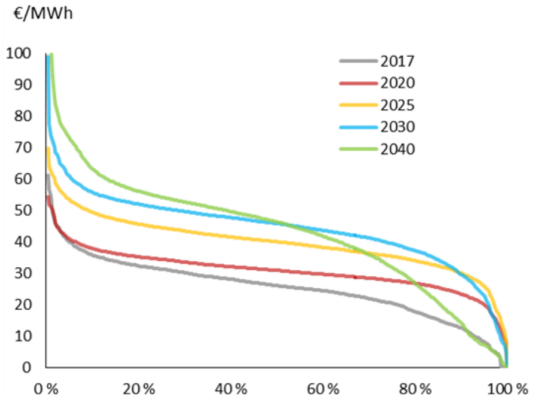

Figure 1.1: *Historical and predicted price duration curve for Norwegian power prices. A price duration curve illustrates a percentage of time in which the price level is over a certain level.[5]*

1.1.3 Consumer Flexibility

The energy market depends on other reliable dispatchable energy sources, energy storage and consumer flexibility in order to balance the production and consumption. Statnett mentions consumer flexibility to be one of the most important measures. The power market will develop into a scenario where the consumer must adapt to the producers. In periods with high renewable energy production and low power prices the consumers should run high power appliances, such as charging their car and various heating. On the other

hand, the high power appliances should be turned off in periods with low renewable energy production and high power prices. This measure is called peak shaving.[3]

There is a big potential of peak shaving amongst households. The introduction of smart metres (AMS) and smart home technology make it easier for households to adapt to the power market. By using less power in times of high spot prices, or focusing on lowering power peaks in considering power tariffs, the consumers can contribute to balancing the power market in addition to save money.[5]

Flexibility by households will have a different impact on the power grid than flexibility amongst more power demanding industry. It will be costly for the industry to be more flexible as this may impact the production etc, but they can in times of power deficit provide flexibility which can be rewarded by economical incentives. This can help balancing the frequency and voltage of the transmission grid, which is considered the grid containing 200 kV or above. The power consumption behavior of the households will affect the distribution grid (22 and 11 kV), both in terms of voltage and bottlenecks. In addition, the distribution grid has fewer options to regulate the production, which emphasize the significance of flexible households.[5]

1.1.4 Household Flexibility Potential

There is a substantial potential for households to provide flexibility through power to heat (P2C) and electric vehicle (EV) charging. Figure 1.2 illustrates that space heating and heating of water stands for the majority of the electricity consumption in Norwegian households in 2017. In that period Norway had a 5.11 % share of electrical cars on the roads. In 2020, 12.06% of the vehicles in Norway were electric cars. The market share of new car sales were 54.3 %. By including plug-in hybrids, which typically are charged at households, the total share of new chargeable car sale in 2020 where 74.7 %. The distribution of electrical energy at Norwegian households will therefore grow substantially.[5–7]

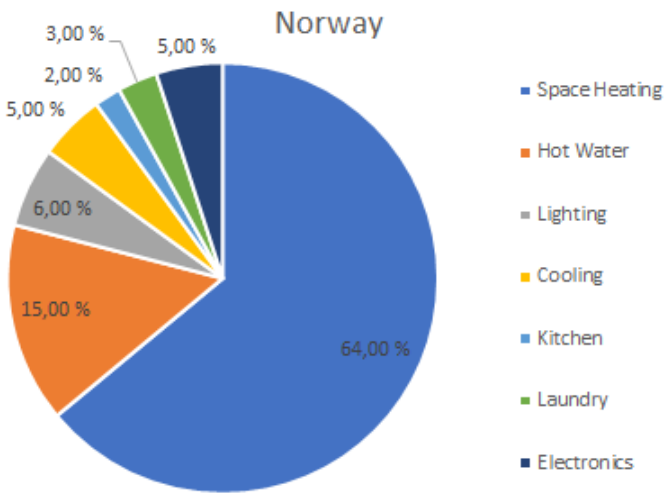

Figure 1.2: *Estimated purpose distribution of electrical energy in Norwegian households in 2017.[5]*

Some of the P2C applications with most potential for flexibility in households of the Northern countries are hot water tanks, heaters and panel heaters, and heat pumps. By exploiting thermal inertia they can stop or reduce the heating in periods of high electricity prices while still maintaining sufficient temperature or comfort. A practical example could be in space heating, where a user can set a comfort level between 19-22 °C. Then a smart home device would have data on the electricity prices for the next day, and suggest a heating schedule for the device.[5]

Typical usage of an EV by households today is commuting to work and to other errands and activities during evenings. A smart charger with inputs of when the user wants the car fully charged, and the spot price for the following hours can then schedule the charging to save money without affecting the user. Typically, the charging would be shifted to nighttime instead of when the user would plug in the charger at afternoon peak hours.[5]

EVs can also function as a balancing energy storage unit. By reversing the energy flow, they can deliver power from vehicle-to-grid (V2G) or from vehicle-to-home (V2H). The technology exists, but is more costly than conventional chargers. In addition, studies show that the expected lifetime of the car battery can be reduced by 50 %. The present spot prices do not fluctuate enough to make this profitable. By 2030 the technology may make it profitable, especially in combination with solar panels and bigger volatility in the electricity prices.[5,8]

1.1.5 Flexibility Market Development

By 2019 Advanced Metering Systems (AMS) were installed in Norwegian households. An AMS is an advanced measurement and control system making consumers able to utilize flexibility in the spot price market. The device measures energy consumption in real time. By default it reports the hourly consumption of a household. By making consumers more aware of their pattern of consumption, they can shift consumption from peak hours benefiting their private economy and the power grid. [5]

1.2 Problem to be addressed

This Master's thesis investigates different models that can represent the temperature dynamics in a household with installed heat pumps. The purpose of the models is to use them in a controller that can minimize costs related to the electricity spot price, while the heat pumps ensure a comfortable temperature. This can be done by a Model Predictive Controller in which of the models calculate a optimal temperature setting of the heat pumps. The problem to be addressed is:

"Develop and investigate power and temperature models of a household that can be used in a Model Predictive Controller that minimizes the electricity spot price of the heat pump power consumption while maintaining a desired comfort temperature."

1.3 Structure of the Thesis

After this introductory section, there is a theory section providing some basic understanding to the work of this Master's thesis. The main part of the thesis consists of the system description and the development and testing of the models. Each model is analyzed at the time. This means that for each model, the model will first be presented, thereafter a parameter estimation of the respective model will be carried out, then the results will be discussed. Some of the models are built on the previous model presented, so it is advised to read them in chronological order. Finally, some predictive capability testing on two combinations of the power and temperature models are performed. This has been done in order to discover strengths and weaknesses on how they may perform as models in a Model Predictive Controller.

1.4 Software

All of the model-based parameter estimation and illustrations made in this thesis are done with Python in Pycharm. For the optimization problem setup and simulations, an open source, software framework for nonlinear optimization and optimal control called CasADi are utilized. The class used for solving the optimization problems is called *Opti* and is applying the algorithm *Ipopt* that is an interior-point filter line-search algorithm for large-scale non-linear programming.[9,10]

2 Theory

2.1 Nord Pool

Nord Pool is a power market where the prices of electricity are decided in 14 countries in Northern Europe. Due to bottlenecks in the transmission lines, the market is split in different bidding areas, whereas the electricity price in each area is called Elspot price. For instance, Norway is normally divided into 5 Elspot areas called NO1-NO5. See figure 2.1 for several Elspot areas in the Nord Pool Power Market.[11]

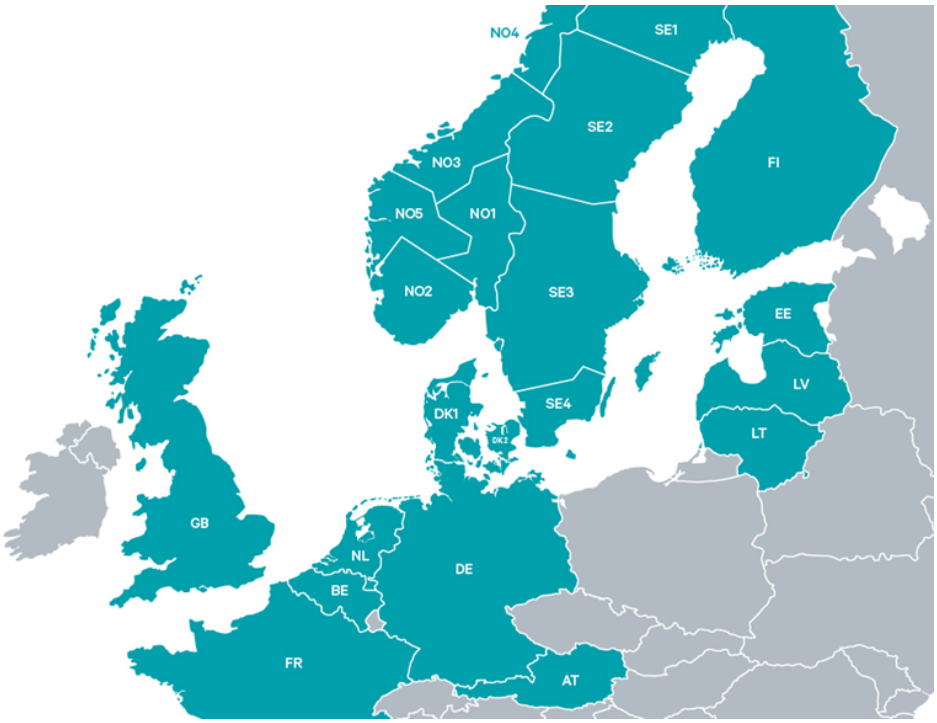

Figure 2.1: *Map over the different Elspot areas in the Nord Pool power market.[11]*

The Elspot price is calculated and determined in a market called the day-ahead market. Each day at 10:00 Central European Time (CET) the available capacity on the transmission lines both between and within the Elspot areas are published. Then buyers and sellers on the market have to make their bids until 12:00 CET. They bid on the hourly prices from 00:00 and 24:00 CET the next day. The bids are then being matched with the market prices from surrounding markets in Europe through an algorithm called Euphemia. This pan-European market coupling process is called the Single Day-Ahead Coupling. Then the Elspot prices for the next day are announced before 13:00 CET.[12]

The Elspot price depends mostly on supply and demand, but also on other factors such as planned maintenance on the transmission lines etc. If the weather forecast predicts a lot of wind and rain the next day, the hydro and wind energy power plants expect high power production that leads to a high level of supply, commonly lowering the prices. However, if the weather forecast predicts low temperatures, the suppliers and consumers expect high energy usage, pushing both the demand and prices up. A region may also experience high prices if the transmission lines is out of service resulting in less supply options. This liberal market form leads to a dynamic where power flows from Elspot areas with low power price to areas with higher power price.[13]

Electricity consumers in Norway normally have a choice of having a fixed, variable or spot price-based electricity bill. By choosing spot price, the consumer will have a price that follows the market price of Nord Pool every hour. This deal gives the consumer the ability to benefit from user flexibility, unlike having a fixed price from the electrical company.[14]

2.2 Heat Pumps

Heat pumps are a source of heating and cooling of households. A common heat pump type is *air-to-air* heat pumps. It uses outside air as heat source to heat up the indoor air. Further in this thesis, when discussing heat pumps, it is *air-to-air* heat pumps that are meant. That is because it is *air-to-air* heat pumps that are investigated later in this thesis. [15].

A heat pump consists of two main parts, an indoor and outdoor unit. The outdoor unit consist of a heat exchanger and a compressor. The heat exchanger gathers heat from the outside air to a circulating heat medium, called refrigerant. In order to transfer heat from the outside air to the refrigerant, the refrigerant needs to be colder than the outside air. The refrigerant is then compressed by the compressor, causing an increase of temperature and pressure. The refrigerant is then sent to the indoor unit where it passes a heat exchanger, transferring heat to the indoor air as it condenses. The pressure and temperature of the refrigerant then drop as it passes through an expansion valve. At last, it returns to the outdoor unit, completing the cycle.[15]

The heat pump compressor type can affect the power consumption of a heat pump. Some

heat pumps have a single speed compressor that run with a fixed speed when it is on. The fixed speed compressor turns on and off as the room temperature is fluctuating below and above the desired temperature. Some heat pumps, however, runs with an inverter that makes the speed of the heat pump compressor motor variable. By using an inverter, the power consumption is 'smoother' than of a fixed speed compressor.[15]

2.3 Heat Transfer

This Master's thesis investigates and develops models that identifies the heat transfer rates between different physical components. In order for heat to transfer a temperature difference between the components is needed, whereas the heat transfers from the hot to the cold component. Depending on the components and what is between them, there three general types of heat transfer exist: conduction, convection and radiation. Conduction and convection will be further described as these types of heat transfer is modelled in this thesis.[16]

2.3.1 Conduction

Conduction is a type of heat transfer where the heat transfers through a component that may be of a solid, liquid or gas. The heat transfers as collisions of atoms and molecules in the component and is triggered by temperature differences. The heat transfer $\dot{Q}[W]$ from the hot to cold side is given as

$$\dot{Q} = kA\frac{T_h - T_c}{\Delta x} \tag{2.1}$$

where T_h and $T_c[K]$ is the temperature of the hot and cold side, respectively. $\Delta x[m]$ is the thickness of the component between the hot and cold side. $A[m^2]$ is the area of the cross section of which the heat is transferred. $k\left[\frac{W}{mK}\right]$ is the thermal conductivity, which is a property that describes the resistance of the heat transfer. The thermal conductivity is positive as of the second Law of Thermodynamics.

2.3.2 Convection

Heat convection is the heat transfer that occurs between a surface of a solid object and its surrounding fluid that is in motion. The fluid can be both liquid or gas. An example may

be heat transfer from a house wall to a colder outside air. The heat transfer $\dot{Q}$ is given by Newton's law of cooling

$$\dot{Q} = hA(T_s - T_f), \tag{2.2}$$

where $T_s[K]$ and $T_f[K]$ is the surface and fluid temperature, respectively. $A[m^2]$ is the surface area, while $h\left[\frac{W}{m^2K}\right]$ is the convection heat transfer coefficient.[16]

2.3.3 Heat Capacity

The heat transfer between two components commonly changes the temperature of the components. A component, such as air or a wall, can be described as a thermal mass with a heat capacity. The heat capacity is the relation between how much energy is added and how much the temperature changes in the substance. The temperature change can be given as

$$\Delta T = \frac{Q}{Cm}, \tag{2.3}$$

where $Q[J]$ is the heat delivered, $C\left[\frac{J}{kg\,K}\right]$ is the specific heat and $m[kg]$ is the mass of the system. The heat capacity of air is $700\frac{J}{kg\,K}$.[17,18]

2.4 Optimization Problem

Optimization is a mathematical tool used in areas such as engineering, science and finance. It can be used to minimize costs, energy or maximize profits to an application or system. Central terms in optimization is an objective, variables/unknowns and constraints. An objective is what is being optimized - it could be time, money, energy etc. The objective f is often referred to as the objective function $f(x)$, as it is a function of the variables x of the system. The constraints c represent restrictions of the system. Such restrictions may be that the energy of a system can not be negative.[19]

A typical representation of an optimization problem can be given as

$$\min_{x} \quad f(x) \tag{2.4}$$

$$\text{subject to} \qquad c_i = 0 \quad i \in \mathcal{E}, \tag{2.5}$$

$$c_i \geq 0 \quad i \in \mathcal{I}. \tag{2.6}$$

By this representation, the objective function $f(x)$ is minimized by the state x. Meanwhile, the system variables c_i is constrained, where $\mathcal{E}$ and $\mathcal{I}$ are sets of indices for equality and inequality constraints.[19]

Optimization algorithms are used for solving optimization problems. An optimization algorithm is an iterative method that starts with an initial guess of the variable x_0 and for each iteration it proposes an improved solution. In a case of a successful sequence of iterations, the algorithm terminates with an optimal solution. The strategy used for finding the improved solution in each iteration is what separates the different optimization algorithms.[19]

2.4.1 Least-Squares Problem

Least-squares problems is a useful technique that can be used in many applications. The way the problem is constructed makes it efficient to estimate unknown parameters of a

model. The general form of a least-square problem is given as

$$f(x) = \frac{1}{2}\sum_{k=1}^{N} r_k^2(x) \tag{2.7}$$

where r is called the residual. When estimating the parameters of a model ϕ, the residual can be given as

$$r_k = \phi_k - y_k \tag{2.8}$$

where y_k is the measurement in time step k. By minimizing the residual squared, the solution will find the optimal parameters for the model. Newton or gradient methods is typically used for solving least-squares problems.[19]

3 System Identification

3.1 System Description

The system that is being modelled in this Master's thesis is of a house located in Trondheim, Norway. There are four rooms in the house that are of interest. They are referred to as *Living*, *Livingdown*, *Main* and *Studio*, and have a volume roughly estimated to 220 m^3, 50 m^3 66 m^3 60 m^3, respectively. The models created assume that all the rooms are separated and do not impact each other, even though the rooms *living* and *main* have an opening between them.

Each room is equipped with one indoor heat pump (HP) unit which is connected to one of two outdoor heat exchanger units, see figure 3.1. The indoor HP unit of *living* is connected to outdoor *Unit 1*. The indoor HP units of *livingdown main* and *studio* are connected to the outdoor *Unit 2*. All of the indoor HP units are of the same manufacturer, *Mitsubishi*.

Note that the HPs are in heating mode. That means that it will not utilize power to cool down the room if the reference temperature of the heat pump is lower than the measured temperature. This is because the general temperature conditions of the house is such that cooling is not needed.

Each unit, both indoor and outdoor experience power saturation effects. That means that due to electrical limitations in the machines, the units have upper power consumption limitations. The saturation levels given in figure 3.1 are further described and identified in section 3.3.

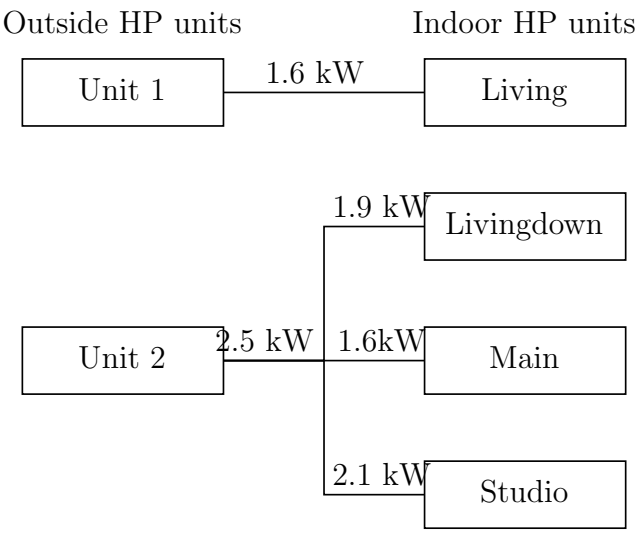

Figure 3.1: *Overview of the heat pump system with associated level of power saturation.*

The measured properties with associated descriptions of the system are given in table 3.1. The power consumption is measured by a device called *Tibber Pulse* by the company *Tibber*. This device is connected to the Advanced Metering System (AMS) of the house that can measure the power with high sample frequency.

The settings (reference temperature etc.) of the HP units are externally controlled through a Rasberry Pi. In addition to the reference temperatures, an MPC controls whether the heat pumps should be on or off. A heat pump is shut off for the next 30 minutes if the controller plans to use less than 50 W the next 30 minutes. Details of the internal controller of the HP units are unknown.(Sebastien Gros, Personal Communication)

There are several aspects of the measured properties that have to be pointed out. One aspect is that the individual HP power consumption is not given explicitly, as the power measured is the total consumption of the HP system. However, by isolating the periods of when only one HP is on at the time, the measured power consumption represents the one HP that is on. Another aspect of the measured properties, is that the temperature measured in each room is done by an external sensor - not by the heat pump control system. That means that the temperature that the heat pump experiences may not be the same as the temperature measured. One last aspect is that the outside temperature property is gathered through an API of the Norwegian Meteorological Institute and is not the exact temperature of the air surrounding the house.

Table 3.1: *Measured properties of the system and associated description.*

Variable Name	Description
t_k	Timestamp
P_k	Total Power consumed
$T_{out,k}$	Outdoor Temperature
$T_{room,k}$	Temperature in each room
$T_{ref,room,k}$	Set Temperature for Heat Pumps in each room
$B_{HP,room,k}$	Boolean telling if Heat Pump is on/off in each room

3.2 System Identification Data Sets

Identification data sets, made by experimental design is made in order to better identify the behaviour of the system. By for example running one heat pump at the time, the behaviour of that unit can be analysed properly. By applying steps in the reference temperature, the step response behaviour can be analysed. Some illustrative examples of the experimental design is presented in this section. All the system identification data sets, given by table 3.2 are illustrated in Appendix A. The data sets are made and handed out by Professor Sebastien Gros, the supervisor of this Master's thesis.

Table 3.2: *System identification data sets summarized with associated start and end time.*

Data Set Name	Start	End
Data Set 1	2021-02-19 19:45	2021-02-20 08:35
Data Set 2	2021-02-20 23:15	2021-02-21 09:45
Data Set 3	2021-02-21 18:30	2021-02-22 04:45
Data Set 4	2021-03-02 08:20	2021-03-04 18:00
Data Set 5	2021-03-02 08:20	2021-03-04 18:00

The power consumption measurements from Data Set 3 are illustrated in figure 3.2. It is observed that the raw measurements fluctuate significantly. In order to better identify the trends and behavior of the power consumption, the series have been re-sampled from an approximately 2 seconds sample rate to a frequency of 5 minutes.

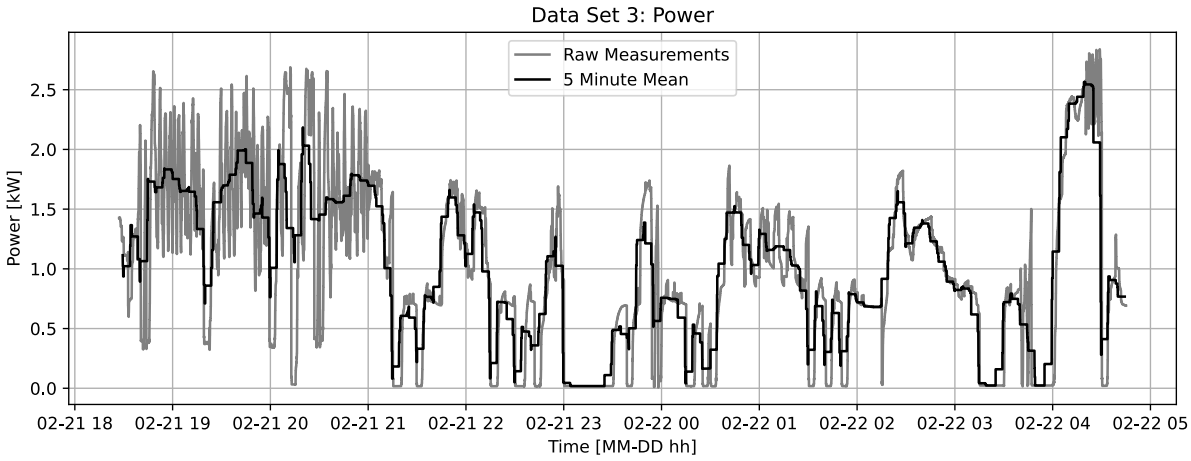

Figure 3.2: *Raw power measurements and their 5-minute mean.*

The measured temperature and the reference temperature in each room of data set 4 are illustrated in figure 3.3. The trajectory of *living* is a good example for the step responses of both lowering and increasing the reference temperature in the room. The measured temperature seems to reach the reference temperature. However, in the trajectories of *main*, the measured temperature in the room does not reach the reference temperature. This may be a consequence of the temperature sensor being an external sensor, not affecting the internal controller of the HP.

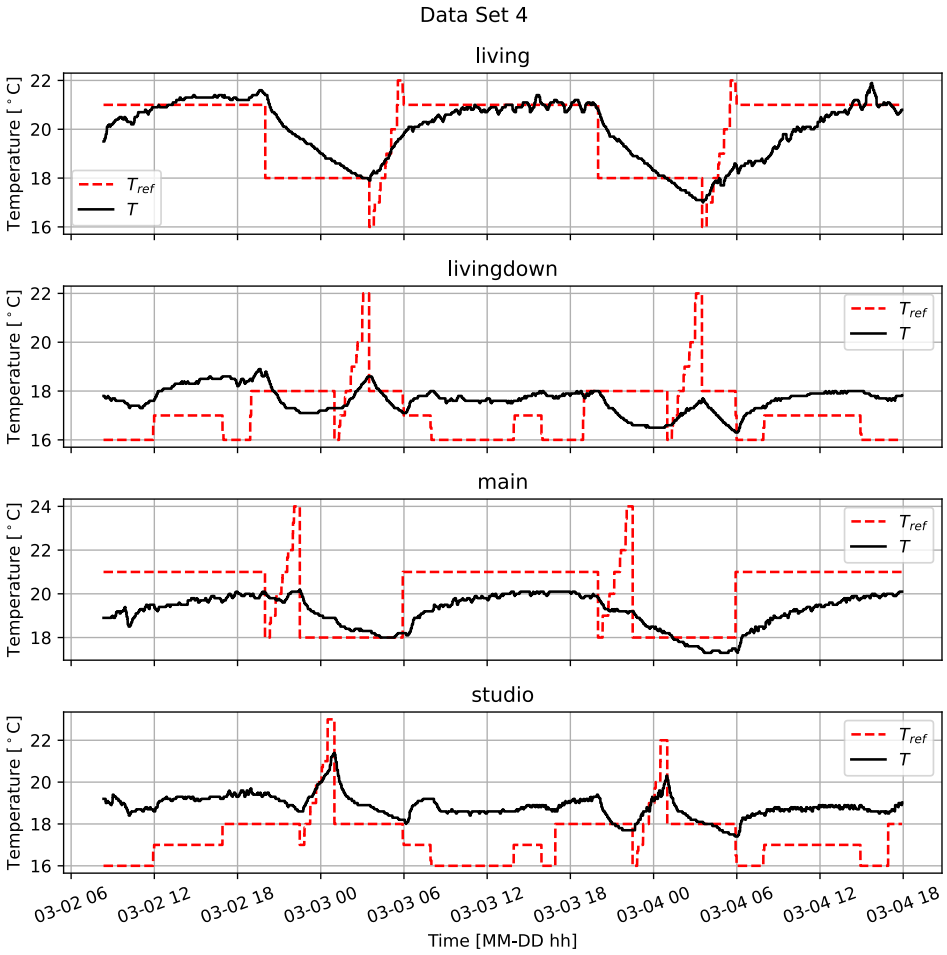

Figure 3.3: *Measured and reference temperatures for each room from Data Set 4.*

The On/Off state of the different heat pumps from Data Set 4 are illustrated in figure 3.4. This figure illustrates the experimental design of the system identification data sets. From start until approximately 03-02 18 all HPs are on. After that and until 03-03 06 one heat pump is on at the time, starting with the HP in *main*. In that way the power measured is representing the one heat pump that is On at the time. Note that the reference temperature can be greater than the measured temperature even though the heat pump is Off.

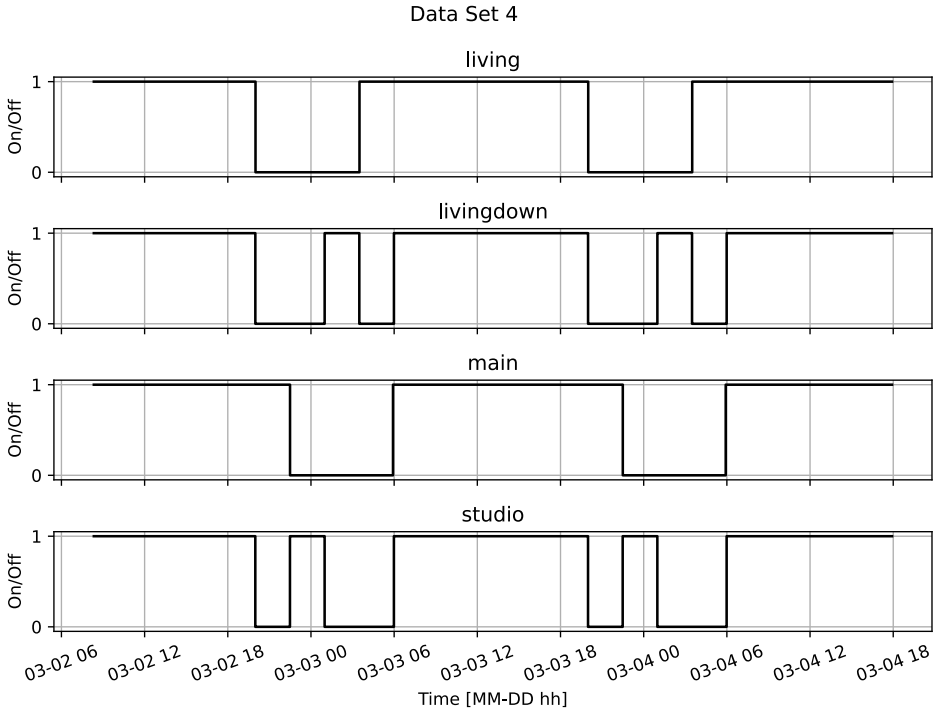

Figure 3.4: *On/Off status of the heat pumps in each room from Data Set 4.*

3.3 Identifying Power Saturation Levels

Before modelling the power consumption of the heat pumps, the power saturation levels of the indoor units in each room, in addition to *Outdoor Unit 2* have to be identified. This is done by analysing the time series of when a single heat pump unit is On at the time in all the system identification data sets. The power series analysed is the 5-minute mean version of the raw data, such that the fluctuation noise of the raw data set is damped. It may be expected that the saturation levels of the indoor units are at the same level, as the units are of the same manufacturer.

3.3.1 Living

The distribution of the power consumption of the HP in *living* when in single operation is illustrated in figure 3.5. The length N of the power series is 2851. The figure shows six instances n over 1.6 kW. This means that six times the raw measurements data set had an average over that level of power. Note that the HP power is over several periods equal to zero, even though the HP setting is *On*.

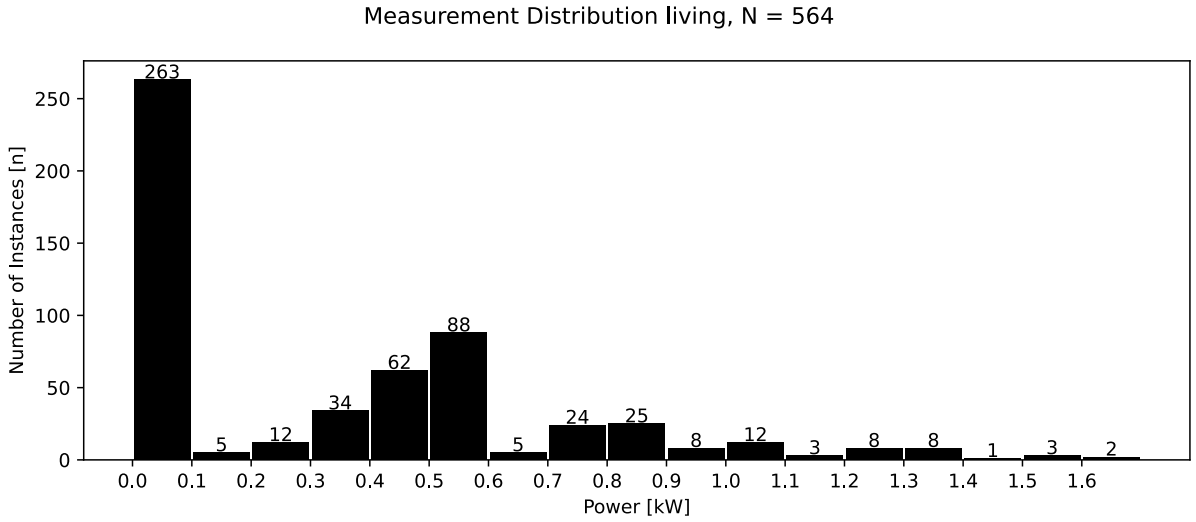

Figure 3.5: *Distribution of the 5-minute mean power measurements of living.*

3.3.2 Livingdown

The distribution of the power consumption of the HP in *livingdown* when in single operation is illustrated in figure 3.6. The figure shows five instances n over 1.9 kW. This is of a total of instances N equal to 1254. There are significantly more instances of power measurements in the interval [1.8 kW, 1.9 kW) than in the intervals of [1.7, 1.8 kW) and [1.9, 2.0 kW].

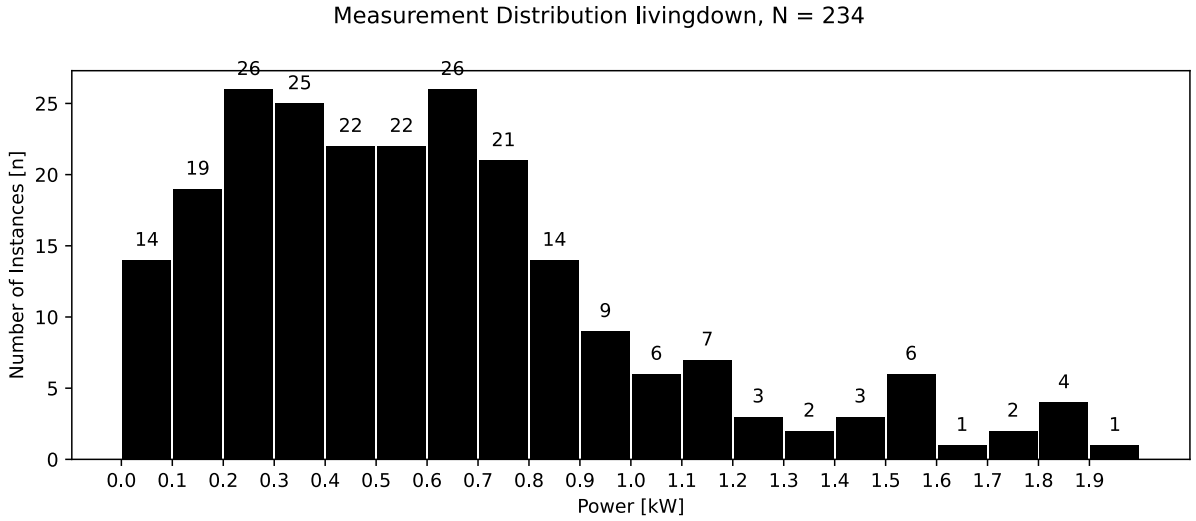

Figure 3.6: *Distribution of the 5-minute mean power measurements of livingdown.*

The distribution of the power consumption of the HP in *main* when in single operation is illustrated in Figure 3.7. As shown by the distribution plot, there were nine instances

above 1.6 kW. Most of the instances were in the lower power interval of [0, 0.1 kW).

3.3.3 Main

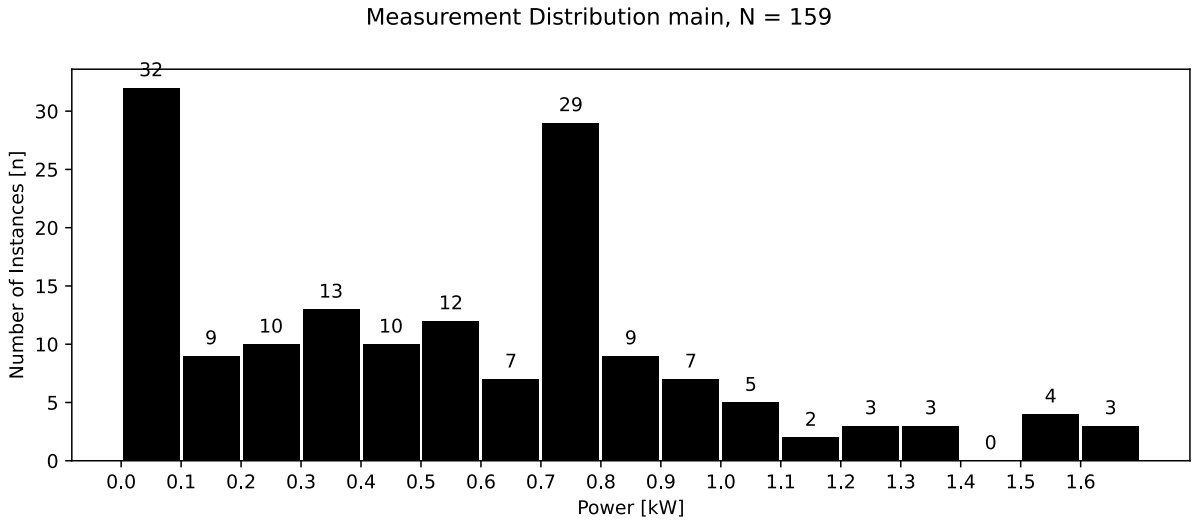

Figure 3.7: *Distribution of the 5-minute mean power measurements of main.*

The distribution of the power consumption of the HP in *studio* when in single operation is illustrated in figure 3.8. This HP unit has measurement instances larger than of the other HP units. The data set of this unit provides with 3 and 2 instances in the power interval of [2.0 kW, 2.1 kW) and [2.1 kW, 2.2kW), respectively. In the power interval [0, 0.1 kW) there were registered six instances, out of a total of N = 767.

3.3.4 Studio

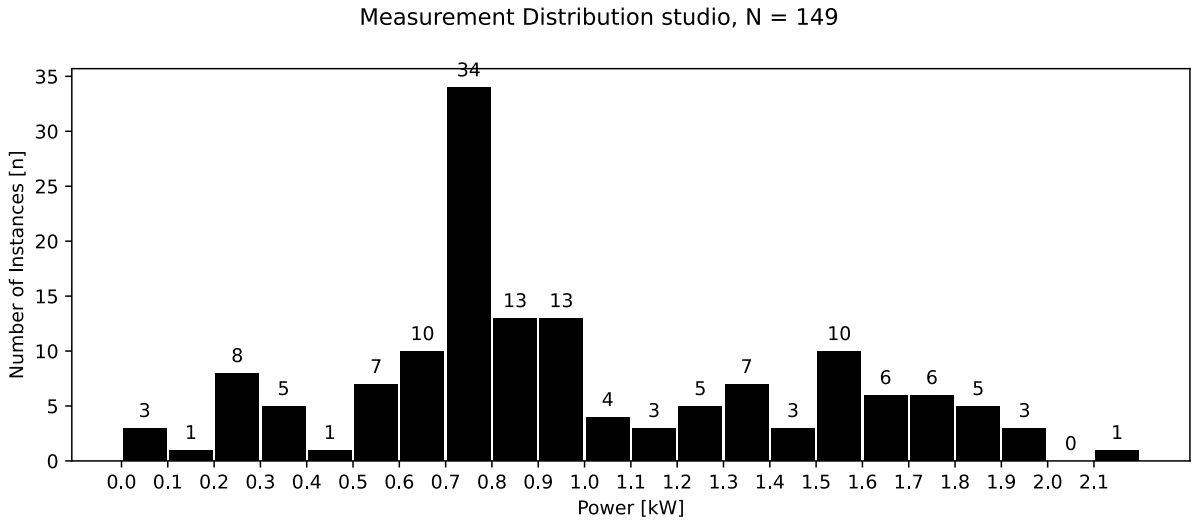

Figure 3.8: *Distribution of the 5-minute mean power measurements of studio.*

Figure 3.9 illustrates the distribution of power measurements when *Unit 2* was operating. That is, all power measurements when the HP unit of *living* was *Off*. As seen from the figure, there were eight instances of power consumption in the interval between [2.5 kW, 2.6 kW).

3.3.5 Outdoor Unit 2

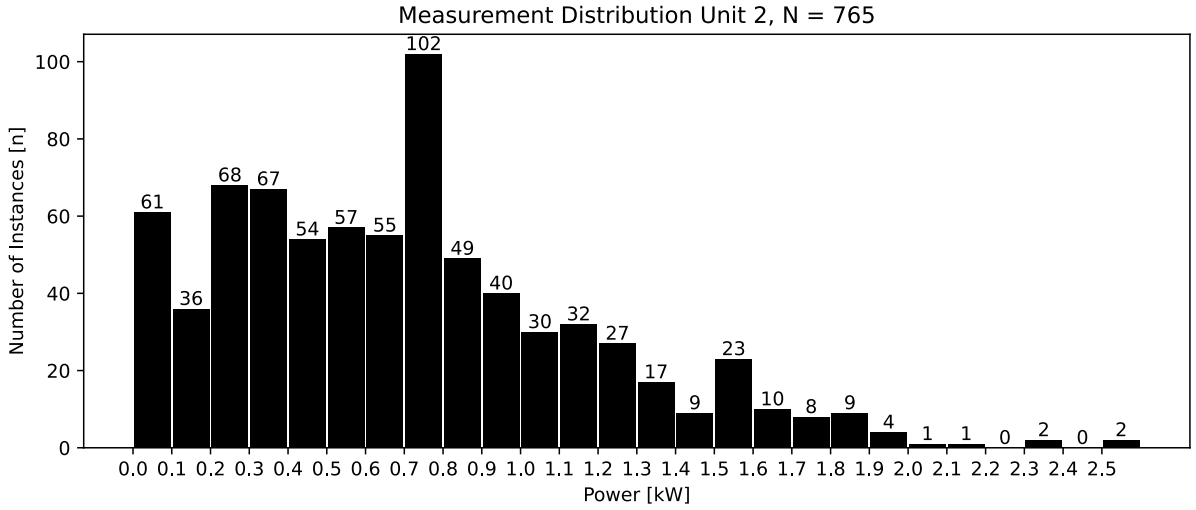

Figure 3.9: *Distribution of the 5-minute mean power measurements of Unit 2.*

3.3.6 Discussion

As the HP units in each room are of the same type and manufacturer, one could expect that the individual level of saturation may be relatively equal. That is not the case according to these data sets. It is a rather large difference(≈0.5 kW) between the highest power measurements of both *living* and *main*, and *studio*. The reason for this difference may be explained by some unknown details of the electrical or heat pump installations. Such details of the system will not be investigated further.

As such individual differences exists, it is reasonable to have individual saturation levels of the HPs. Even though there are few instances of the highest power measurements, one can argue that this represents the level of saturation. As these measurements are a 5-minute average of the raw data sets, noise should be cancelled out. The saturation levels chosen for the system is summarised in table 3.3

One aspect that is noticed by the distribution plots is that the number of instances in the lower power interval varies significantly between the HPs. In particular, the room *living* has many samples in the lower interval. There may be two reasons for this. First, that is gets heating from external sources such as from the open corridor from *main*, or from the sun through windows. Secondly, it may be that the room heats up more quickly to the reference temperature of the HP. However, as *living* by far is the largest in terms of the air volume, that is unlikely that it gets heated more quickly.

Table 3.3: *Heat pump saturation levels in each room and for Outdoor Unit 2.*

Units	**Power Saturation** $[kW]$
Living	1.6
Livingdown	1.9
Main	1.6
Studio	2.1
Outdoor Unit 2	2.5

3.4 General Model Based Parameter Estimation Problem

This section presents a general model based parameter estimation problem that is used in this Master's thesis. Some changes are done in the different models, but it will be presented in their respective sections. To cover the most general methods, two versions of the parameter estimation will be presented, one for static functions and one for dynamic functions. The constraints of the parameter estimation problem vary whether the model is static or dynamic. If the model is static, it depends on input states from the same time step. If the model is dynamic, it depends on input states and its own estimates from earlier time steps.

The goal of the optimization problem is to find the optimal parameter vector p^* that makes the model replicates the real system behaviour. The least-square optimization problem does that by minimizing the accumulated residual error squared r^2 over all time steps k. The residual is defined as

$$r_k = \phi_k(p) - y_k \tag{3.1}$$

where y_k is the measured property in which the model is trying to estimate. $\phi_k(p)$ is the model estimate trajectory in time step k in function of the parameter vector p.

The optimization problem for parameter estimating the static models is given in equation 3.2. The model trajectory ϕ_k in time step k is equal to the model estimates $f_k(p, z_k)$ in function of the variable parameters and the input state vector z_k in a time step k. For some of the models, there are optimal parameters p_i^* that is defined as positive. The constrained parameters is presented in the parameter estimation section for each respective model presented.

$$\min_{p} \quad \sum_{k=1}^{N} r_k^2. \tag{3.2a}$$

$$\text{subject to} \quad \text{for } k \in [0, \text{N}] : \tag{3.2b}$$

$$\phi_k = f_k(p, z_k) \tag{3.2c}$$

$$p_i^* > 0. \tag{3.2d}$$

The optimization problem for parameter estimations of dynamic models is given in 3.3. To ensure that the model estimate trajectory ϕ is continuous, each time step of the model estimate trajectory is calculated in function of the previous estimate. Some of the training data sets contain a longer gap than 5 minutes. This is because several data sets form separate time periods are merged to achieve longer training data sets. After each gap of over 5 minutes, the optimization will continue with new initial values.

$$\min_{p,\, \phi_{gap}} \quad \sum_{k=1}^{N} r_k^2, \tag{3.3a}$$

$$\text{subject to} \quad \text{for } k \in [1, \text{N}] : \tag{3.3b}$$

$$\text{if } \textit{not} \text{ gap:} \tag{3.3c}$$

$$\phi_k = f_k(p, z_k, \phi_{k-1}) \tag{3.3d}$$

$$p_i^* > 0. \tag{3.3e}$$

Since the initial values are free variables decided by the optimization solver for the dynamic models, the minimizing is done with the parameter vector p and ϕ_{gap}, which is the initial model estimate.

3.4.1 Standard Deviation of the Residual

For each parameter estimation that is done later in this thesis, the distribution of the residual is presented. This is to get a visual presentation of how well the model is performing. Ideally, the form of the residual distribution will be Gaussian and narrow around 0. To be able to compare the different parameter estimation results not only visually, the standard deviation of the residual is calculated by equation 3.4, where $\bar{r}$ is the mean value of the residual samples.

$$\sigma_r = \sqrt{\frac{\sum_{k=1}^{N}(r_i - \bar{r})^2}{N-1}} \tag{3.4}$$

4 Power Models

The purpose of the power models is to estimate the power consumption $\hat{P}_k$ of the heat pump at time step k in each room based on an input state vector z and a parameter vector p. This section starts with a presentation of the saturation and non-negativity model that is included in all power models. Then, for each power model the model itself is presented, followed by an explanation of how the optimal parameter vector p^* were estimated, and its results. At last, for each model a discussion of the parameter estimation results is presented.

Some sorting of the data sets has been done in order to achieve better parameter estimation. The measured power consumption given by the data set gives the total power consumption of all the heat pumps, but the model and parameter estimation is representing one heat pump at the time. Therefore the data sets had to be sorted. The data sets were sorted such that the the input data of the parameter scheme was the measured data from the time steps where only one heat pump where On. In this way, the measured power consumption $y_{P,k}$ is representing the heat pump that is On. The consequence of this method is that it shrinks the data set, such that the training data becomes relatively small. Therefore the first four data sets of February and March are combined into one data set called Winter Data Set. The data set of May is called Spring Data Set. From Spring Data Set, there was not enough single unit power measurements on the HP units in *Main* and *Studio* in order to estimate the parameters. It is therefore only results from the Winter Data Set in those rooms.

4.1 Modelling Saturation and Non-negativity

As the level of power saturation for the different rooms and the outdoor units has been identified, these effects have to be modelled. In addition to an upper limit of the power, it is desirable that the model has a lower limit equal to zero as the heat pumps (HPs) cannot draw negative power.

The upper and lower limits of the power consumption are decided to be constrained in the model itself and not by the constraints in the optimization problem of the parameter estimation. An example of why, could be if the difference between the measured

and reference temperature is causing the power to exceed the saturation level limits. Optimization constraints would then force down the proportional parameter such that the power consumption is in the feasible set. However, by modelling these effects, the parameters that are found will be representative for power consumption within and at the limits of saturation.

To model the saturation and non-negativity, it is desirable to have a model behaviour that inputs an estimated power $\bar{P}$ and limits that such that the saturated power estimation $\hat{P}$ is within the limits of zero and the level of saturation P_{sat}. This model behaviour can be expressed as

$$\hat{P}(\bar{P}) \approx \begin{cases} 0, & \text{for } \bar{P} < 0, \\ \bar{P} & \text{for } 0 < \bar{P} < P_{sat}, \\ P_{sat} & \text{for } \bar{P} > P_{sat}, \end{cases} \tag{4.1}$$

To model the saturation and non-negativity effects in a time step k, a modified Sigmoid function is used. This function makes the model smooth, which is important for a Newton-based optimization strategy like *Ipopt*. The Saturation and Non-negativity model is given as

$$\alpha_k(\bar{P}_k) = \ln\left(\frac{1 + \exp(ReLu\,\bar{P}_k)}{ReLu}\right) \tag{4.2a}$$

$$\hat{P}_k(\alpha_k(\bar{P}_k)) = P_{sat} - \ln\left(\frac{1 + \exp(ReLu\,(P_{sat} - \alpha_k(\bar{P}_k))}{ReLu}\right) \tag{4.2b}$$

where the constant $ReLu$ is equal to 10, which affects the slope of the saturation curve. To increase readability, an intermediate calculation is done by the function α_k. An example of the model behaviour with $ReLu = 10$ and $P_{max} = 2kW$ is illustrated in figure 4.1.

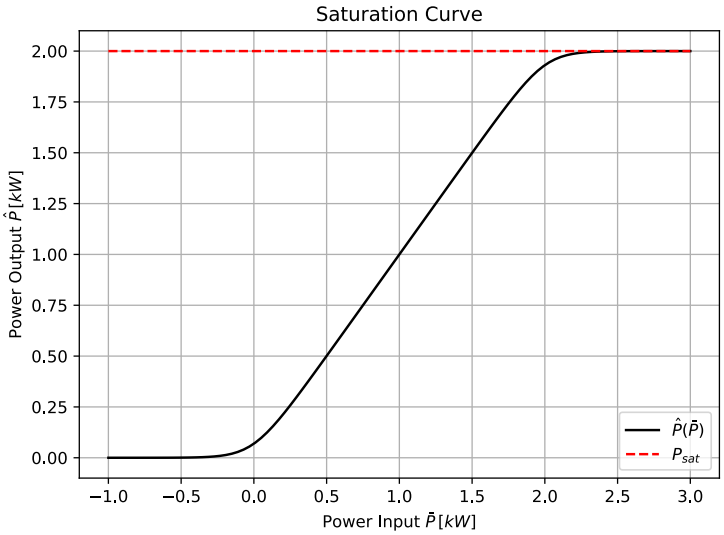

Figure 4.1: *The saturation function for power saturation at 2 kW. The illustration is self-made in Python.*

4.2 Power Model 1

Power Model 1, given by equation 4.3 is first calculating the unsaturated power consumption of a heat pump $\bar{P}_{mod1,k}$ in time step k based on the reference temperature $T_{ref,k}$ and the measured room temperature T_k. It is done by replicating a proportional (P) controller, where p_1 is equivalent to the proportional term K_p of a standard P-controller. Finally the model calculates the saturated power estimation $\hat{P}_{mod1,k}$ by the saturation function given by equation 4.2.

$$\bar{P}_{mod1,k} = p_1 \left(T_{ref,k} - T_k\right) \tag{4.3a}$$

$$\hat{P}_{mod1,k} = \hat{P}_k(\bar{P}_{mod1,k}) \tag{4.3b}$$

Even though the model is simple, it may give useful results and insight into the system behavior. Hopefully, this model will to a certain extent replicate the heat pump controller as the difference between the set temperature and the current temperature in the room should be a dominant factor of the heat pump power consumption. It is a simple and static model where the parameter is intuitive, and can be subsequently built on with more parameters and inputs.

Ideally, the measured temperature T_k would be the same as the temperature that the actual internal HP controller experiences. Any bias between these temperatures could affect this model negatively, especially when the reference temperature is approximately equal to the measured temperature. In some cases, by the reference temperature being slightly below the measured one, the model will tell that the power should be zero, when the internal HP controller experiences a temperature above the reference, making the power consumption greater than zero.

4.2.1 Parameter Estimation Problem

The parameter estimation of Power Model 1 is based of the general parameter estimation problem of section 3.4. As Power Model 1 is static, the problem is given by 3.2, where y_k is the power measurements from the winter and spring data sets. The model trajectory estimates are defined by the constraints in equation 3.2c, where

$$\phi_k = f_k(p, z_k) = \hat{P}_{mod1,k}(p, z_k), \tag{4.4}$$

where $z_k = [T_{ref,k}, T_k]$. The parameter vector p is redefined as a scalar $p = p_1$, and is constrained in equation 3.2d where $i = 1$. This parameter is positive definite because it is the proportional gain of the modelled controller.

4.2.2 Parameter Results

The results of the parameter estimation for each room is summarised in table 4.1. p_1^* and σ_r is the parameter at the solution and the standard deviation of r in the respective rooms. There was not sufficient single operation samples of the heat pumps *main* and *studio* in Spring Data Set for making good model estimations. The illustrations of the model estimates presented in this section are included for illustrative purposes, and rest of the results is presented in appendix B.1.

The parameter at the solution for Winter Data Set - *living* resulted in more than twice as large as of the Spring Data Set. The Winter Data Set estimations of *livingdown* also resulted in a larger parameter value than for the Spring Data Set, but not as big of a difference. Both winter sets also gave the biggest σ_r for both *living* and *livingdown*. The

parameters of *main* is not too far off the other results and gave a standard deviation of 0.35. p_1^* of *Studio* resulted in the highest parameter value of 6.38. In addition, this result gave the highest $\sigma_r = 0.57$.

Table 4.1: *The parameter estimation results of Power Model 1 summarised.*

Living	$\boldsymbol{p_1^* \times 10^1 \left[\frac{kW}{^\circ C}\right]}$	$\boldsymbol{\sigma_r}$
Winter Data Set	5.41	0.45
Spring Data Set	1.59	0.21
Livingdown		
Winter Data Set	3.0	0.42
Spring Data Set	2.36	0.25
Main		
Winter Data Set	2.71	0.35
Studio		
Winter Data Set	6.38	0.57

The parameter estimation of Power Model 1 in *living* resulted in both the lowest parameter p_1 and standard deviation σ_r. Figure 4.2 shows that the model estimation $\phi(p^*)$ follows the measurements y, but only at low power levels close or equal to zero. There are two exceptions, one at the beginning and another at approximately time step 60-70, where the estimates follow the measurements at higher power levels. The distribution of r is clearly affected by the fact that the estimation is close to the lowest levels of power.

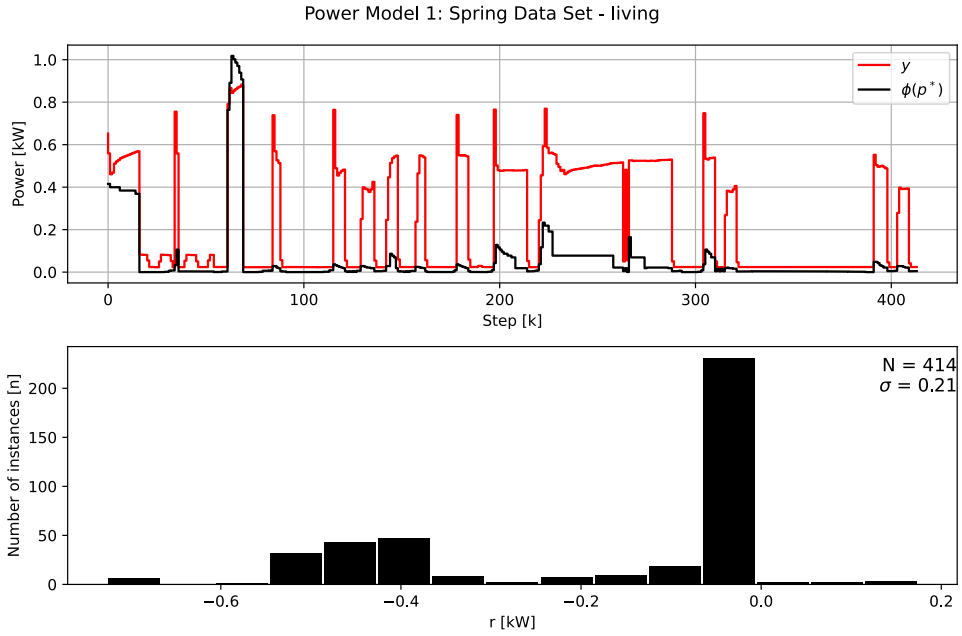

Figure 4.2: *Upper plot compares the estimate trajectory of Power Model 2 and the power measurements for Living - Spring Data Set. The lower plot illustrates the distribution of the residual.*

The parameter estimation of Power Model 1 in *livingdown*, based on Spring Data Set, resulted in a $\sigma = 0.25$ and $p_1 = 2.36$. From figure 4.3 it can be observed that the model estimation trajectory $\phi(p_1^*)$ follows the mean of the power measurements y quite well until approximately time step 50. After that it is lower than the trend of y. The distribution plot resembles a skew normal distribution with a peak lower than zero. Based on equation 3.1 it verifies that $\phi(p^*)$ is generally lower than y.

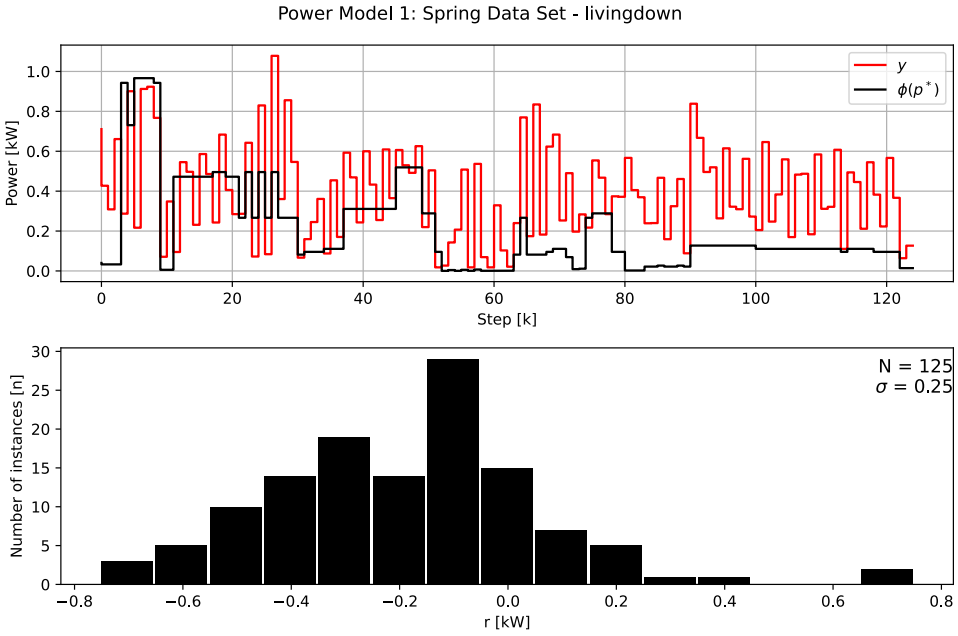

Figure 4.3: *Upper plot compares the estimate trajectory of Power Model 1 and the power measurements for Livingdown - Spring Data Set. The lower plot illustrates the distribution of the residual.*

4.2.3 Discussion

The estimation of Power Model 1 in *living* gave the lowest σ off all estimations, but it is not necessarily the optimal one for replicating the system behaviour. Since the data set measurements have a lot of values close to zero, the solution is more satisfied at being close to the low power levels, rather than the power peaks. The reason for that the model cannot follow the fluctuations of power, may be that there is a bias between the measured temperature and the temperature experienced by the indoor HP unit. This model would not be recommended as a model in a Model Predictive Controller (MPC), as it is rather inaccurate.

The estimation of Power Model 1 in *livingdown* by Spring Data set resulted in the second lowest σ_r out of the other estimates. Even though it follows the trends at some extent, it is not sufficiently accurate to utilize it in an MPC. The skew distribution of r indicates that there is a bias in the system.

The results presented in this section has similar trends as the other estimates presented in the appendix, and is indicating that a bias is restricting the model. A new proposed model

should deal with this issue. It may be advantageous to add a new parameter p_2 that shifts the power estimation up, as the results of this model is generally too low.

4.3 Power Model 2

Power Model 2 is a model that builds further on Power Model 1, which is described in section 4.2. The input states z remains the same, but it is a parameter. The new parameter p_2 is representing the bias in the model - especially with respect to the expected bias between the measured temperature from the external sensor and the experienced temperature of the internal controller of the HP.

Power Model 2 is given by 4.5 where p_1 is equivalent to the proportional gain K_p of a P-controller and is defined as positive definite. p_1 is scaling the power proportional to the difference between the reference temperature of the heat pump T_{ref} and the temperature measured by the external temperature sensor T_k. The model estimates $\bar{P}_{mod2,k}(p, z)$ is then an input to the saturation function $\hat{P}$ in equation 4.5b, which calculates the saturated power estimates.

$$\bar{P}_{mod2,k} = p_1 \left(T_{ref,k} - T_k\right) + p_2 \tag{4.5a}$$

$$\hat{P}_{mod2,k} = \hat{P}_k(\bar{P}_{mod2,k}) \tag{4.5b}$$

It is expected that this model will perform better than Power Model 1. Ideally, the new bias term fixes the issue where Power Model 1 estimated too low power consumption. As Power Model 1 generally estimated too low values, the bias term is expected to shift the estimates up, hence it should be positive.

4.3.1 Parameter Estimation Problem

The parameter estimation problem is similar to the parameter estimation of Power Model 1. The model is static, which means the problem can be defined by equation 3.2, where y_k is the power measurements from the winter and spring Data Set. The model trajectory

estimates is defined by the constraints in equation 3.2c, where

$$\phi_k = f_k(p, z_k) = \hat{P}_{mod2,k}(p, z_k), \tag{4.6}$$

where the input states $z_k = [T_{ref,k}, T_k]$ of time step k and the parameter vector $p = [p_1, p_2]$. Parameter p_1 is constrained in equation 3.2d where $i = 1$, because the proportional gain is defined as positive. Parameter p_2 is unconstrained as it can both be positive or negative.

4.3.2 Parameter Results

The results of the parameter estimation for each room are summarised in table 4.2. p^* and σ_r are the parameter vector at the solution and the standard deviation of r in the respective rooms. There was not enough single operation samples of the heat pumps *main* and *studio* in Spring Data Set for generating good model estimates. The illustrations of the model estimates presented in this section are included for illustrative purposes. The rest of the results are presented in appendix B.2.

The parameter results of *living* show that both parameters where larger of the Winter Data Set results. The bias based parameter p_2^* is nearly twice as large of the Winter Data Set. The Spring Data Set gave the lowest standard deviation of $\sigma_r = 0.14$. The results of *livingdown* also gave the highest parameters of the Winter Data Set results, and lowest standard deviation. The parameter results of *main* and *studio* gave parameters within reasonable range of the other parameter results. The highest bias term of the parameter estimation is of *studio*.

Table 4.2: *The parameter estimation results of Power Model 2 summarised.*

Living	$\boldsymbol{p_1^* \times 10^1 \left[\frac{kW}{^\circ C}\right]}$	$\boldsymbol{p_2^* \times 10^1 [kW]}$	$\boldsymbol{\sigma_r}$
Winter Data Set	1.57	7.09	0.29
Spring Data Set	1.28	3.89	0.14
Livingdown			
Winter Data Set	1.39	5.78	0.32
Spring Data Set	0.8	3.53	0.21
Main			
Winter Data Set	1.35	4.35	0.31
Studio			
Winter Data Set	1.42	9.65	0.38

The parameter estimation of Power Model 2 of *living* and Spring Data Set resulted in the lowest σ_r. As illustrated in figure 4.4, the model estimation trajectory $\phi(p^*)$ follows the trends of the measurements y. Even though it follows the trends, it does not estimate the correct amplitude of the power peaks. It usually estimates approximately 0.1 kW higher or lower. This observation is verified by the distribution plot.

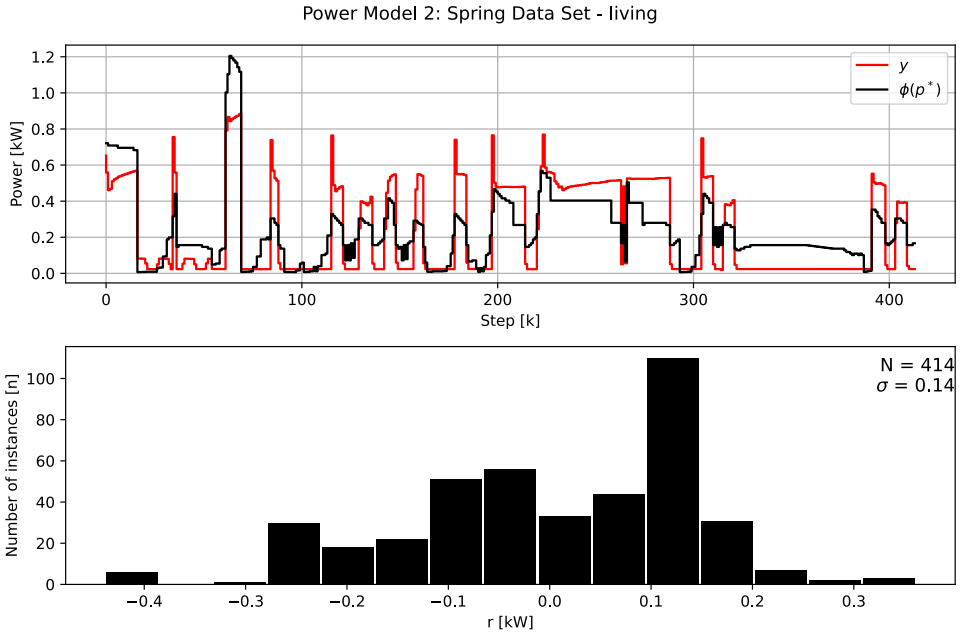

Figure 4.4: *Upper plot compares the estimate trajectory of Power Model 2 and the power measurements for living - Spring Data Set. The lower plot illustrates the distribution of the residual.*

By figure 4.5 it can be observed that the measurements y fluctuate around the trajectory of the model estimates $\phi(p^*)$. The model estimate trajectory is mostly at an approximate of the fluctuation mean. The distribution plot of r indicates a Gaussian distribution with a peak at $r \approx 0$. The other results from Power Model 2 parameter estimation presented in appendix B.2 have similar results as in figure 4.5.

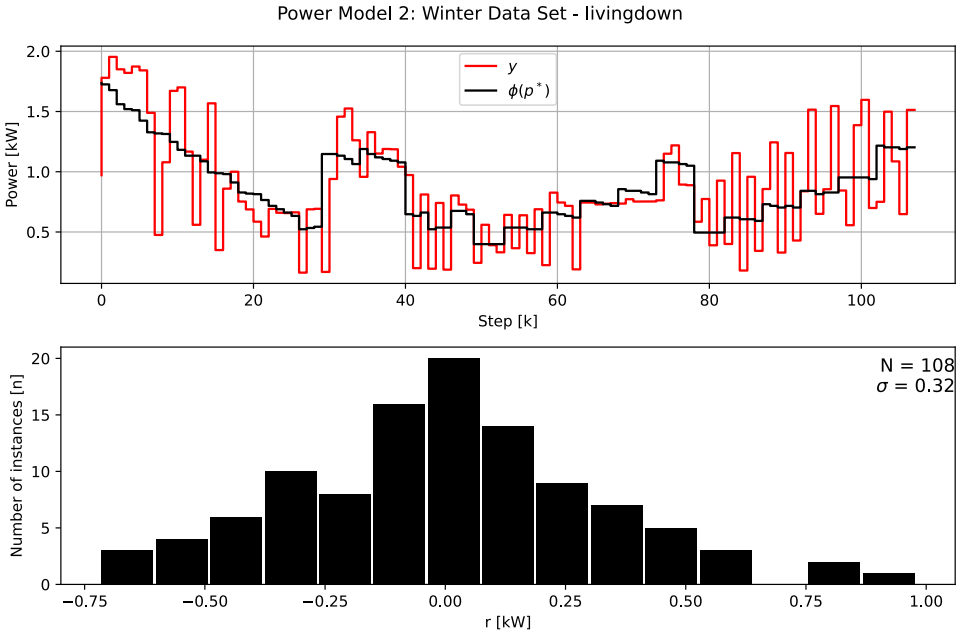

Figure 4.5: *Upper plot compares the estimate trajectory of Power Model 2 and the power measurements for ivingdown - Winter Data Set. The lower plot illustrates the distribution of the residual.*

4.3.3 Discussion

The estimation results of *living - Spring Data Set* illustrates the impact of the bias term in comparison with Power Model 1. As expected $p_2^* > 0$ for all solutions. Power Model 2 seems to be able to estimate the trends of the power consumption fairly well. It is hard to conclude whether the estimation of the peaks is good enough if the model is to be used in an MPC. The predictive capabilities of the model should be tested to verify any strengths and weaknesses.

The results of *livingdown - Winter Data Set* show that the model is not capable of estimating the frequent oscillations of the measurements. However, it seems to estimate the mean value of these fluctuations, which can be sufficient as a model in an MPC. It can be argued that the impact the HP power has on the room temperate can be represented by the mean of the fluctuations as well as the fluctuating measurements. This is because the heating of the room is a rather slow process. In addition, the fluctuation of the power consumption may originate from the HP compressor, finding the right pressure and heat combination of refrigerant. This is also a rather slow process with regard regard to the

temperature changes in the room. In terms of energy usage per hour, which the electricity bill is depended on, the model estimate trajectory may have little difference from the fluctuating power measurements.

4.4 Power Model 3

Power Model 3 builds on Power Model 2, a new term is added that consists of a new parameter and input state. The purpose of the new term is to model any changes in performance of the heat pump with regard to the outdoor temperature. It would identify if the HP uses more power in times of lower outdoor temperatures compared to the indoor temperature.

The model given by equation 4.7 is first estimating the unsaturated power $\bar{P}_{mod3,k}$ at time step k, where p_1 is equivalent to the proportional gain of a P-controller and p_3 is the bias term. p_2 is the new parameter that is related to the performance of the heat pump with regard to the outdoor temperature $T_{out,k}$. Finally, the model calculates the saturated power estimation $\hat{P}_{mod3,k}$ based on the saturation function given by equation 4.2.

$$\bar{P}_{mod3,k} = p_1 \left(T_{ref,k} - T_k + p_3\right) \left(1 - p_2 \left(T_{out} - T_k + p_3\right)\right) \tag{4.7a}$$

$$\hat{P}_{mod3,k} = \hat{P}_k(\bar{P}_{mod3,k}) \tag{4.7b}$$

p_1 and p_2 are defined as positive, but the bias term p_3 can be both negative and positive.

The estimation result of this model is expected to give some improvement compared to Power Model 2. The parameter p_2 is expected to be between [0,1]. As the bias term was positive for all rooms in Power Model 2, it is expected that will be the case of Power Model 3.

4.4.1 Parameter Estimation Problem

The parameter estimation by Power Model 3 is done on the basis of the general estimation problem described in section 3.4. The model is static and the problem can therefore be described by equation 3.2 where y_k is the power measurements from *Winter* and *Spring*

Data Set. The model estimate at time step k is defined by equation 3.2c where

$$\phi_k = f_k(p, z_k) = \hat{P}_{mod3,k}(p, z_k). \tag{4.8}$$

The parameter and input state vectors are defined as

$$p = [p_1, p_2, p_3], \tag{4.9a}$$
$$z_k = [T_{ref,k}, T_k, T_{out,k}]. \tag{4.9b}$$

Parameter p_1 is constrained by equation 3.2d, hence $i = 1$. The parameters p_2 and p_3 are unconstrained. The parameter p_2 could be constrained as it is expected to be greater than 0, but is left unconstrained to test if the parameter estimation identifies the expected behavior. By having both p_2 and p_3 unconstrained, there is more freedom in the optimization problem, hence it strengthens the results if it manages to identify the expected results.

4.4.2 Parameter Results

The parameter estimation results of Power Model 3 are summarised in table 4.3. p^* is the optimal parameters at the solution, and σ_r is the standard deviation of the residual r of each room. For all of the rooms and data set combinations, except Spring Data Set - *living*, parameter p_2^* was between [0,1]. The unconstrained parameter p_3^* is positive for all rooms.

Table 4.3: *Parameter estimation results of Model 3.*

Living	$p_1^* \times 10^2 \left[\frac{kW}{^\circ C}\right]$	$p_2^* \times 10^2 \left[\frac{1}{^\circ C}\right]$	$p_3^*[^\circ C]$	σ_r
Winter Data Set	7.43	8.79	4.55	0.27
Spring Data Set	13.3	-0.340	3.02	0.14
Livingdown				
Winter Data Set	9.44	3.57	4.27	0.32
Spring Data Set	8.92	2.7	3.78	0.20
Main				
Winter Data Set	10.2	2.08	3.26	0.30
Studio				
Winter Data Set	4.16	21.3	6.62	0.37

The model trajectories are presented in appendix B.3, and are not included in this section as they resemble the trajectories from previous model estimates from Power Model 2.

4.4.3 Discussion

The model based parameter estimation identified a relation between the power and the difference of the outside and inside temperature for all rooms and data set combinations, except one. This means that the heat pump may require more power when it is cold outside because it requires more to heat the refrigerant. The results may also be affected by the fact that there is more heat loss in the room itself. Hence, the heat pump is running at higher power over longer periods of time.

The standard deviation of the residual is lower compared to Power Model 2 for the rooms and data set combinations that had $p_2^* > 0$, except for Winter Data Set - *livingdown*, they had the same σ_r. For Winter Data Set - *living* it improved by 0.02, while the rest improved by 0.01.

The fact that p_2 and p_3 were unconstrained, indicates that the model is identifying the system behaviour. As p_3^* were positive for all rooms and data set combination indicates that the bias term from Power Model 2 is also replicating the system behaviour. As it is positive, it may indicate that the measured temperature is less than temperature that the

internal controller of the heat pump experiences.

4.5 Power Model 4

The internal controllers of the HPs in the house may be PI-controllers. This is a common control strategy in systems regarding heating, as the integral term deals with the disturbance caused by heat loss. Power Model 4 given in equation 4.10 represents such a controller. The integration term I_k of time step k by equation 4.10c is accumulating the error between the mean reference temperature $\bar{T}_{ref,k}$ and the mean measured room temperature $\bar{T}_k$. The mean temperatures of time step k are given by equations 4.10a and 4.10b. By taking the mean of the temperature between time step k and k-1, it is assumed that the temperature changes linearly between the time steps.

The unsaturated power estimation $\bar{P}_{mod4,k}$ by equation 4.10d is calculated as a PI-controller where p_2 and p_3 are equivalent to the proportional gain K_p and the integration gain K_I, respectively. The parameter p_1 is representing the measurement bias between the external temperature sensor and the experienced temperature of the internal HP controller. The saturated power estimation $\hat{P}_{mod4,k}$ is given by equation 4.10e, where the function $\hat{P}_k$ is given by equation 4.2.

$$\bar{T}_{ref,k} = \frac{T_{ref,k} + T_{ref,k-1}}{2} \tag{4.10a}$$

$$\bar{T}_k = \frac{T_k + T_{k-1}}{2} \tag{4.10b}$$

$$I_k = I_{k-1} + (\bar{T}_{ref,k} - \bar{T}_k + p_1)\,\Delta t_k \tag{4.10c}$$

$$\bar{P}_{mod4,k} = p_2\,(T_{ref,k} - T_k + p_1) + p3\,I_k \tag{4.10d}$$

$$\hat{P}_{mod4,k} = \hat{P}_k(\bar{P}_{mod4,k}) \tag{4.10e}$$

4.5.1 Parameter Estimation Problem

The parameter estimation problem of finding the optimal parameter vector p^* is based on the general estimation setup described in section 3.4. Power Model 4 is a dynamic model, which means that the optimization problem can be given by equation 3.3, where ϕ_k is the model estimates in time step k, and y_k is the measured power from the data sets *Winter Data Set* and *Spring Data Set*.

The model estimate trajectory is defined by the constraints in equation 3.3d where

$$\phi_k = f_k(p, z_k, \phi_{k-1}) = \hat{P}_{mod4,k}(p, z_k, \phi_{k-1}), \tag{4.11}$$

and the input states and parameter vector are defined as

$$z_k = [T_{ref,k}, T_k, T_{ref,k-1}, T_{k-1}, I_k, \Delta t_k], \tag{4.12a}$$

$$p = [p_1, p_2, p_3]. \tag{4.12b}$$

Parameters p_2 and p_3 are defined as positive, hence i = [2,3] in 3.3e. The bias parameter p_1 is unconstrained as it can be both positive and negative. Δt is given in minutes, and not seconds to achieve parameter values with lower magnitude.

The initial values of the integration term I_0 and I_{gap} are also unconstrained. As it is unknown if the HP is resetting the integrated error back to zero after each time it has been turned off, we let the solver find the most appropriate values.

4.5.2 Parameter Results

The parameter estimation results of Power Model 4 are summarised in table 4.4, where p^* is the parameter vector at the solution and σ_r are the standard deviation of r. There was not a sufficient of single operation samples of the heat pumps of *main* and *studio* in Spring Data Set for making good model estimations. It was not found a solution for *livingdown - Winter Data Set*. The illustrations of the model estimates presented in this section are included for illustrative purposes. The remaining results is presented in appendix B.4.

The bias parameter p_1^* is changing signs from room to room. The greatest absolute value of p_1^* is for *living - Spring Data Set* and would be equivalent to 0.8 °C bias. Parameter p_2^* that is equivalent to the proportional gain is ranging from 0.134 to 0.257. The integrator gain based parameter p_3^* is varying a bit more. For *living* the Winter Data Set gave approximately ten times higher parameter value than from the Spring Data Set. The lowest standard deviation is of *living - Spring Data Set* at 0.09.

Table 4.4: *The parameter estimation results of Power Model 2.*

Living	$p_1^* \times 10^1 [°C]$	$p_2^* \times 10^1 \left[\frac{kW}{°C}\right]$	$p_3^* \times 10^3 \left[\frac{kW}{°Cmin}\right]$	σ_r
Winter Data Set	-1.98	1.37	4.76	0.24
Spring Data Set	8.11	2.40	0.459	0.09
Livingdown				
Winter Data Set	-	-	-	-
Spring Data Set	-3.87	2.57	2.46	0.18
Main				
Winter Data Set	5.89	1.34	0.625	0.30
Studio				
Winter Data Set	0.777	1.51	2.20	0.36

Figure 4.6 show that the model estimates $\phi(p^*)$ track the measurements y. There are a few exceptions where $\phi(p^*)$ fall before y, as y was lagging behind. The distribution plot verifies that most of the estimates are near the true values.

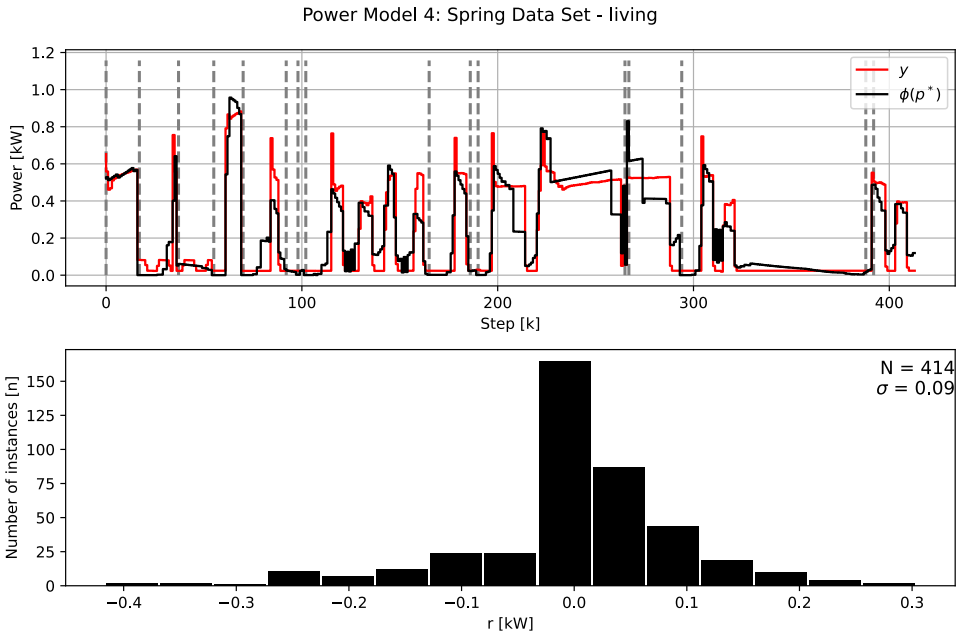

Figure 4.6: *Upper plot compares the estimate trajectory of Power Model 4 and the power measurements for Living - Spring Data Set. The vertical grey dotted lines indicate gaps in the time series. The lower plot illustrates the distribution of the residual.*

The model estimates $\phi(p^*)$ of *livingdown* are compared with the measurements y in figure 4.7. y has an oscillating tendency. This tendency seems to be replicated by the model in some instances at around time steps 20-27 and 50-58. The model estimate trajectory is mostly able to follow an approximately average of the fluctuations in measurements. The distribution of r has a block shape with edges slightly larger than $\pm 0.2kW$. The results presented in appendix B.4 show the same trends as in figure 4.7.

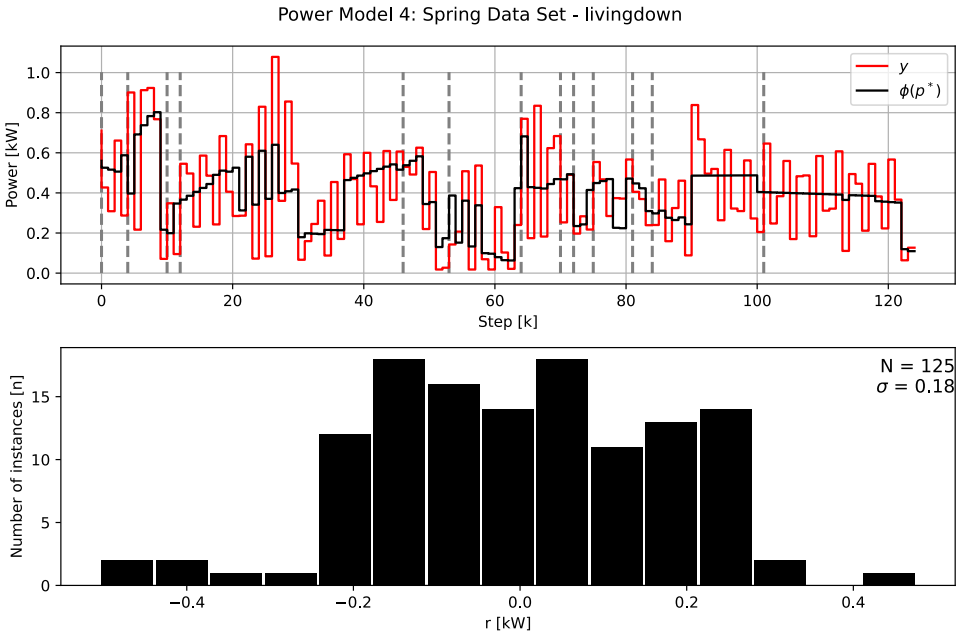

Figure 4.7: *Upper plot compares the estimate trajectory of Power Model 4 and the power measurements for livingdown - Spring Data Set. The vertical grey dotted lines indicate gaps in the time series. The lower plot illustrates the distribution of the residual.*

Figure 4.8 and 4.9 illustrate the evolution of the integration term I. For each gap in the data set, the new initial values steps up or down significantly. I of *living* ranges from approximately ± 2000, while I of *livingdown* ranges from approximately -130 to 400.

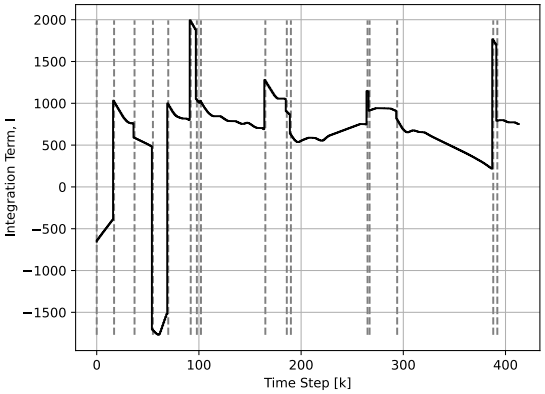

Figure 4.8: *The integration evolution term over the time step k from the parameter estimation of living - Spring Data Set results. The vertical grey dotted lines indicate gaps in the time series.*

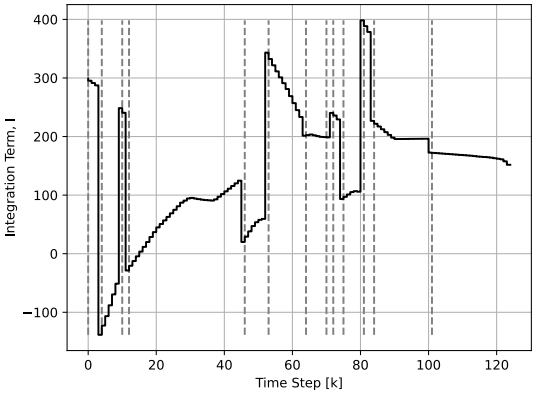

Figure 4.9: *The integration evolution term over the time step k from the parameter estimation of livingdown - Spring Data Set results. The vertical grey dotted lines indicate gaps in the time series.*

4.5.3 Discussion

Power Model seems to identify the system behaviour, as it does a proper job of tracking the measurements. Comparing the standard deviation with the ones from Power Model 3, it improves for all rooms and data set combinations. The largest improvements have been made in *living*, where it reduced from 0.28 to 0.24 and from 0.14 to 0.09. The remaining standard deviations have been reduced from 0.01 and 0.02.

Some of the improved results may be explained by the fact that the solver finds the optimal initial integration values for each gap in the time series. This helps the model estimates towards the measurement values, even though it might not replicate the true integration behaviour of the internal controller of the HPs. The different amplitudes of the integration terms presented, may be an indication of that it "exploits" the initial values, instead of replicating the behaviour of the internal HP controller. It can not be verified however that the HP resets the accumulated integration term after it has been shut off, or if it saves it until it is turned on again.

This model has a high potential, and has unlike the previous models been able to identify

some of the faster fluctuations of the power measurements. However, the parameters are quite varying, such as the trajectory of the integration terms. It is recommended to investigate and analyse this model further before implementing it in an MPC.

5 Temperature Models

The purpose of the temperature models is to estimate the temperature $\hat{T}_k$ at the time step k in each room based on an input state vector z_k and a parameter vector p. This section will first cover common aspects about the temperature models. Then, each model will be presented with a description, parameter estimation method and results and at last, a discussion section.

One common input state for all the temperature models is the heat pump power consumption. This input state is calculated by Power Model 2. Power Model 2 is chosen based on the discussions in section 4. It is a simple model, yet it follows the trends of the measurements well. If the PI-controller based Power Model 4 where to be used, uncertainties would arise in terms of the initial value of the integration term. Even though the model did not estimate all the fast fluctuation of the measurements, an approximate mean value of these were found. As the thermal system is expected to be slower, the estimations of Power Model 2 should should be sufficient.

The power model function used to calculate the input power to the temperature models is defined as

$$\bar{P}_k = p_1 \left(T_{ref,k} - T_k\right) + p_2, \tag{5.1a}$$

$$P_k = on\, \hat{P}_k(\bar{P}_k), \tag{5.1b}$$

where $\bar{P}_k$ is the unsaturated power estimate and P_k is the saturated power estimate calculated by the saturation function $\hat{P}_k$ given by equation 4.2. The variable inputs of the function is defined as $z_{P,k} = [T_{ref}, T_k, on]$. T_{ref} is the reference temperature of the heat pump internal controller and T_k is the room temperature. On is a Boolean value that activates the function when the heat pump is on. This is necessary because the estimated power output is depended on the difference between T_{ref} and T_k that may vary, even though the system HP is Off. The parameters p for each room is given by table 5.1. They are found by the parameter results of table 4.2. These parameters were chosen based on how well they performed in the parameter estimation.

Table 5.1: *Power Model parameters used in the temperature models.*

Rooms	$\boldsymbol{p_1 \times 10^1 \left[\frac{kW}{^\circ C}\right]}$	$\boldsymbol{p_2 \times 10^1 [^\circ C]}$
Living	1.28	3.98
Livingdown	0.80	3.53
Main	1.35	4.35
Studio	1.42	9.65

An alternative way to get the power input state could be directly from the data sets. But then, as in the system identification data sets of the parameter estimation of the power models, the data would have been severely limited. As the power measurements from the data sets are the total combined power consumption of all the heat pumps (HPs), the power measurements would be from whether the HP is the only one 'On' and when it is 'Off'. Any other instances where a HP is running at the same time as another, the actual power consumption of the HP would be unknown. Another reason for using calculations of the power model to get the power measurements is that the temperature models will 'fit' with the power model. This way may make the model perform better, than if the power and temperature models were parameter estimated separately.

5.1 Temperature Model 1

Temperature Model 1 uses the principles of heat transfer to calculate the temperature dynamics of the rooms. The HP is considered a heat source, while the outside air is considered a heat source/sink, depending on whether the outside air temperature is lower or higher than the room temperature. The energy flow between the outdoor and indoor air is depends on the heat conduction through the windows and walls of the rooms.

The temperature model is given by equation 5.2. First, it calculates the rate of change in temperature $\Delta T_{mod1,k}$ in the time step k by the power usage of the HP heat source and the heat conduction between the outside air $T_{out,k-1}$ and the room temperature T_{k-1} of the previous time step $k-1$. The parameter p_1 is the relation between the power used and the rate of temperature change in the room. The parameter p_2 includes the thermal conductivity of the walls and windows, in addition to the specific heat capacity of the air

in the room. Both parameters are defined as positive definite because of the Second Law of Thermodynamics and Newton's Law of cooling. The inside air is treated as a thermal mass where $T_{mod1,k}$ is the estimated temperature at time step k. T_{k-1} is the temperature in the room at the previous time step and Δt_k is the time difference between time step k and k-1, and is given in days.

$$\Delta T_{mod1,k} = p_1 \, P_{k-1}(T_{ref,k-1}, T_{k-1}) + p_2 \, (T_{out,k-1} - T_{k-1}) \tag{5.2a}$$

$$T_{mod1,k} = T_{k-1} + \Delta T_{mod1,k} \, \Delta t_k \tag{5.2b}$$

5.1.1 Parameter Estimation Problem

The parameter estimation of Temperature Model 1 is done on the basis of the optimization scheme described in section 3.4. The temperature model is a dynamic model, and therefore the problem of the estimation can be described by equation 3.3, where ϕ_k is the model estimate trajectory and y_k is the temperature measurements at time step k. The measurements are from the *Winter* and *Spring Data Set*.

The model estimate trajectory is defined by the constraints in equation 3.3d, where

$$\phi_k = f_k(p, z_k, \phi_{k-1}) = T_{mod1,k}(p, z_k, \phi_{k-1}), \tag{5.3}$$

where ϕ_{k-1} is the model estimates in previous the time step. This input makes the trajectory continuous. The input state and parameter vectors z_k and p are defined as

$$z_k = [T_{ref,k-1}, T_{out,k-1}, T_{k-1}, on, \Delta t_k], \tag{5.4a}$$

$$p = [p_1, p_2], \tag{5.4b}$$

where both parameters are constrained to be positive definite, hence $i = [1, 2]$ by equation 3.3e.

5.1.2 Parameter Results

The parameter estimation results of Temperature Model 1 are summarised in table 5.2. p^* is the parameter vector at the solution and σ_r is the standard deviation of the residual r. The model estimation trajectory and the residual of *living - Winter Data Set* and *main - Winter Data Set* is presented in this section for illustrative reasons. The other resulting trajectories and residuals is presented in Appendix C.1.

The parameter results in table 5.2 show that for the Winter Data Sets, both p_1^* and p_2^* are higher than for the Spring Data Sets. Within some of the rooms, the same parameters differ with over 100 %. For *living* and *livingdown* the Winter Data Set resulted in the lowest standard deviation of 0.40 and 0.37. For *main* and *studio*, Spring Data Set resulted in the lowest standard deviation of 0.47.

Table 5.2: *The parameter estimation results of Temperature model 1.*

Living	$\boldsymbol{p_1^*}\left[\frac{°C}{kW\ day}\right]$	$\boldsymbol{p_2^*}\left[\frac{1}{day}\right]$	$\boldsymbol{\sigma_r}$
Winter Data Set	35.4	0.617	0.40
Spring Data Set	16.5	0.502	0.64
Livingdown			
Winter Data Set	35.3	0.448	0.37
Spring Data Set	12.6	0.373	0.69
Main			
Winter Data Set	17.1	0.438	0.48
Spring Data Set	9.00	0.133	0.47
Studio			
Winter Data Set	11.8	0.359	0.59
Spring Data Set	4.82	0.174	0.47

Figure 5.1 shows that the optimal model estimate trajectory $\phi(p^*)$ follows closely the measurements y, both in times of temperature rise with contribution of the heat pump, and in times of temperature drops. Notice that the temperature drop of the system is nonlinear, while the model is approximately linear. The distribution of the residual r has a Gaussian shape and illustrates that most of the model estimates are within ± 1 °C.

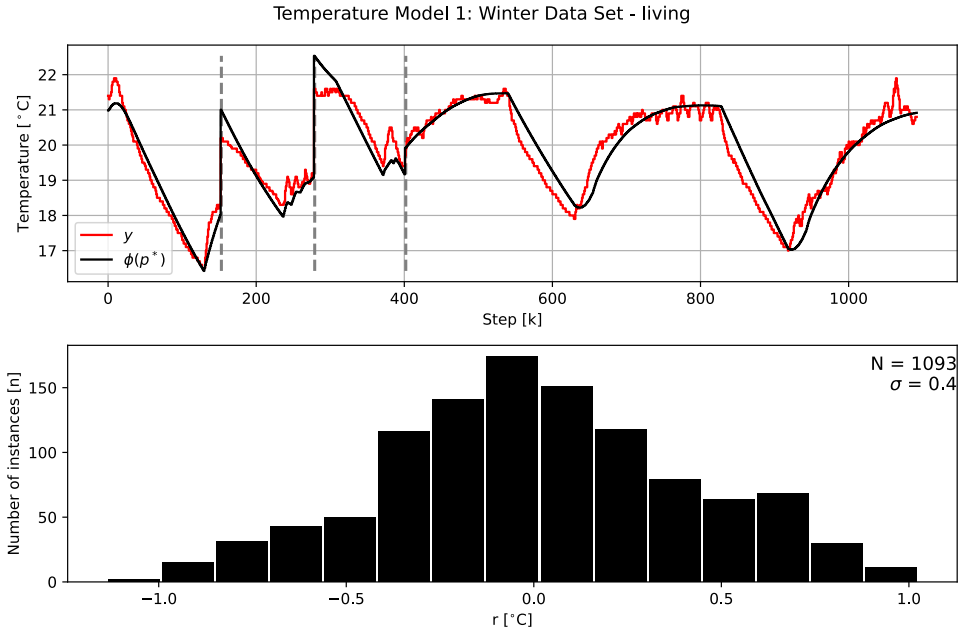

Figure 5.1: *Upper plot compares the optimal model trajectory in black with the temperature measurements in red of Winter Data Set - living. The grey vertical dotted lines mark the gaps in the time series of over five minutes. The lower plot illustrates the distribution of the residual.*

Figure 5.2 show that the optimal model estimate trajectory $\phi(p^*)$ is following the trends of the measured temperature y. However, the transient responses of the temperature changes differ more at the last half of the time series. The model estimates a more linear temperature response than the real system measurements indicate. The distribution of the residual r resembles a subgaussian form and illustrates that most of the model estimates are within ± 1 °C.

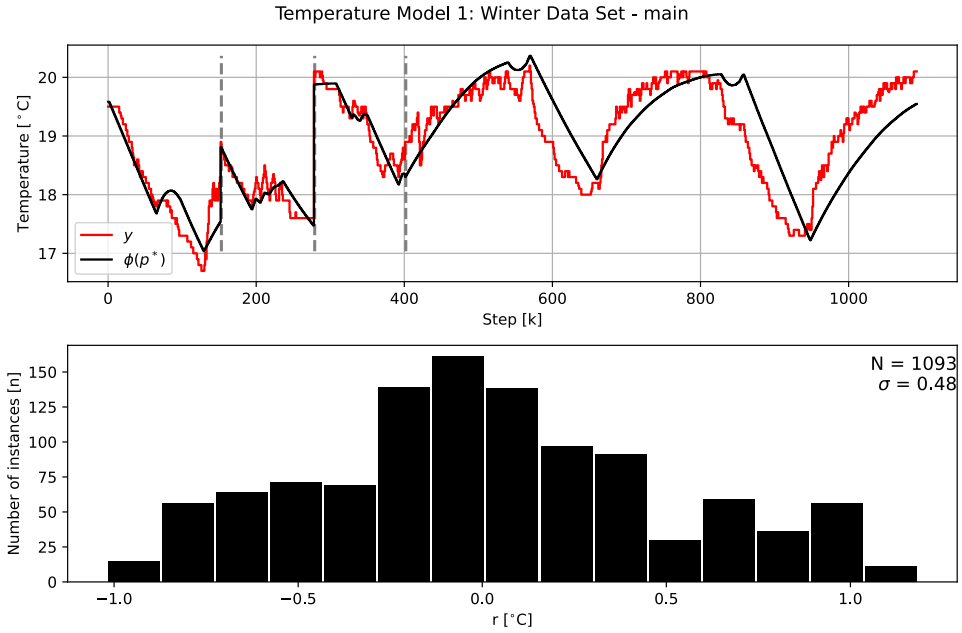

Figure 5.2: *Upper plot compares the optimal model trajectory in black with the temperature measurements in red of Winter Data Set - main. The grey vertical dotted lines mark the gaps in the time series of over five minutes. The lower plot illustrates the distribution of the residual.*

5.1.3 Discussion

Both of the estimation results presented in this section shows that the temperature model follows the trends of the system. Some of the other results given in appendix C.1 show that the model follows the trends, but is inaccurate in terms of the amplitude of the temperature fluctuations. This may be explained by the fact that the time series of these current results are twice the length of the better ones. The optimal solution for the long series would then be to be at a level close to the mean of the fluctuations. This could explain the resulting parameters of Spring Data sets are lower than the ones from the winter data sets.

Another cause for the lower parameters of the spring data sets could be explained by the outdoor temperature. As the outdoor temperature of the spring is higher than the winter, the HP requires less power to compress the refrigerant. In addition, there is less heat loss through the shell of the house.

By analysing the temperature changes of the measurements, it seems that the room temperature is experiencing thermal inertia. This could be either from the room shell, but also furniture and air from other rooms in the house. A new proposed model could

add a state that identifies the suspected thermal inertia.

5.2 Temperature Model 2

Temperature Model 2 is based on Temperature Model 1 described in section 5.1. As the previous model did not manage to recreate the system behaviour in the temperature step responses, a model may perform better by adding a new state that replicates a thermal inertia of the room. This thermal inertia could be the temperature of the shell of the rooms, furniture and air temperature of the other rooms.

Temperature Model 2 is given by equation 5.5, where the new thermal inertia state is given as the thermal mass temperature $T_{I,k}$ at time step k. The rate of temperature change in the thermal inertia $\Delta T_{I,k}$ is calculated with the principles of heat transfer and heat capacity. The heat transfers between the inertia mass and the surrounding inside and outside air. The transfer depends on the temperature difference between the temperature of the inertia mass $T_{I,k-1}$ and the temperature of the room T_{k-1} and outside air $T_{out,k-1}$. The parameters p_1 and p_2 include the convection coefficients, the conductivity and the physical dimensions of the system. As of Thermodynamics Second Law and Newton's Law of Cooling the parameters are defined positive.

The rate of change in the room temperature depends on three terms, see equation 5.5c. The first term is providing heat from the HP heat source that is proportional to the parameter p_3 and the estimated power P_{k-1}. The second term includes the convective heat transfer between the room air and the thermal inertia of the room that is proportional to the parameter p_4. The third term is the term from Temperature Model 1 where there is a heat transfer related to the indoor and outdoor air temperature. The parameter p_5 includes the conductivity, convection coefficient and the specific heat of the walls, windows ventilation, etc. All parameters are defined as positive. Δt_k is the time difference between time step k and k-1, and is given in days.

$$\Delta T_{I,k} = p_1 \left(T_{k-1} - T_{I,k-1}\right) + p_2 \left(T_{out,k-1} - T_{I,k-1}\right) \tag{5.5a}$$

$$T_{I,k} = T_{I,k-1} + \Delta T_{I,k}\, \Delta t_k \tag{5.5b}$$

$$\Delta T_{mod2,k} = p_3\, P_{k-1}(T_{ref,k-1}, T_{k-1}, on) + p_4 \left(T_{I,k-1} - T_{k-1}\right) + p_5 \left(T_{out,k-1} - T_{k-1}\right) \tag{5.5c}$$

$$T_{mod2,k} = T_{k-1} + \Delta T_{mod1,k}\, \Delta t_k \tag{5.5d}$$

5.2.1 Parameter Estimation

The parameter estimation of the Temperature Model 2 parameters are based on the general problem described in section 3.4. The model is dynamic, which means that the optimization problem can be given by equation 3.3, where r_k is the residual of the model estimate ϕ_k and the temperature measurements y_k in time step k. The measurements are from *Winter Data Set* and *Spring Data Set*. The model trajectory is defined in the constraints by equation 3.3d, where

$$\phi_k = f_k(p, z_k, \phi_{k-1}) = T_{mod2,k}(p, z_k, \phi_{k-1}), \tag{5.6}$$

where ϕ_{k-1} is the model estimates in previous time step $k-1$. This input makes the trajectory continuous. The input state and parameter vectors z_k and p are defined as

$$z_k = [T_{ref,k-1}, T_{out,k-1}, T_{k-1}, T_{I,k-1}, on, \Delta t_k], \tag{5.7a}$$

$$p = [p_1, p_2, p_3, p_4, p_5]. \tag{5.7b}$$

All parameters is constrained to be positive, hence $i = [1, 2, 3, 4, 5]$ in equation 3.3e. The initial temperature of both the inertia heat mass $T_{I,gap}$ and the room air temperature $T_{I,gap}$ is calculated by the solver to find the optimal temperature.

5.2.2 Parameter Results

The parameter estimation results of Temperature Model 2 are summarised in table 5.3. The table includes the parameter p^* at the solution and the standard deviation σ_r of

the residual r for each room and data set combination. The resulting trajectories and residual distribution that are presented in this section are for *livingdown - Winter Data Set*, *main - Spring Data Set* and *studio - Winter Data Set*. The remaining room and data set combinations are given in appendix C.2.

Table 5.3 shows that five out of eight p_2^* were zero. The model based parameter estimation only identified p_2^* greater than zero for *livingdown - Spring Data Set* and *studio*. Three other p^* equal to zero, one for p_1^* and two for p_5^*. *Studio - Winter Data Set* were also found and were the only result where none of the optimal parameters were zero.

The parameter p_1^* is significantly deviating between the data sets for each room, while p_3^* and p_4^* show less variation between the data sets. The standard deviation is lowest for Winter Data Set for *living*, *livingdown* and *main*, while greater for Spring Data Set for the room *studio*.

Table 5.3: *The parameter estimation results of Temperature model 2.*

Living	$\boldsymbol{p_1^*}\left[\frac{1}{day}\right]$	$\boldsymbol{p_2^* \times 10^{-1}}\left[\frac{1}{day}\right]$	$\boldsymbol{p_3^* \times 10^{1}}\left[\frac{°C}{kW\,day}\right]$	$\boldsymbol{p_4^* \times 10^{1}}\left[\frac{1}{day}\right]$	$\boldsymbol{p_5^* \times 10^{-1}}\left[\frac{1}{day}\right]$	$\boldsymbol{\sigma_r}$
Winter Data Set	9.42	-0.0	7.08	1.1	12.12	0.24
Spring Data Set	0.02	-0.0	3.7	0.72	27.22	0.33
Livingdown						
Winter Data Set	3.93	-0.0	7.4	1.2	9.53	0.2
Spring Data Set	1.22	1.75	4.8	1.01	-0.0	0.28
Main						
Winter Data Set	-0.0	-0.0	2.43	0.51	7.5	0.26
Spring Data Set	4.53	-0.0	3.44	1.71	4.7	0.34
Studio						
Winter Data Set	2.76	0.82	5.9	2.76	9.84	0.29
Spring Data Set	1.99	1.41	2.59	1.27	-0.0	0.21

Figure 5.3 show that the model estimates $\phi(p^*)$ track the measurements y. For these model estimates the optimal parameter p_2^* was zero. The temperature of the inertia thermal mass T_I stays within the lower and upper peaks of the temperature fluctuations. The distribution of r has a Gaussian form and has lower and upper values at approximately ± 0.4 °C.

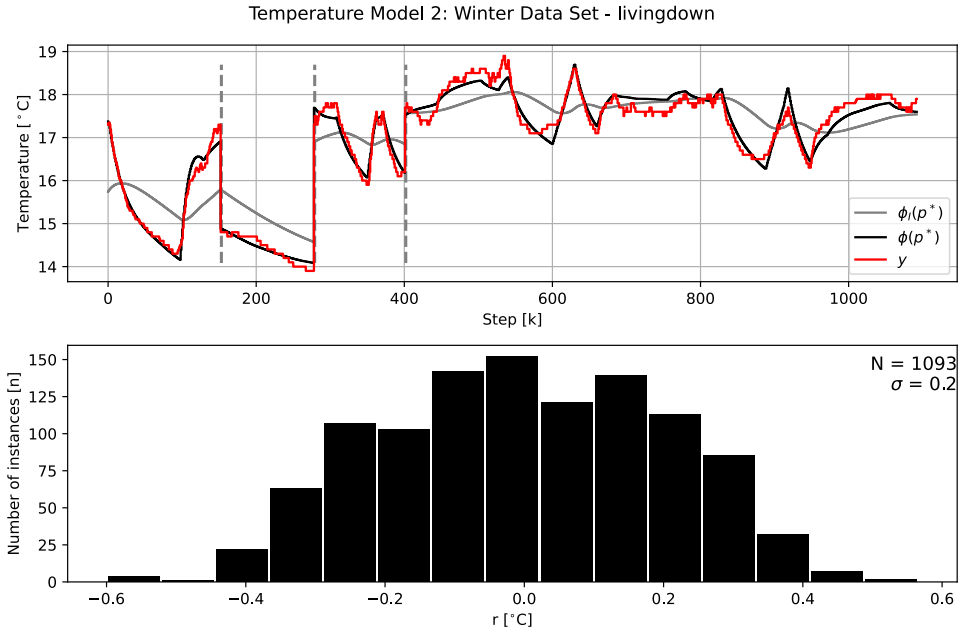

Figure 5.3: *Upper plot compares the optimal model trajectory in black with the temperature measurements in red of Winter Data Set - livingdown. The grey solid trajectory illustrates the temperature of the inertia thermal mass, while the grey vertical dotted lines mark gaps in the time series of over five minutes. The lower plot illustrates the distribution of the residual.*

Figure 5.4 shows that the model estimates $\phi(p^*)$ follow y, with a few exceptions. At some periods, such as at time step 500, the measured room temperature suddenly peaks. These peaks is synchronous with the temperature rise in figure C.8 given in Appendix C.2. This model also has an optimal parameter p_2 equal to zero. The distribution of r has a somewhat Gaussian form, but is clearly impacted by the peaks of disturbance.

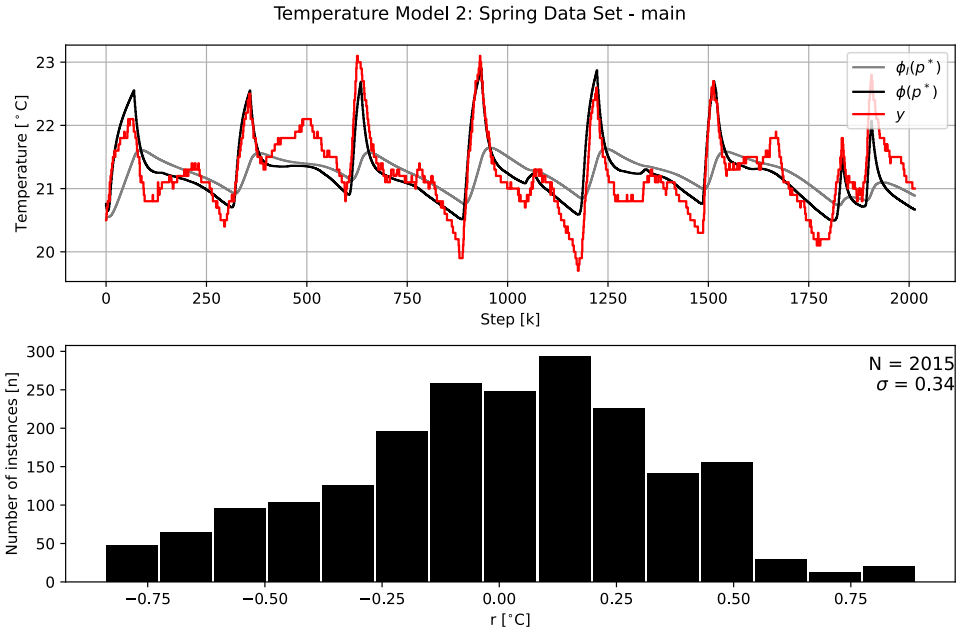

Figure 5.4: *Upper plot compares the optimal model trajectory in black with the temperature measurements in red of Spring Data Set - main. The grey solid trajectory illustrates the temperature of the inertia thermal mass, while the grey vertical dotted lines mark gaps in the time series of over five minutes. The lower plot illustrates the distribution of the residual.*

Figure 5.5 shows that the model estimates $\phi(p^*)$ track the temperature measurements y. None of the optimal parameters of this model was equal to zero. The distribution of r is a bit shifted to the right, caused by a period around time step 500 to 800 where the estimates are significantly greater than the measurements.

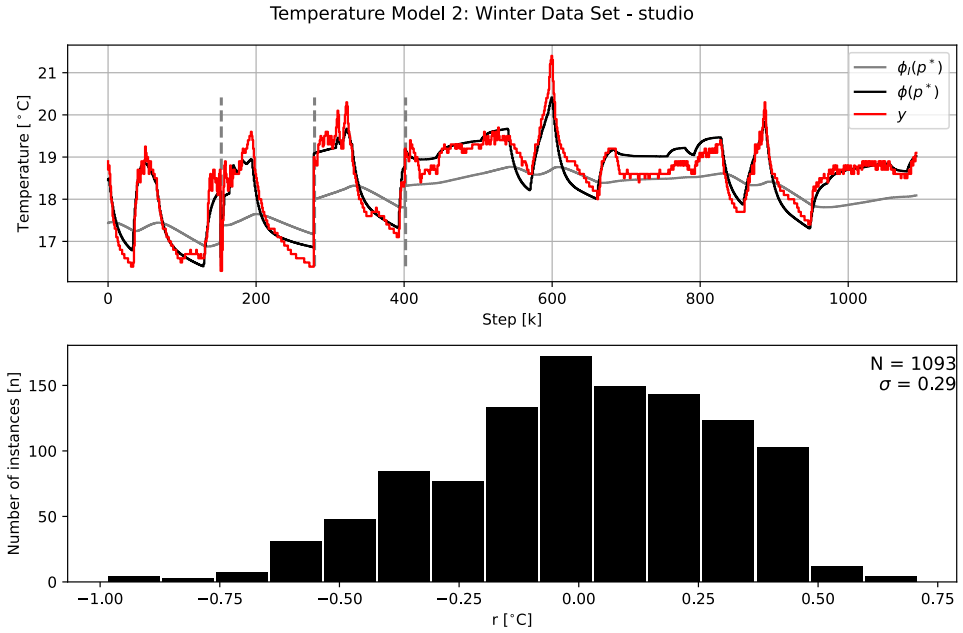

Figure 5.5: *Upper plot compares the optimal model trajectory in black with the temperature measurements in red of Spring Data Set - main. The grey solid trajectory illustrates the temperature of the inertia thermal mass, while the grey vertical dotted lines mark gaps in the time series of over five minutes. The lower plot illustrates the distribution of the residual.*

5.2.3 Discussion

The fact that there were several optimal parameters p_2^* that were equal to zero may indicate two things. Firstly, it may indicate that the model has trouble identifying the behaviour of the system. Secondly, it may also indicate that the heat transfer between the inertia thermal mass and the outside air is negligible. This may be be caused by that the shell of the rooms is significantly less exposed to the outside air than to the rest of the house. In addition, the model already has a term that depends on the room temperature and outside temperature. A proposed new model may neglect the term containing p_2.

Both *living* and *main* experience this unexpected temperature rise that happened seven times and with a fixed interval. It may result from sun radiation as the data set time series of seven days. Both rooms may experience the same temperature rise as they are not physically separated, or they both have sun exposed windows. The house also contains a chimney, which may have been used at the time, causing the temperature peaks.

The parameter estimation of Winter Data Set - **studio** was the only estimation where the

optimal parameter vector p^* was greater than zero. The model tracked the measurements, and the inertia thermal mass was reasonable. Unfortunately, the other rooms and data set combinations could not identify the same behaviour that for this room and data set combination. Again, a new proposed model could neglect the p_2 term in order to identify all the parameters properly.

5.3 Temperature Model 3

Temperature Model 3 is based on Temperature Model 2 described in section 5.2. The difference between the two models is that Temperature Model 3 is neglecting the term that included the heat transfer between the inertia thermal mass and the outside air. The main reason for this is that the previous parameter estimations did not recognize that behaviour of the system, leaving the associated parameter equal to zero.

Temperature Model 3 is given by equation 5.8, where the inertia thermal mass of the room in time step k is given as $T_{I,k}$. The rate of change of the inertia thermal mass $\Delta T_{I,k}$ depends on the temperature difference between the inertia thermal mass and the temperature of the air in the room and the parameter p_1, which includes the convection coefficient, the heat capacity and the physical dimensions.

The rate of change in the room temperature depends on three terms, see equation 5.8c. The first term is providing heat from the HP heat source that is proportional to the parameter p_2 and the estimated power P_{k-1}. The second term is the heat transfer between the room air and the thermal inertia of the room that is proportional to parameter p_3. The third term is modelling the heat transfer between the indoor and outdoor air. The parameter p_4 contains the conductivity, convection coefficient, the heat capacity and the physical properties of the walls, windows, ventilation, etc. All parameters are defined as positive as of The Second Law of Thermodynamics and Newton's Law of Cooling.

$$\Delta T_{I,k} = p_1 \left(T_{k-1} - T_{I,k-1}\right) \tag{5.8a}$$

$$T_{I,k} = T_{I,k-1} + \Delta T_{I,k}\, \Delta t_k \tag{5.8b}$$

$$\Delta T_{mod3,k} = p_2\, P_{k-1}(T_{ref,k-1}, T_{k-1}, on) + p_3 \left(T_{I,k-1} - T_{k-1}\right) + p_4 \left(T_{out,k-1} - T_{k-1}\right) \tag{5.8c}$$

$$T_{mod3,k} = T_{k-1} + \Delta T_{mod3,k}\, \Delta t_k \tag{5.8d}$$

5.3.1 Parameter Estimation Problem

The parameter estimation of Temperature Model 3 is based on the general optimization problem described in section 3.4. Since the model is dynamic, its problem can be described by equation 3.3 where y_k is the temperature measurements from the data sets.

The model state trajectory is defined in the constraints in equation 3.3d, where

$$\phi_k = f_k(p, z_k, \phi_{k-1}) = T_{mod3,k}(p, z_k, \phi_{k-1}), \tag{5.9}$$

where ϕ_{k-1} is the model estimates in previous time step k-1. This input makes the trajectory continuous. The input state and parameter vectors z_k and p is defined as

$$z_k = [T_{ref,k-1}, T_{out,k-1}, T_{k-1}, T_{I,k-1}, on, \Delta t_k], \tag{5.10a}$$

$$p = [p_1, p_2, p_3, p_4]. \tag{5.10b}$$

All of the parameters are constrained to be positive, hence $i = [1, 2, 3, 4]$ in equation 3.3e. The initial temperature of both the inertia heat mass $T_{I,gap}$ and the room air temperature $T_{I,gap}$ are calculated by the solver to find the optimal temperature.

5.3.2 Parameter Results

The parameter estimation results of Temperature Model 2 are summarised in table 5.3. The table includes the parameter p^* at the solution and the standard deviation σ_r of the residual r for each room and data set combination. The resulting trajectories and residual

distribution presented in this section is for *living - Spring Data Set*, *livingdown - Winter Data Set*. The remaining rooms and data set combinations are presented in Appendix C.3.

Table 5.4 that two parameters were equal to zero: p_4^* of Spring Data Set - *livingdown* and p_1^* of Winter Data Set - *Main*. The remaining parameters are within reasonable range of each other. The lowest standard deviation is of Winter Data Set - *livingdown*. Each room has at least one optimal parameter vector that is positive.

Table 5.4: *The parameter estimation results of Temperature Model 3.*

Living	$\boldsymbol{p_1^*}\left[\frac{1}{day}\right]$	$\boldsymbol{p_2^* \times 10^1}\left[\frac{°C}{kW\,day}\right]$	$\boldsymbol{p_3^* \times 10^1}\left[\frac{1}{day}\right]$	$\boldsymbol{p_4^* \times 10^{-1}}\left[\frac{1}{day}\right]$	$\boldsymbol{\sigma_r}$
Winter Data Set	9.42	7.08	1.10	12.1	0.24
Spring Data Set	6.89	5.42	2.07	15.6	0.48
Livingdown					
Winter Data Set	3.93	7.40	1.20	9.53	0.20
Spring Data Set	0.110	4.49	0.910	-0.00	0.32
Main					
Winter Data Set	-0.00	2.43	0.510	7.50	0.26
Spring Data Set	4.53	3.44	1.71	4.70	0.34
Studio					
Winter Data Set	3.11	5.96	2.72	17.4	0.29
Spring Data Set	1.69	2.34	1.20	7.33	0.29

Figure 5.6 shows that the optimal model estimates trajectories $\phi(p^*)$ are tracking the measurements y, with some exceptions. There are some peaks of temperature that the model do not manage to identify at approximately time step 200, 500, 1400 and 1600. The inertia thermal mass temperature T_I trajectory is lagging behind $\phi(p^*)$ throughout the time series. The distribution of the residual r has a Gaussian form.

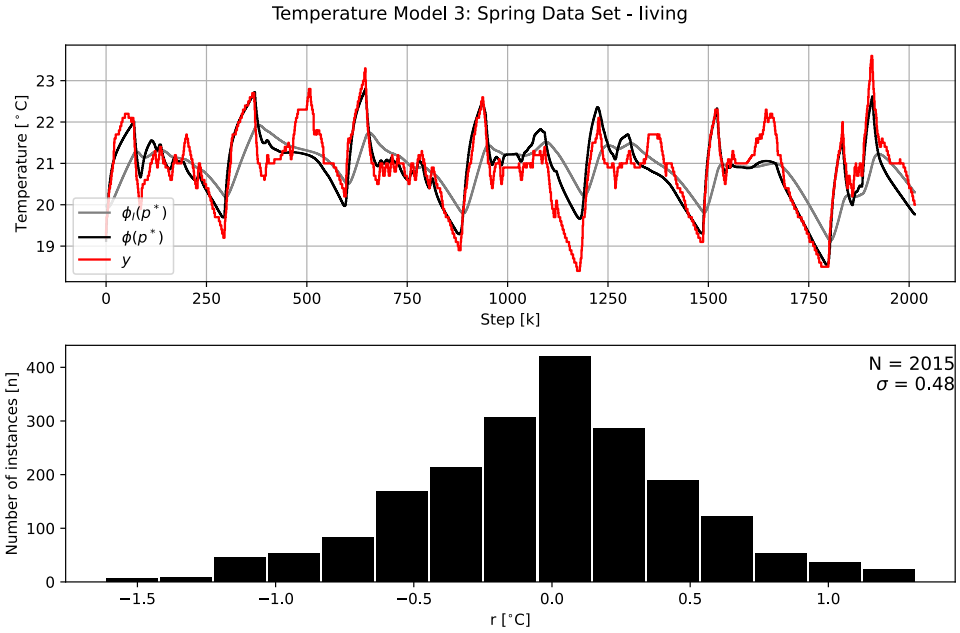

Figure 5.6: *Upper plot compares the optimal model trajectory in black with the temperature measurements in red of Spring Data Set - living. The grey solid trajectory illustrates the temperature of the inertia thermal mass. The lower plot illustrates the distribution of the residual.*

Figure 5.7 shows that the optimal model estimates $\phi(p^*)$ track the temperature measurements y. The inertia thermal mass temperature is approximately at the mean of the room temperature fluctuations. The distribution of the residual r has a Gaussian form with edges at approximately ± 0.4 °C.

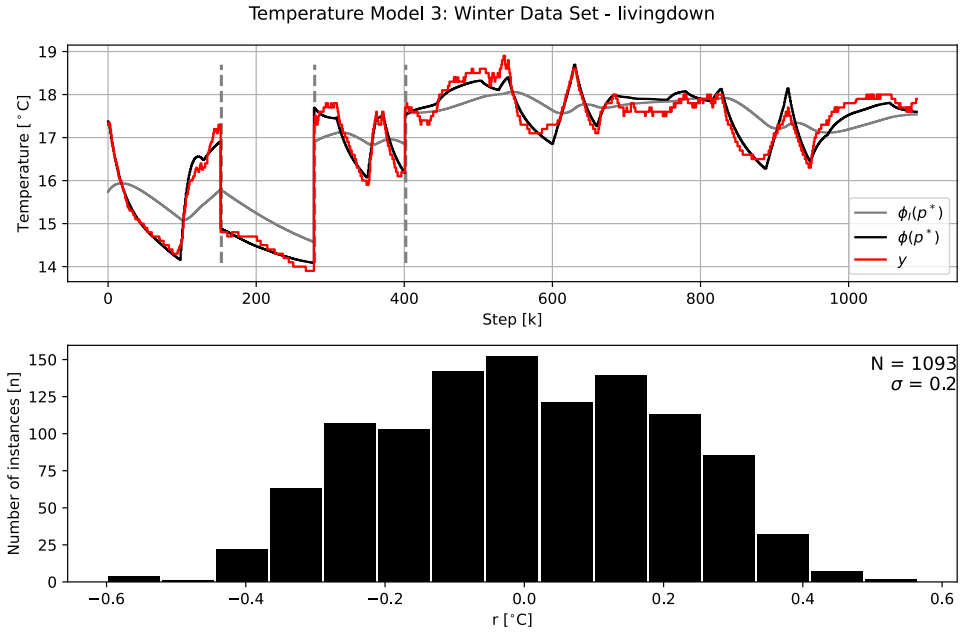

Figure 5.7: *Upper plot compares the optimal model trajectory in black with the temperature measurements in red of Winter Data Set - livingdown. The grey solid trajectory illustrate the temperature of the inertia thermal mass, while the grey vertical dotted lines mark gaps in the time series of over five minutes. The lower plot illustrates the distribution of the residual.*

The resulting trajectory of Spring Data Set *main* and *studio*(figures C.15, C.16 and C.17) also got similar behavior as presented in this section. From Winter Data Set - *living* the initial temperature of the thermal inertia was higher than of the other parameter estimation results. The model trajectories of Spring Data Set *livingdown* and Winter Set *main* was different from the others as one of the parameters in the model where equal to zero.

5.3.3 Discussion

Compared to Temperature Model 2, it seems that the parameter estimation of Temperature Model 3 identified the system behavior in a better way, as more of the parameters were greater than zero and relatively consistent. As the thermal inertia temperature is within the fluctuations of the room temperature, the second order transient response is as desired. Indications of that the model is capable of replicating the system behaviour is that the distribution of the residual has an approximate Gaussian form.

As discussed in section 5.2 the reason for the unexpected peaks of the measured temperature in the results of Spring Data Set in *living* and *main* could be from an

unknown heat source that may be from sun exposed windows. The rooms are not physically separated, which could be the reason for the rooms to experience the same temperature peaks. The house also contains a chimney, which may have been used at the time, causing the temperature peaks.

The initial temperature of the thermal inertia was usually within a mean of the modelled room temperature, which is reasonable, as it is supposed to replicate an inertia of the air mass. However, the result of Winter Set *living* had two initial values of the inertia temperature were it was a bit higher than the room temperature. This could be for two reasons. One reason could be that the temperature was descending from previous time period. A more likely explanation, may be that the initial temperature of the thermal inertia was set this high in order to shift the room temperature up in order to fit the measurements better.

Before implementing this model in an MPC, more testing should be done. It could be advantageous to estimate the parameters over different seasons, as the parameters tends to be different from winter to spring. The model predictive capabilities should also be tested as it is important in an MPC.

6 Predictive Capability Review

It is of to analyze the predictive capabilities of a system model as this is their most important task in a Model Predictive Controller (MPC). The better a model can predict the states, the better the MPC will perform. This may lead to reduced costs and increased comfort in an MPC scheme with the objective of controlling the heat pumps with regard to the spot price market.

6.1 Models

The predictive capabilities of two combined power and temperature models are be analysed. The first model, M_1 consists of a combination of Power Model 2 from section 4.3 and Temperature Model 1 of section 5.1. The second model, M_2, consists of Power Model 2 and of Temperature Model 3 from section 5.3. Each model will has distinctive parameters, depending on which room they represent. Power Model 2 were chosen as it was used in the estimation of the parameters of the temperature models. Temperature Model 1 and 2 were chosen based on the results and discussions in sections 5.1 and 5.3.

M_1 is given by equation 6.1. The predicted power consumption $\hat{P}_{1,k}$ is calculated by equation 6.1a and 6.1b, while the predicted temperature in time step k is given by equation 6.1c and 6.1d. The power related parameters for each room $p_{1,1}$ and $p_{1,2}$ are given in table 5.1, while the temperature related parameters $p_{1,3}$ and $p_{1,4}$ are given in table 6.2. $P_{sat,k}$ is the saturation and non-negativity function given by equation 4.2.

$$\bar{P}_{1,k} = p_{1,1}\,(T_{ref,k} - T_{1,k}) + p_{1,2} \tag{6.1a}$$

$$\hat{P}_{1,k} = P_{sat,k}(\bar{P}_{1,k}) \tag{6.1b}$$

$$\Delta T_{1,k} = p_{1,3}\,\hat{P}_{1,k-1}(T_{ref,k-1}, T_{1,k-1}) + p_{1,4}\,(T_{out,k-1} - T_{1,k-1}) \tag{6.1c}$$

$$T_{1,k} = T_{1,k-1} + \Delta T_{1,k}\,\Delta t_k \tag{6.1d}$$

M_2 is given by equation 6.2, where the power related parameters $p_{2,1}$ and $p_{2,2}$ are the same as in M_1 and is given by table 5.1. The temperature related parameters $p_{2,3}$ to $p_{2,6}$ are given in table 6.3. Equation 6.2a and 6.2b, which originate from Power Model

2, calculate the predicted power $\hat{P}_{2,k}$ of time step k. Equations 6.2c-6.2f calculate the predicted temperature $T_{2,k}$ in time step k and are based on Temperature Model 3. $P_{sat,k}$ is the saturation and non-negativity function given by equation 4.2.

$$\bar{P}_{2,k} = p_{2,1}\,(T_{ref,k} - T_{2,k}) + p_{2,2} \tag{6.2a}$$

$$\hat{P}_{2,k} = P_{sat,k}(\bar{P}_{2,k}) \tag{6.2b}$$

$$\Delta T_{I,k} = p_{2,3}\,(T_{2,k-1} - T_{I,k-1}) \tag{6.2c}$$

$$T_{I,k} = T_{I,k-1} + \Delta T_{I,k}\,\Delta t_k \tag{6.2d}$$

$$\Delta T_{2,k} = p_{2,4}\,P_{2,k-1}(T_{ref,k-1}, T_{2,k-1}) + p_{2,5}\,(T_{I,k-1} - T_{2,k-1}) + p_{2,6}\,(T_{out,k-1} - T_{2,k-1}) \tag{6.2e}$$

$$T_{2,k} = T_{2,k-1} + \Delta T_{2,k}\,\Delta t_k \tag{6.2f}$$

There are two true state trajectories that are input to the simulations. The first is the outdoor temperature, that in an MPC scheme would be known through weather forecasts. The second state vector is the reference temperature, which would be calculated by the MPC. Other than the initial temperature, the remaining states are estimated by the power and temperature models.

6.2 Parameters

As M_1 and M_2 consist of Power Model 2 they both use the same parameters and are given in table 6.1. These are the same parameters that were used in the parameter estimation of the temperature models.

Table 6.1: *Power Model parameters originating from the parameter estimation of Power Model 2 used in M_1 and M_2.*

Rooms	$\boldsymbol{p_{i,1} \times 10^1 \left[\frac{kW}{^\circ C}\right]}$	$\boldsymbol{p_{i,2} \times 10^1 [kW]}$
Living	1.28	3.98
Livingdown	0.80	3.53
Main	1.35	4.35
Studio	1.42	9.65

The temperature related parameters of M_1 are given in table 6.2. These parameters originate from the previous parameter estimation of Temperature Model 1. The decision of utilizing these parameters is based on the discussions in section 5.1.3, with the purpose of developing accurate predictive models.

Table 6.2: *Parameters of Temperature Model 1 used in the simulation.*

Rooms	$\boldsymbol{p_{1,3}}\left[\frac{°C}{kW\ day}\right]$	$\boldsymbol{p_{1,4}}\left[\frac{1}{day}\right]$
Living	35.4	0.617
Livingdown	35.3	0.448
Main	17.2	0.438
Studio	11.8	0.359

The temperature related parameters of M_2 are given by table 6.3. These parameters originate from the previous parameter estimation of Temperature Model 3. The decision of utilizing these parameters is based on the discussions in section 5.3.3, with the purpose of developing accurate predictive models.

Table 6.3: *Parameters of Temperature Model 3 used in the simulation.*

Rooms	$\boldsymbol{p_{2,3}}\left[\frac{1}{day}\right]$	$\boldsymbol{p_{2,4}} \times \mathbf{10^1}\left[\frac{°C}{kW\ day}\right]$	$\boldsymbol{p_{2,5}} \times \mathbf{10^1}\left[\frac{1}{day}\right]$	$\boldsymbol{p_{2,6}} \times \mathbf{10^{-1}}\left[\frac{1}{day}\right]$
Living	9.42	7.08	1.10	12.1
Livingdown	3.93	7.40	1.20	9.53
Main	4.53	3.44	1.71	4.70
Studio	3.11	5.96	2.72	17.4

6.3 Simulation Results

The simulations were done on a test data set that are from a different time period than the system identification data sets. This is to prevent potential overfitting. The time horizon of the simulations was set to 35 hours. This is the longest horizon of the known spot price. The shortest horizon for known spot prices is 11 hours. It can be argued that for a use in an MPC the predictive capability performance of the models is more relevant at shorter horizons than 35 hours. However, by utilizing longer simulations, more valuable

information on whether the models can predict different scenarios can be analysed, even though it loses track of the measured state trajectory by an accumulated error.

The saturation effect of *Unit 2* is included in this simulation. If the indoor heat pump units of *Unit 2* requests more power than 2.5 kW, the power is restricted. An even proportion of the power of the indoor units is then reduced such that the total power consumption is equal to the saturation level. The saturation level of 2.5 kW is found in section 3.3.

The starting inertia temperature of Model 2 is set to the previous mean temperature in the room. This is done based on the behaviour observed on the parameter estimation and the illustrations of the inertia temperature of the room.

6.3.1 Power

The power prediction of Model 1 and Model 2, $\hat{P}_1$ and $\hat{P}_2$ is based on the same power model, but is receiving different input temperatures. As seen from figure 6.1 the two models do not deviate significantly from each other. They start off by being approximately 1 kW higher than the measured power y_P. After about 1 hour, the three trajectories are approximately the same, and both models predict the drop in power consumption after 3 hours. The models keep tracking y_P until about 7 hours, where y_P peaks at 2 kW and shortly after drops to slightly above 0 kW. Meanwhile, $\hat{P}_1$ and $\hat{P}_2$ predict a relatively stable power consumption at 1 kW. Between 10 and 15 hours the models predict a power that seems to be slightly below the mean y_P fluctuations. From 15 to 29 hours the models track y_P. However, between 29 and until the end of the simulation, y_P is at zero before it peaks at almost 3 kW, while the models predict a power consumption of slightly above zero, followed by a peak at 1 kW.

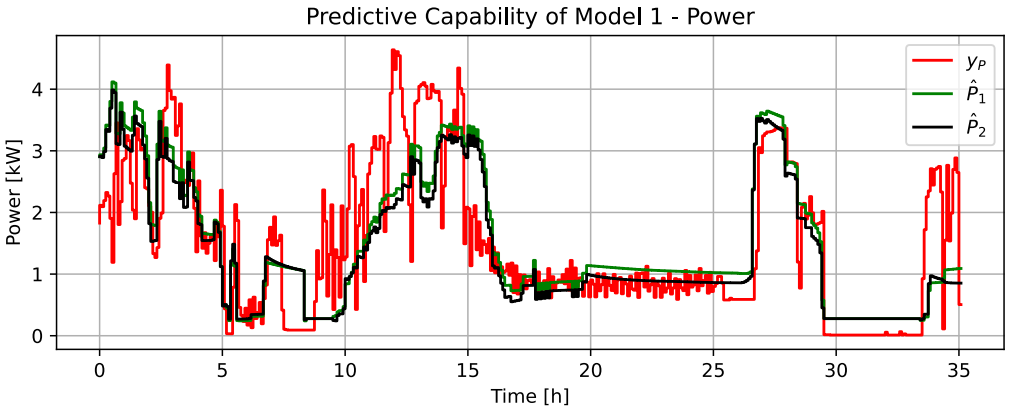

Figure 6.1: *The predictive capabilities of power by M_1 in green and M_2 in black, compared to the measured power y_P in red.*

6.3.2 Living

The temperature predictive capabilities of the models of room living are illustrated by figure 6.2, where T_1 is the estimated temperature of M_1 and T_2 is the estimated temperature of M_2. During the three first hours of the simulation, both models track the measured room temperature y_T. The following hours, until about 7 h, y_T drops down to 19 °C with some smaller peaks. The two models predict the peaks (T_1 with smaller amplitude), but drop to 21.1 and 21.7 °C.

Between 7-12 h there is a bigger peak in temperature followed by a temperature drop. y_T rises from approximately 1 °C, the same as T_1 predicts, while T_2 predict an increase of about 2 °C. The amplitude of the drop of y_T is slightly above 2 °C, T_1 slightly less than 2 °C and T_2 approximately 2.5 °C.

Between 12-27 h y_T increases gradually with some minor peaks. The models predict approximately the same through this period, correctly predicting some of the minor peaks. However, the temperature does not rise with the same magnitude of y_T. After 27 h, y_T drops about 3 °C, T_1 drops about the same, while T_2 drops almost 4 °C.

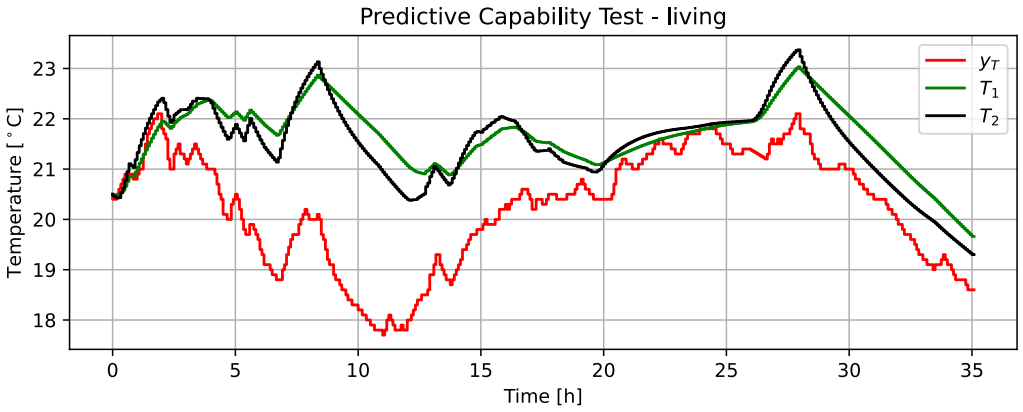

Figure 6.2: *The predictive capability test of the temperature of M_1 and M_2 in living. The temperature estimation of Model 1 T_1 in green and the temperature estimation of Model 2 T_2 in black are compared to the measured temperature of the room y_T.*

6.3.3 Livingdown

The temperature predictive capabilities of the models of room living are illustrated by figure 6.2, where T_1 is the estimated temperature of M_1 and T_2 is the estimated temperature of M_2. The first three hours of the simulation, T_2 is tracking the measured temperature y_T. T_1 has the same trend, but has a slower increase rate. Between 3-11 h the y_T drops 3 °C. T_2 mostly followed but decreased at a slower rate. T_1 shows a more linear decrease, and even at a lower rate than T_2, dropping 1 °C.

Between 11-16 h there was an increase of temperature. y_T changes approximately 3 °C, which is about the same as T_1 and T_2. After 16 hours, and until 27 hours there was an decrease in temperature. y_t dropped approximately 4 °C. Again, T_2 has the about the same trajectory form, but dropped slower than y_T. T_1 dropped more linearly and like T_2, it dropped approximately 3 °C.

From 27 hours and until the end of the simulation, y_T of *livingdown* showed an increase of almost 4 °C, followed by a drop of about 3 °C. T_1 has at the same time predicted both an increase and decrease of slightly above 1 °C. T_2 predicted an increase of 1.5 °C and a decrease of about 2 °C.

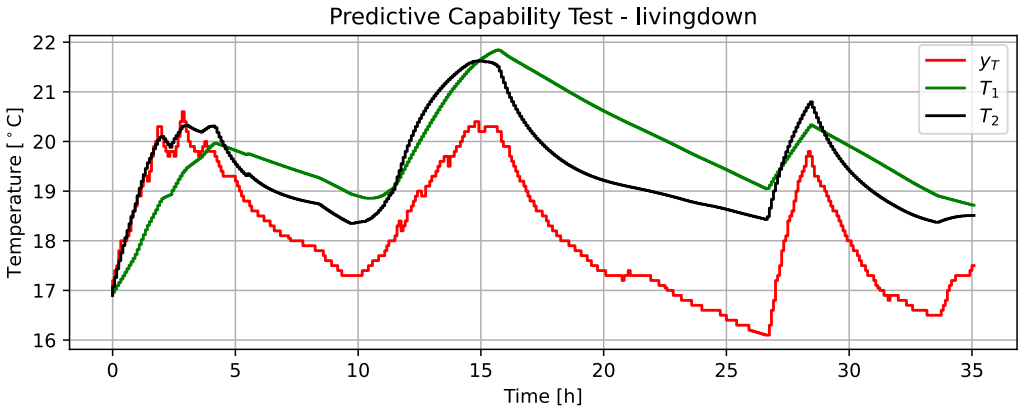

Figure 6.3: *The predictive capability test of the temperature of M_1 and M_2 in livingdown. The temperature estimation of Model 1 T_1 in green and the temperature estimation of Model 2 T_2 in black are compared to the measured temperature of the room y_T.*

6.3.4 Main

The temperature predictive capabilities of the models in room *main* are illustrated by figure 6.4, where T_1 is the estimated temperature of M_1 and T_2 is the estimated temperature of M_2. The first 10 hours of the simulation show that the three trajectories have three distinctive behaviours. The measured room temperature of *main* y_T first experienced a slight increase of temperature, before it dropped 2 °C. T_1 dropped 2.5 °C linearly, while T_2 dropped approximately 1 °C. Between 10-27 hours y_T experienced a period of 1.5 °C increase, followed by a period of stable temperatures. Both models predict an increase of 1 °C and is both stable like y_T. From 27 h until the end of the simulation, y_T dropped 1.5 °C, while T_1 dropped more than 2 °C, and T_2 dropped slightly less than 1 °C.

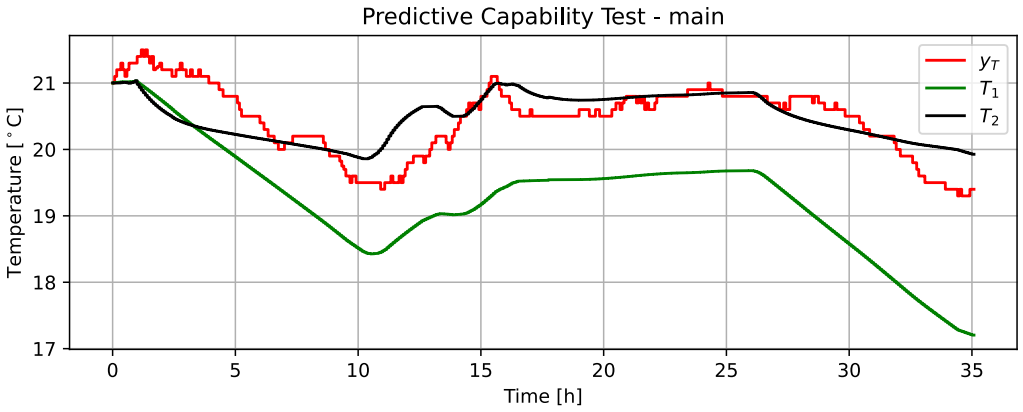

Figure 6.4: *The predictive capability test of the temperature of M_1 and M_2 in main. The temperature estimation of Model 1 T_1 in green and the temperature estimation of Model 2 T_2 in black are compared to the measured temperature of the room y_T.*

6.3.5 Studio

The temperature predictive capabilities of the models of room studio are illustrated in figure 6.5, where T_1 is the estimated temperature of M_1 and T_2 is the estimated temperature of M_2. The first 5 hours of the simulation showed that the different models have distinctive behaviour. The increase of T_1 is more linear than T_2, which has more similar trajectory form to the measured temperature of studio y_T. T_1 and T_2 are predicting 0.5 and 1 °C higher than y_T at 5 hours. The next five hours, until 10 h, the measured temperature dropped 2 °C. Meanwhile, T_1 dropped 1 °C linearly and T_2 dropped 2.5 °C with the same transient response as y_T.

Between 10-15 h y_T increased by 2 °C. T_2 predicted approximately the same increase with the same form of the trajectories. T_1 is at the same time a little off with an increase of approximately 1 °C. From about 16 h to 27 h there is a decrease of temperature. Again, T_2 and y_T have similar magnitude of the change and with same transient response. The last part of the simulation, from 27 to 35 h, T_2 and y_T showed the same transient response, while T_1 had less magnitudes, and was linear.

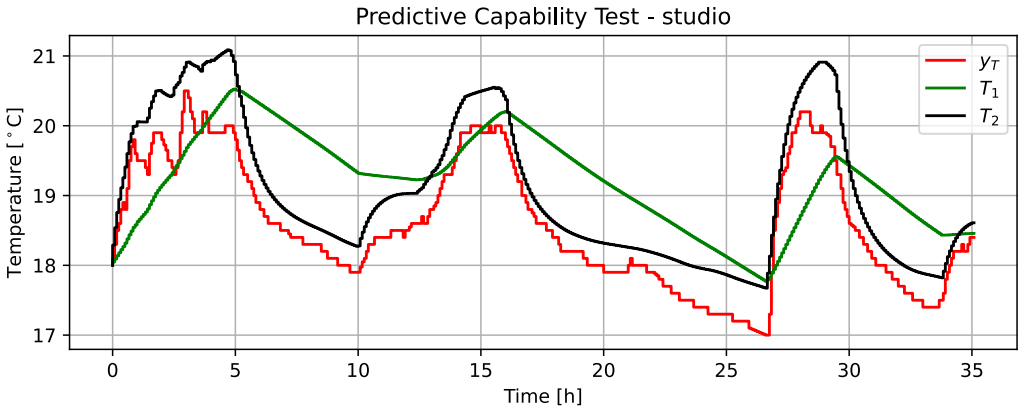

Figure 6.5: *The predictive capability test of the temperature of M_1 and M_2 in studio. The temperature estimation of Model 1 T_1 in green and the temperature estimation of Model 2 T_2 in black are compared to the measured temperature of the room y_T.*

6.4 Discussion

The analyses of the predictive capability test of both models, show that they perform relatively good by predicting the power consumption of the heat pumps. The biased proportional controller based model seems to identify the most significant triggering factors and characteristics of the system. Even though the measured power fluctuated more, the models stayed at an approximate mean, which is important in an hourly priced based MPC. However, as the results show, there are some periods where the error between the model and measurements is up to 2 kW.

The reason for any significant errors between the power prediction and the measured power can be of several reasons. One can argue that the accumulated temperature error in each rooms gets larger and this will impact the power prediction error. However, in the start of the simulation, both models predicts 1 kW too high power consumption when the temperature error of each room is minimal. It is hard to conclude what causes this deviation, but it may be that the power model is not able to identify a triggering factor in that specific scenario.

As the known power consumption is for the whole system combined and not for each unit isolated, it is hard to identify and analyze the performance of the model and associated parameter for each room. It may be that the models and parameters chosen are more

suitable for one room than another. However, the magnitude of the individual error of each room should be constrained by the saturation and non-negativity properties of the models. One indicator of how the power model performs in each room could be found by analyses of the temperature dynamics in each room.

The Predictive Capability Test of *living* illustrated that the temperature estimation by Model 1 and Model 2 was relatively equal. The most noticeable deviation was that Model 1 was more linear and slower. The transient responses of the measured temperature was more equal to the estimated temperature of Model 2. This is due to the inertia term from Temperature Model 3.

Both models struggled to predict the rate of the first temperature drop in the trajectory of figure 6.2, causing a large prediction error. However, they were more accurate during other temperature changes in the same time series. The cause of the error may be that the model parameters were not tuned for that scenario, or it could be caused by some external properties not factored in the model. Such a factor could be that some of the heat being transported to the room *main*. As observed by the early stages of *main*, the temperature increased, while the models predicted a decrease. The temperature dynamic of *living* and *main* may also have affected each other. The rise of temperature could also have been caused by sun radiation through windows.

The Predictive Capability Test of *livingdown* illustrated clearly the differences of the two models. Due to the temperature inertia term in Model 2, the transient response of the temperature was similar to the measured one. This means that Model 2 and its parameters related to both power and temperature, replicate the real system to a certain extent. Both models did accumulate some prediction error, estimating too high temperatures. This could be that the parameters scaling the heat loss should be higher, or the parameters scaling the heat pump power effect should be lower for this scenario. Model 1 did replicate the system behavior to some degree, but not as good as Model 2, as it was too linear in the transient responses.

The Predictive Capability Test of *main* had lower measured temperature fluctuations, spanning from slightly above 19 °C to slightly above 21 °C. It is interesting to see how well the model performs under more stable conditions, as this will most likely be the operation

scenario in use in an MPC of a household.

As previously discussed, the reason for the early peak of the measured temperature could be of heat being transported from the room of *living*, or it could originate from another source, such as the sun. After this peak, the prediction followed the measured temperature trajectory well. The predictions of Model 2 were more damped, but also followed the trends in the measured temperature.

The Predictive Capability Test of *studio* illustrates the different dynamics of the two models. Model 1 is more linear than Model 2 that includes the thermal inertia of the room. The transient response of Model 2 is very similar to the measured temperature trajectory. This means that the model and parameters are well suited for the system of this time period.

To verify if the models developed are sufficiently good for implementation in an MPC more testing should be done. This section only did one test, which may discover weaknesses and rule away models, but to verify if the models are sufficiently good, other scenarios from example different seasons should be done. Other combinations of the power and temperature model may also be analyzed. Another way to improve the models may be by choosing other parameters, and/or tuning them manually.

New models could also be proposed to achieve better accuracy. One could be where it is implemented a term that connects the heat mass of *living* and *main*, as it is a physical opening there. Another model could implement the COP factor in the temperature function, where the relation between the heat pump power and temperature changes depend on the outside and indoor air temperature. A model could also investigate if there is a relation between the unexpected temperature peaks in *living* and *main* is caused by sun radiation.

A source of error in the simulations done in this section could be that the initial temperature of the inertia heat mass is set equal to the mean temperature of the room. This is only a thought based on the parameter estimations, and may vary from room to room. By running the model on the previous historic data, one could find a more likely starting temperature.

7 Conclusion

By the predictive capability tests completed, it is Model 2, which is a combination of Power Model 2 and Temperature Model 3, that perform best, especially regarding the temperature prediction, replicating the transient response in the rooms *livingdown* and *studio*. As Model 2 is only tested on one data set, it is too early to conclude whether it would perform well if implemented in an MPC driven system. There are some weaknesses with the model that need to be further investigated, as there are some unknown factors that lead to prediction error in both the power prediction and the temperature predictions.

Model 1, by the predictive capability tests done, does not replicate the system behaviour as accurate as Model 2. As the model does not consider thermal inertia, the transient response was more linear then the system behaviour. As this model contains Temperature Model 1, it is not recommended to use that model in an MPC.

Power Model 4, which is a proportional-integrator controller based model, performed well by the parameter estimation results. It managed to identify some of the faster fluctuations of the power measurements. This model is a good candidate for implementation in future model combinations of the system.

Temperature Model 2 is also a good candidate for future models. However, by the parameter estimation of this thesis, it struggled to identify a consistent behaviour for all the rooms. The one room where all of the parameters where found to be greater than zero gave good results.

8 Further Work

There is a potential for improvement of both parameter estimation and model developing for this project. Based on the results and experiences of working with this thesis, following future tests are proposed:

- Run several predictive capability tests with different starting points and investige statistical errors at different future times.
- Investigate heat transfers between the different rooms
- Investigate the impact of sun radiation
- Investigate the impact of COP and season-varying parameter values
- Perform a parameter estimation of the entire system at once, and not each room individually. The results from the individual parameter estimates can be used as initial values

References

[1] *Aldri før har vi brukt mer strøm i Norge*. no. URL: https://www.statnett.no/om-statnett/nyheter-og-pressemeldinger/nyhetsarkiv-2021/aldri-for-har-vi-brukt-mer-strom-i-norge/ (visited on 02/09/2021).

[2] *Ny rekord i strømforbruket i dag*. no. URL: https://www.statnett.no/om-statnett/nyheter-og-pressemeldinger/nyhetsarkiv-2021/ny-rekord-i-stromforbruket-i-dag/ (visited on 02/09/2021).

[3] Statnett. *Langsiktig markedsanalyse, Norden og Europa 2020 - 2050*. URL: https://www.statnett.no/globalassets/for-aktorer-i-kraftsystemet/planer-og-analyser/langsiktig-markedsanalyse-norden-og-europa-2020-50_revidert.pdf.

[4] Norges vassdrags- og energidirektorat. "Elektrifiseringstiltak i Norge - Hva er konsekvensene for kraftsystemet?" In: (Oct. 2020). URL: https://publikasjoner.nve.no/rapport/2020/rapport2020_36.pdf.

[5] Statnett. *Fleksibilitet i det nordiske kraftmarkedet, 2018 - 2040*. URL: https://www.statnett.no/globalassets/for-aktorer-i-kraftsystemet/planer-og-analyser/2018-Fleksibilitet-i-det-nordiske-kraftmarkedet-2018-2040.

[6] *Antall elbiler og ladestasjoner i Norge*. nb-NO. URL: https://elbil.no/elbilstatistikk/ (visited on 02/12/2021).

[7] *Elbilbestand*. nb-NO. URL: https://elbil.no/elbilstatistikk/elbilbestand/ (visited on 02/12/2021).

[8] Hallgeir Horne. "Smarte ladesystemer og Vehicle-to-Grid". no. In: (), p. 3.

[9] Joel A E Andersson et al. "CasADi – A software framework for nonlinear optimization and optimal control". In: *Mathematical Programming Computation* 11.1 (2019), pp. 1–36. DOI: 10.1007/s12532-018-0139-4.

[10] Andreas Wächter and Lorenz T. Biegler. "On the implementation of an interior-point filter line-search algorithm for large-scale nonlinear programming". In: *Mathematical Programming* 106.1 (Mar. 1, 2006), pp. 25–57. ISSN: 1436-4646. DOI: 10.1007/s10107-004-0559-y. URL: https://doi.org/10.1007/s10107-004-0559-y (visited on 06/18/2021).

[11] Nord Pool. *Bidding areas*. URL: https://www.nordpoolgroup.com/the-power-market/Bidding-areas/ (visited on 01/20/2021).

[12] Nord Pool. *The main arena for trading power.* URL: https://www.nordpoolgroup.com/the-power-market/Day-ahead-market/ (visited on 01/21/2021).

[13] Nord Pool. *The Power Market.* URL: https://www.nordpoolgroup.com/the-power-market/ (visited on 01/25/2021).

[14] Forbrukervalget. *Forskjellen på spotpris, fastpris og variabel pris.* Strømvalget. URL: https://stromvalget.no/artikkel/1443/forskjellen-paa-spotpris-fastpris-og-variabel-pris (visited on 06/18/2021).

[15] *How does a heat pump work // Mitsubishi Electric.* URL: https://www.mitsubishi-electric.co.nz/heatpump/how.aspx (visited on 06/16/2021).

[16] Majid Ghassemi and Azadeh Shahidian. "Chapter 3 - Biosystems Heat and Mass Transfer". In: *Nano and Bio Heat Transfer and Fluid Flow.* Ed. by Majid Ghassemi and Azadeh Shahidian. Oxford: Academic Press, Jan. 1, 2017, pp. 31–56. ISBN: 978-0-12-803779-9. DOI: 10.1016/B978-0-12-803779-9.00003-0. URL: https://www.sciencedirect.com/science/article/pii/B9780128037799000030 (visited on 06/18/2021).

[17] Grady Hanrahan. "Chapter 3 - Aqueous Chemistry". In: *Key Concepts in Environmental Chemistry.* Ed. by Grady Hanrahan. Boston: Academic Press, Jan. 1, 2012, pp. 73–106. ISBN: 978-0-12-374993-2. DOI: 10.1016/B978-0-12-374993-2.10003-2. URL: https://www.sciencedirect.com/science/article/pii/B9780123749932100032 (visited on 06/20/2021).

[18] *Heat Capacity and Energy Storage — EARTH 103: Earth in the Future.* URL: https://www.e-education.psu.edu/earth103/node/1005 (visited on 06/20/2021).

[19] Jorge Nocedal and Stephen J. Wright. *Numerical optimization.* en. 2nd ed. Springer series in operations research. OCLC: ocm68629100. New York: Springer, 2006. ISBN: 978-0-387-30303-1.

Appendix A: System Identification Data Sets

This appendix contains illustrations of the data sets that are used for the model based parameter estimation. First, the power measurements are presented, then the reference and measured temperature are given. Finally, the heat pump setting "On/Off" and the outdoor temperature are presented. An overview of the data sets with time of start and end are given in table A.1.

Table A.1: *An overview of the intervals of the measurements associated with the various data sets.*

No. Data set	Start	End
1	2021-02-19 19:45	2021-02-20 08:35
2	2021-02-20 23:15	2021-02-21 09:45
3	2021-02-21 18:30	2021-02-22 04:45
4	2021-03-02 08:20	2021-03-04 18:00
5	2021-03-02 08:20	2021-03-04 18:00

A.1 Power

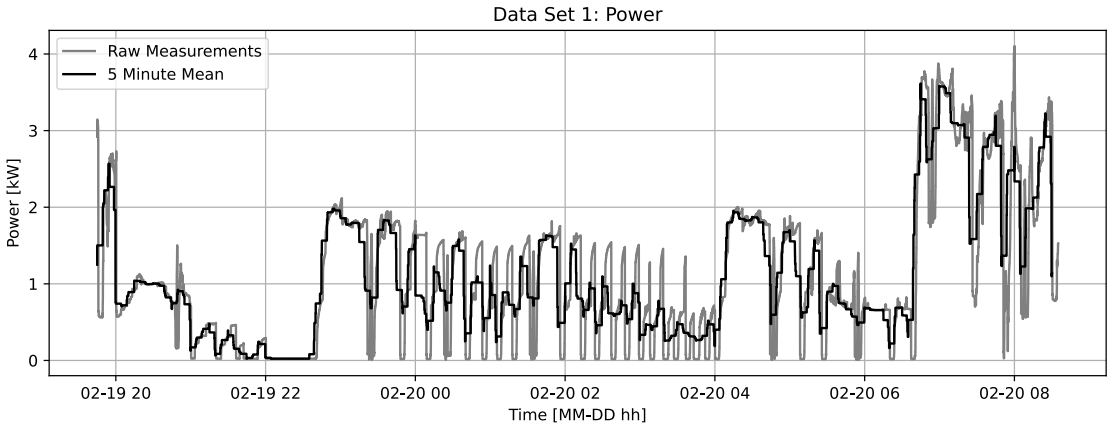

Figure A.1: *Raw and 5-minute mean power measurements of data set 1 used in the model based parameter estimation.*

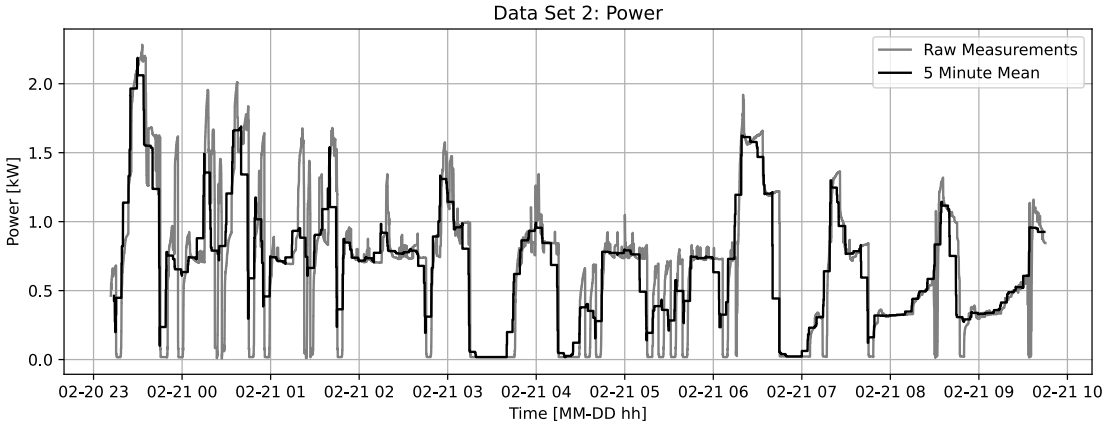

Figure A.2: *Raw and five-minute-mean power measurements of data set 2 used in the model based parameter estimation.*

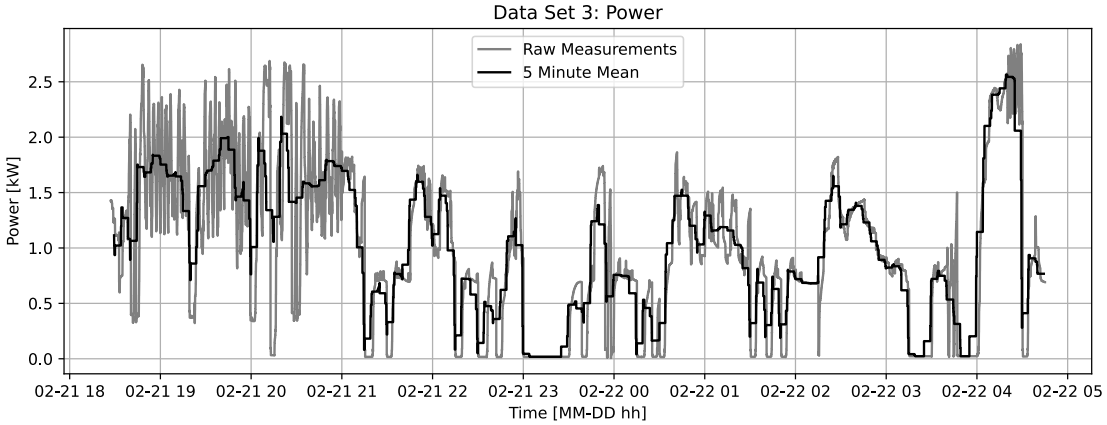

Figure A.3: *Raw and 5-minute mean power measurements of data set 3 used in the model based parameter estimation.*

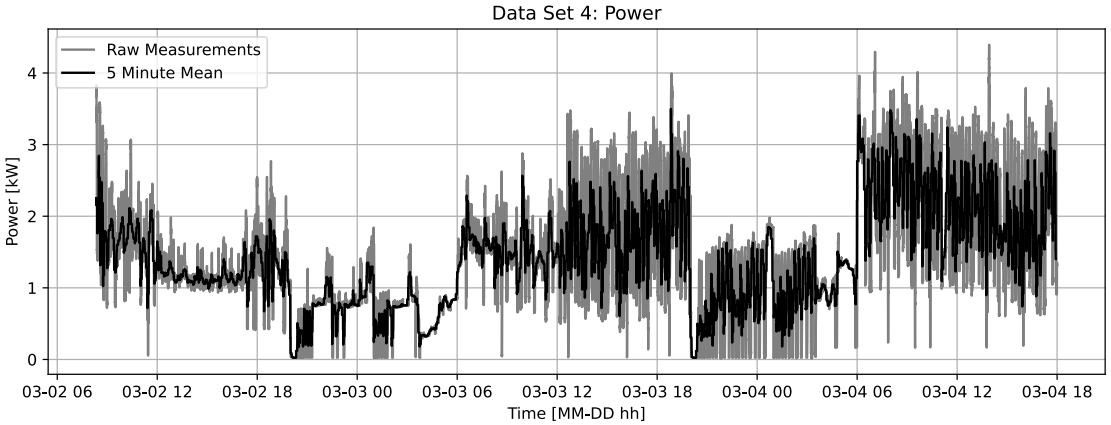

Figure A.4: *Raw and 5-minute mean power measurements of data set 4 used in the model based parameter estimation.*

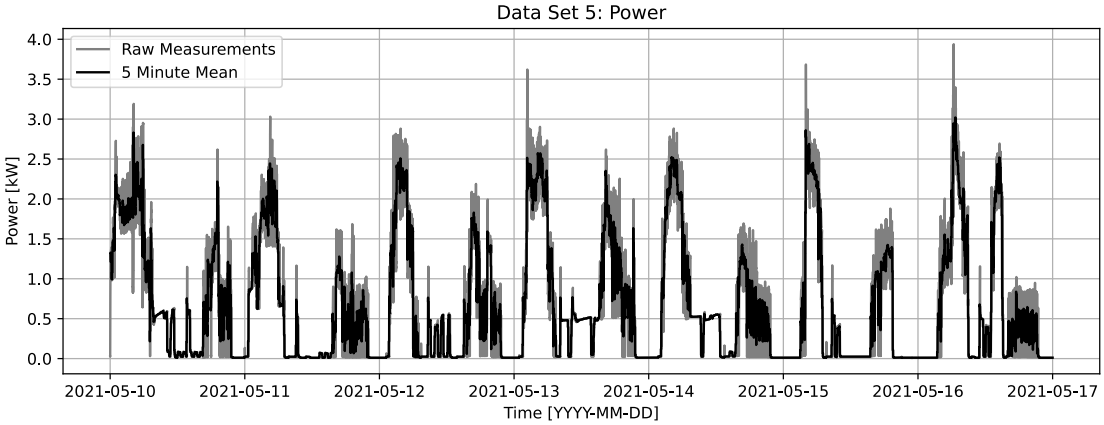

Figure A.5: *Raw and 5-minute mean power measurements of data set 5 used in the model based parameter estimation.*

A.2 Measured and Reference Temperature

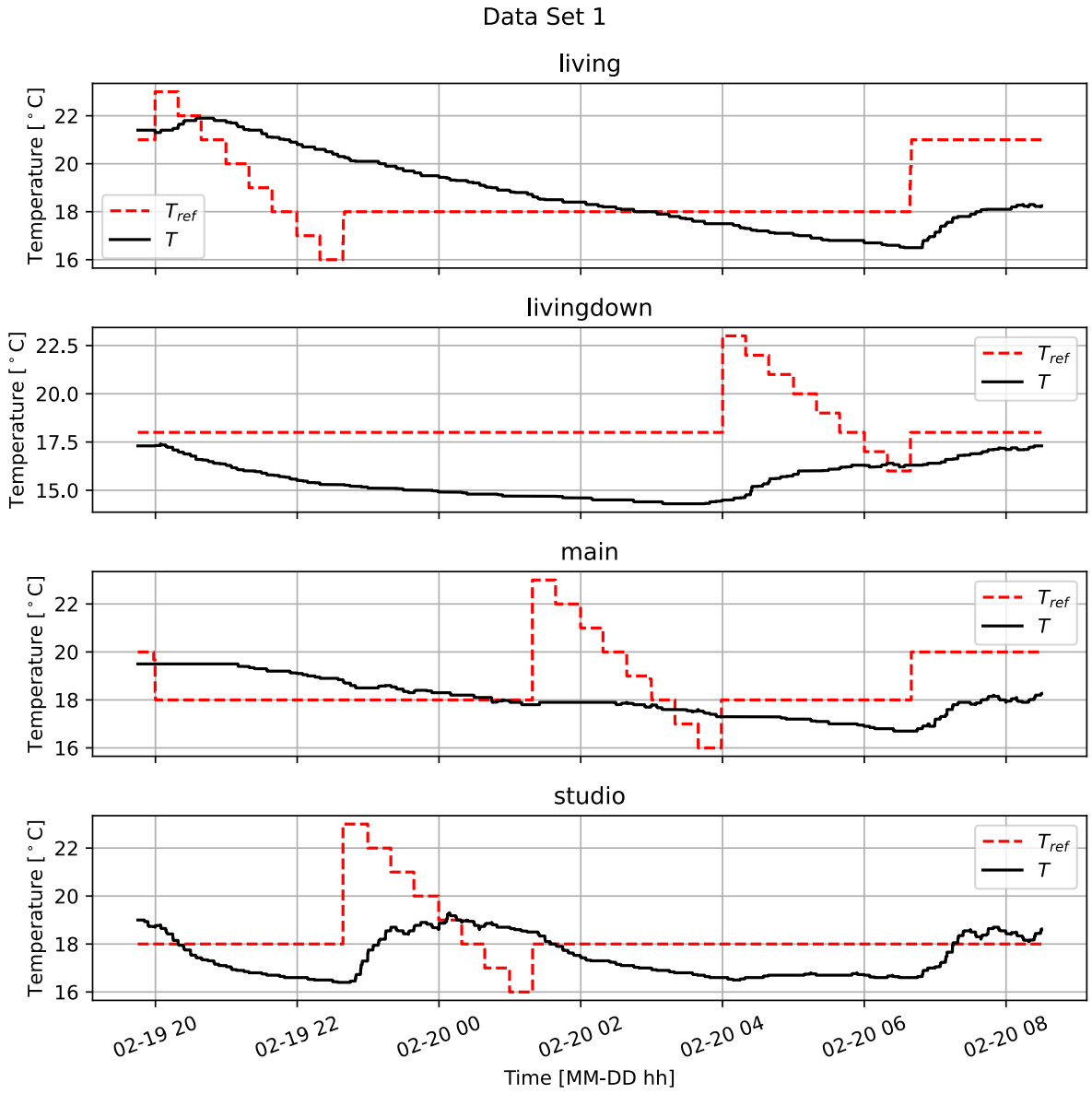

Figure A.6: *The reference temperature in stippled red and the measured temperature in black for each room from Data Set 1.*

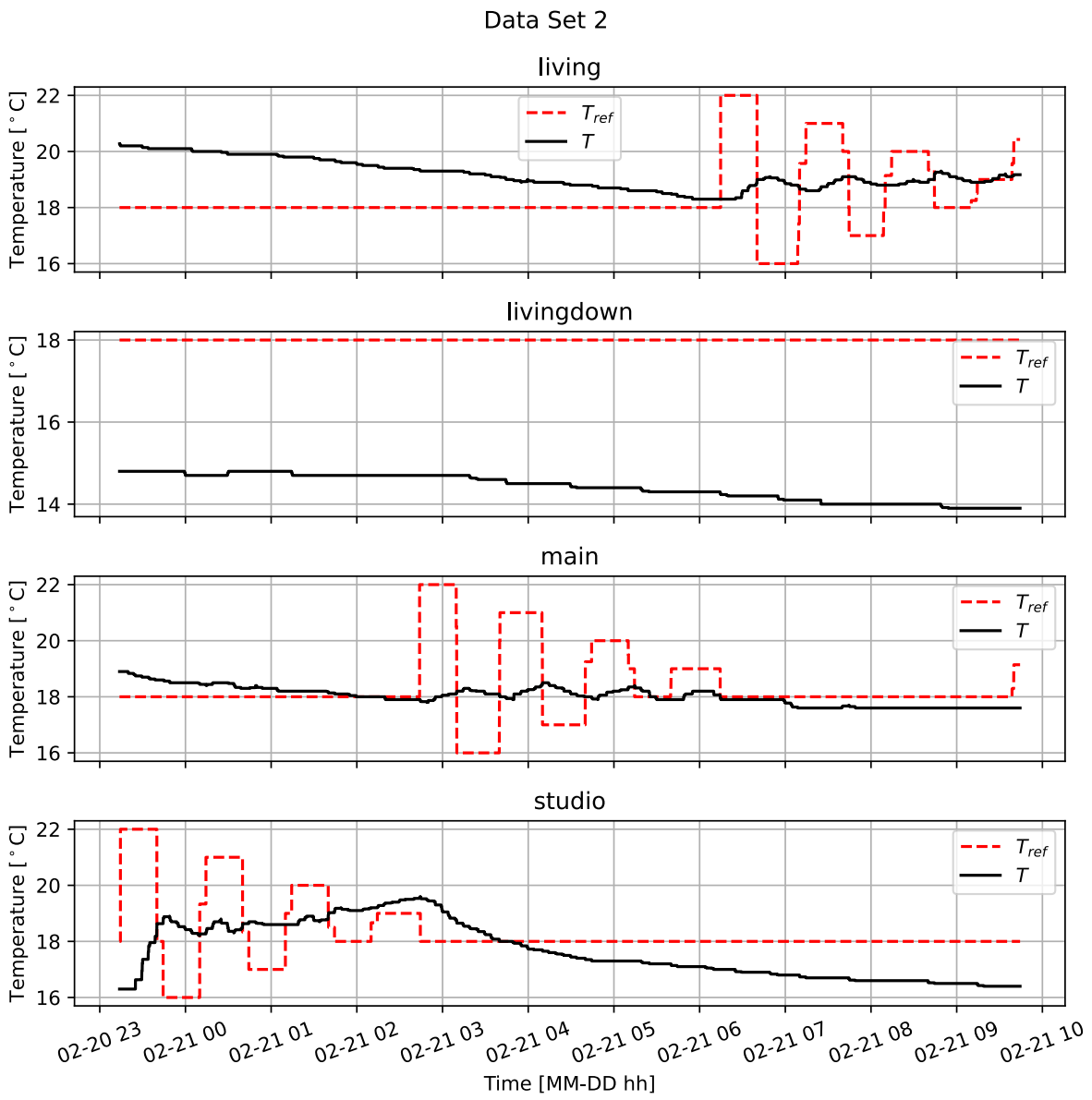

Figure A.7: *The reference temperature in stippled red and the measured temperature in black for each room from Data Set 2.*

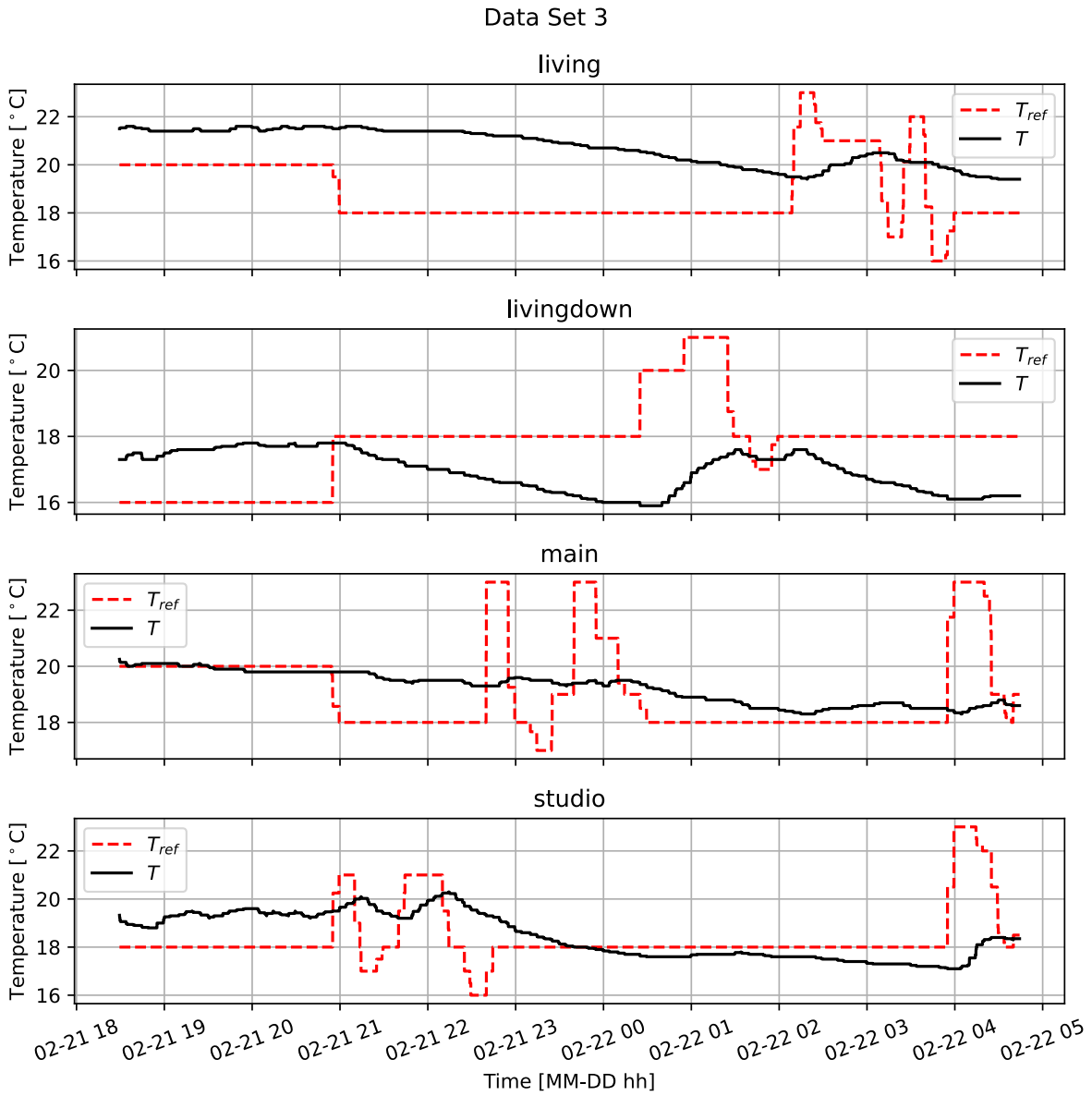

Figure A.8: *The reference temperature in stippled red and the measured temperature in black for each room from Data Set 3.*

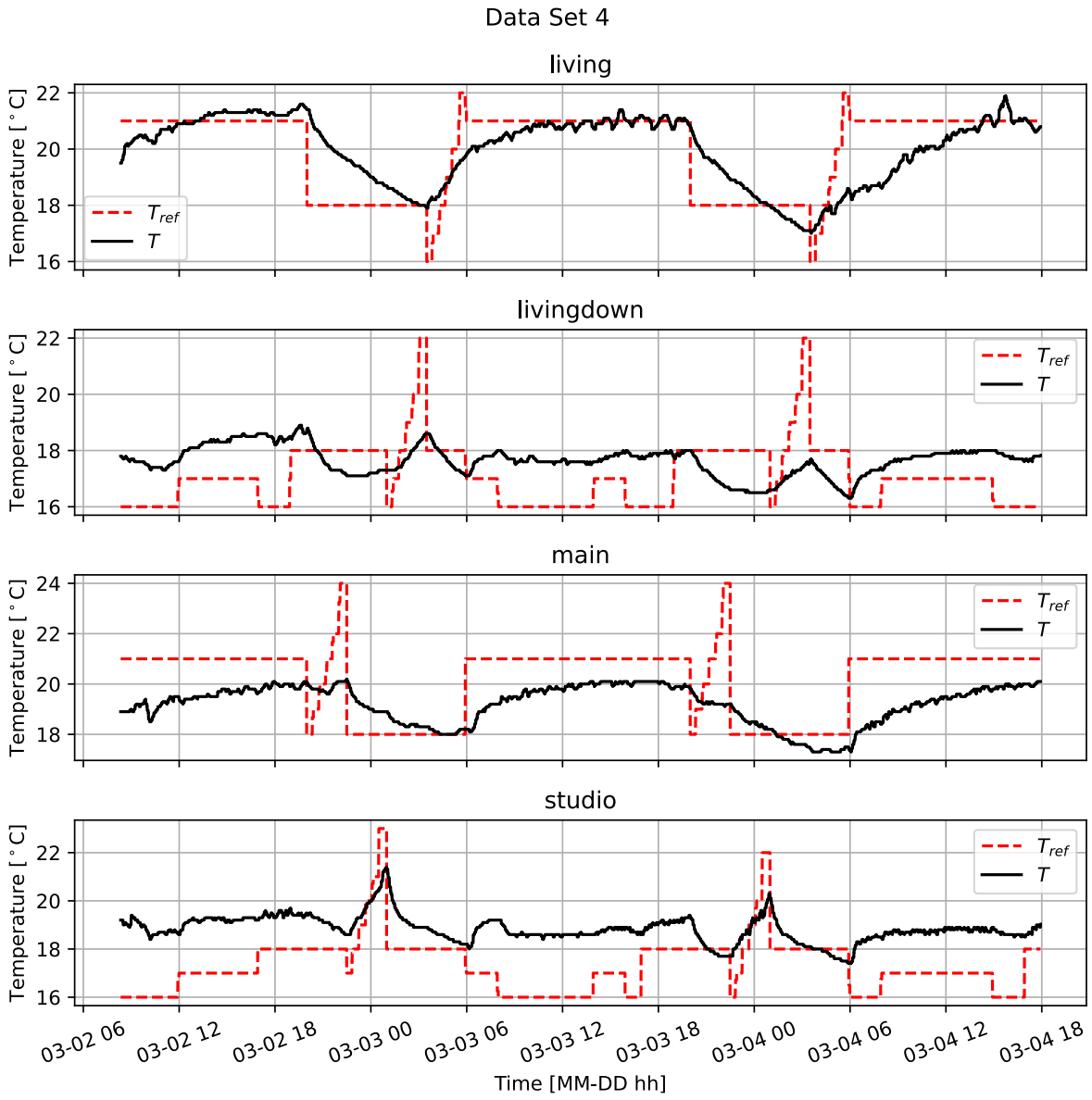

Figure A.9: *The reference temperature in stippled red and the measured temperature in black for each room from Data Set 4.*

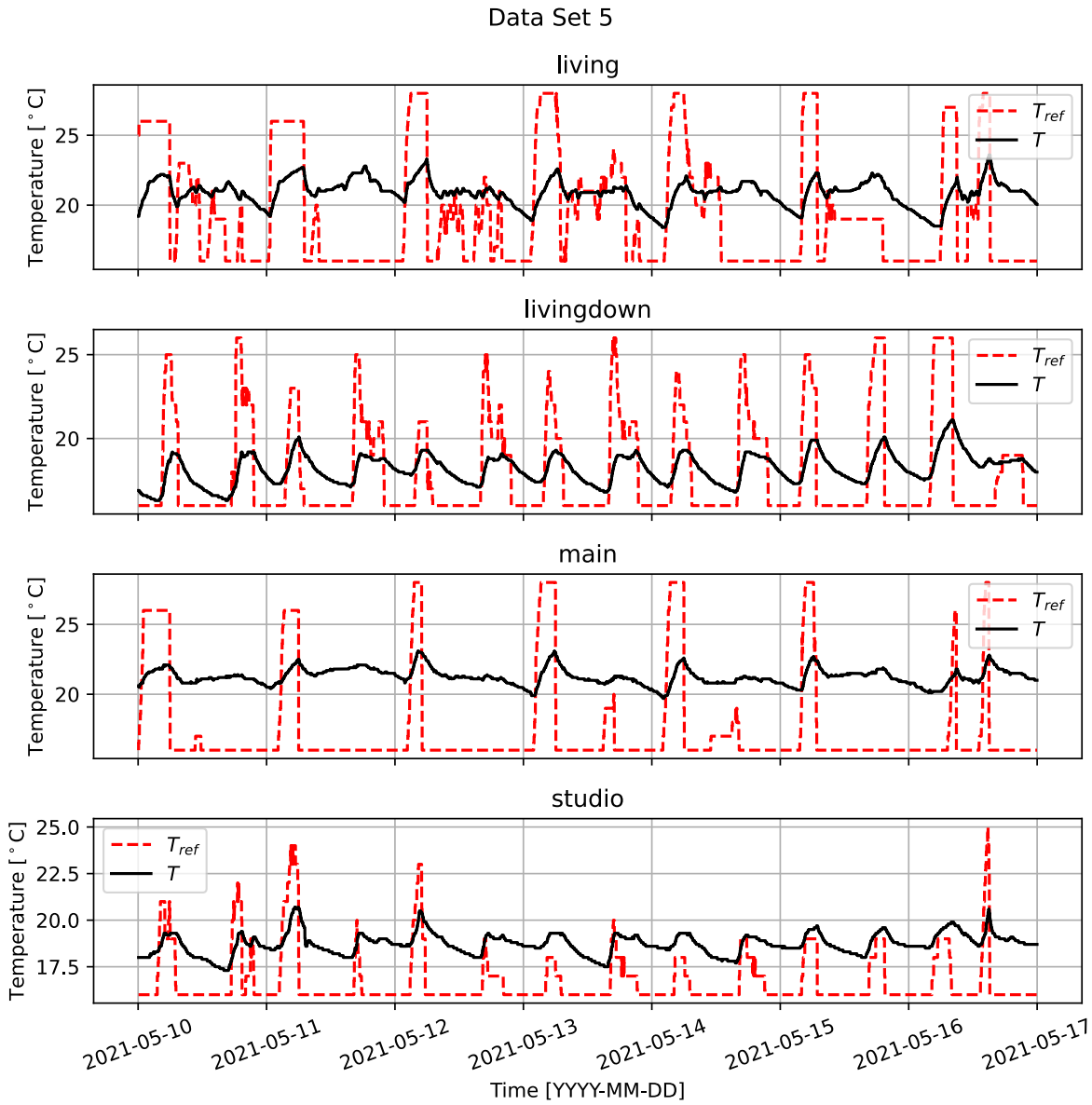

Figure A.10: *The reference temperature in stippled red and the measured temperature in black for each room from Data Set 5.*

A.3 On/Off

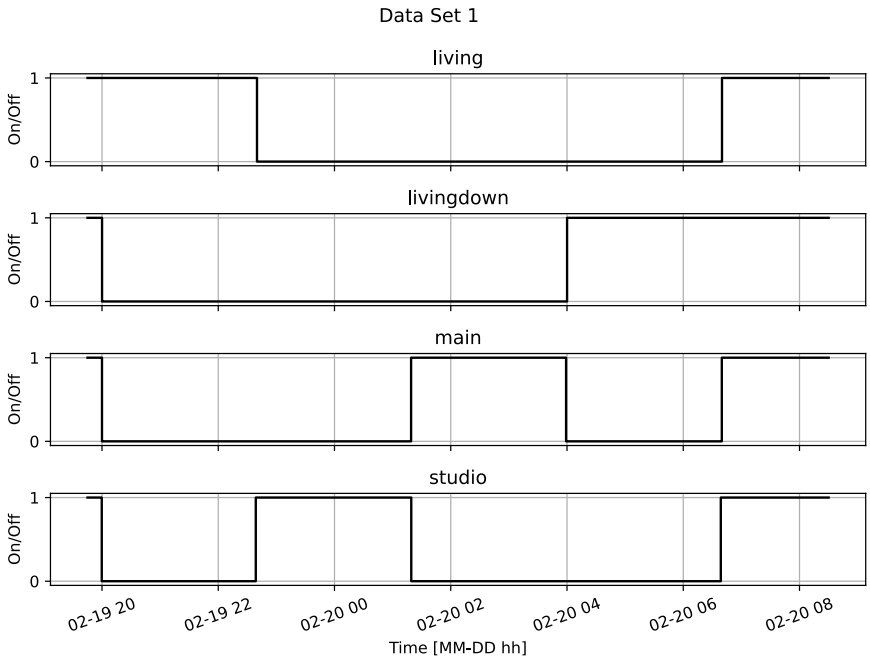

Figure A.11: *Boolean representation of the "On/Off" setting of the heat pump in each room from Data Set 1.*

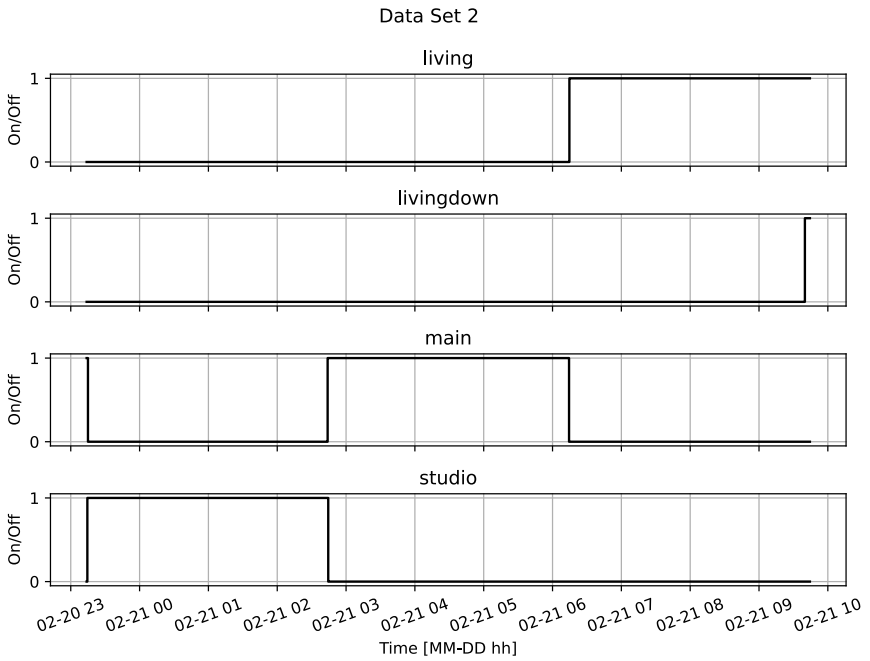

Figure A.12: *Boolean representation of the "On/Off" setting of the heat pump in each room from Data Set 1.*

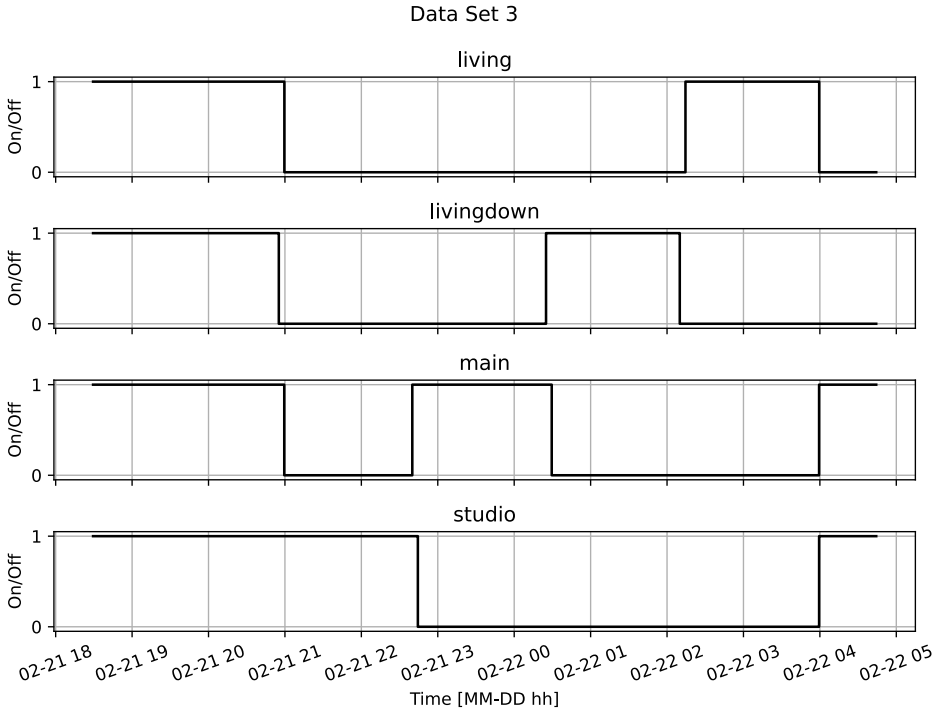

Figure A.13: *Boolean representation of the "On/Off" setting of the heat pump in each room from Data Set 1.*

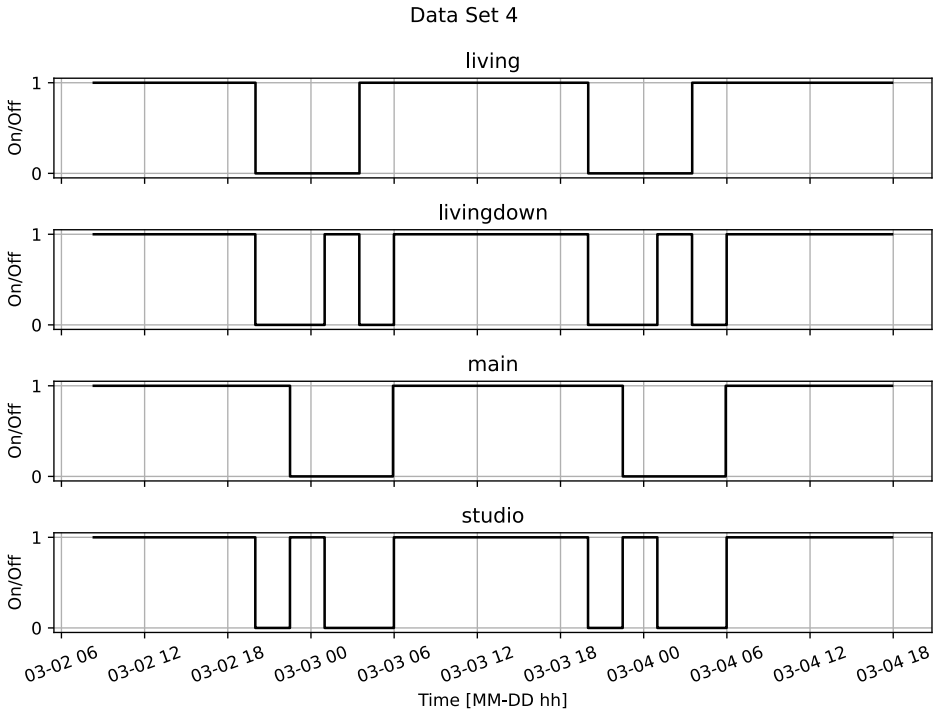

Figure A.14: *Boolean representation of the "On/Off" setting of the heat pump in each room from Data Set 1.*

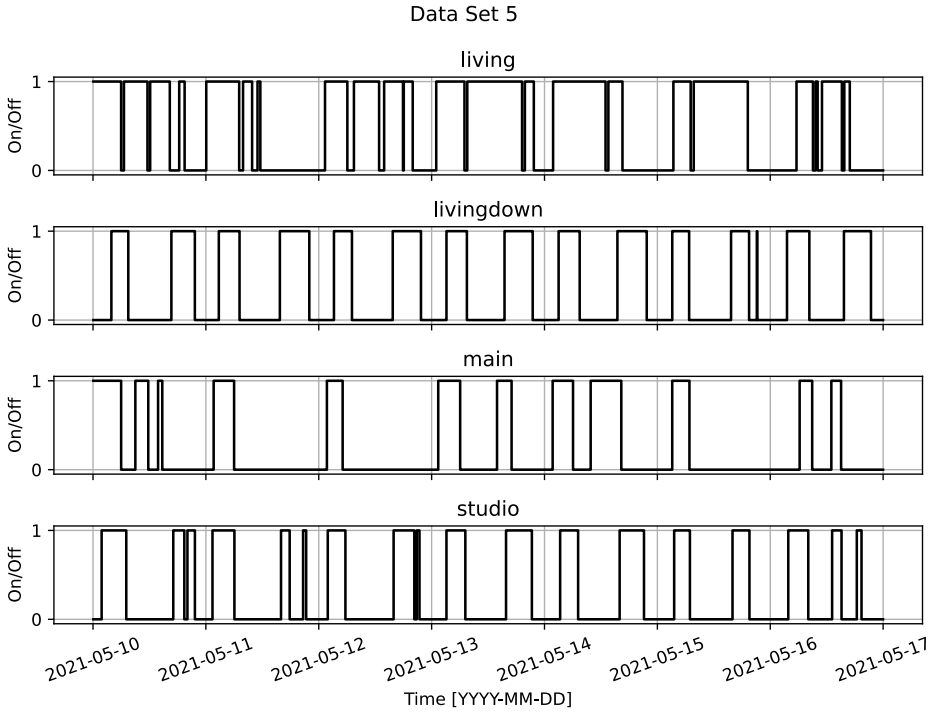

Figure A.15: *Boolean representation of the "On/Off" setting of the heat pump in each room from Data Set 1.*

A.4 Outdoor Temperature

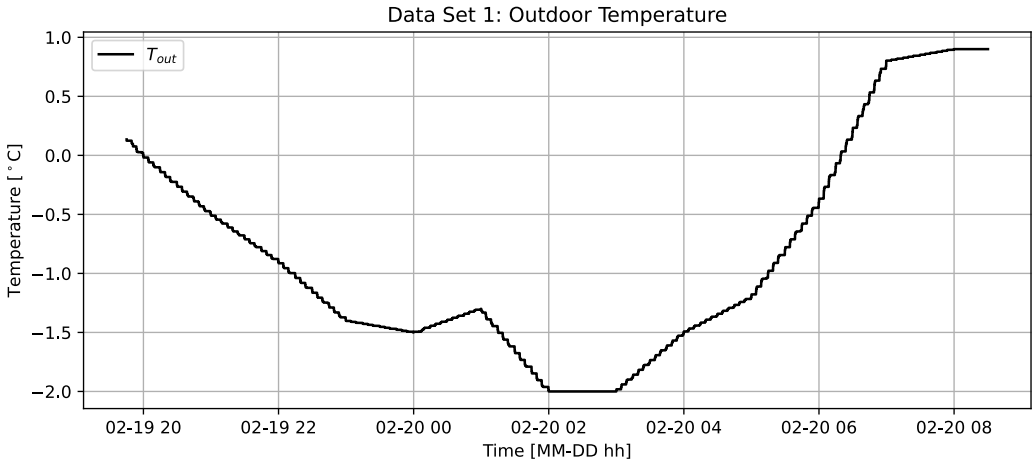

Figure A.16: *The outdoor temperature trajectory from Data Set 1.*

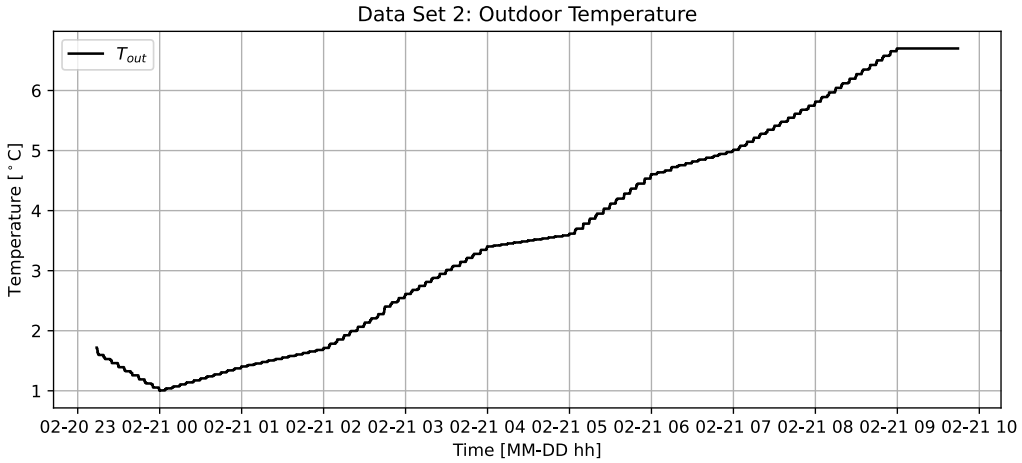

Figure A.17: *The outdoor temperature trajectory from Data Set 2.*

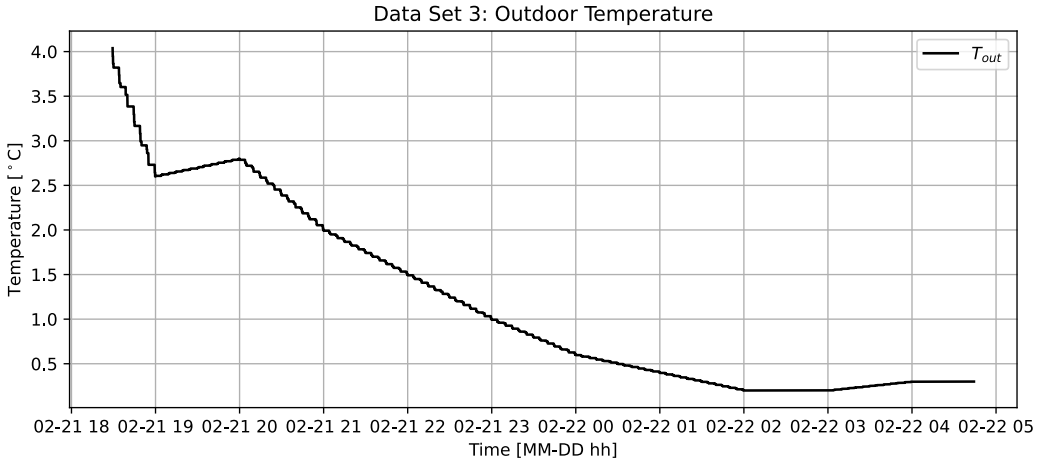

Figure A.18: *The outdoor temperature trajectory from Data Set 3.*

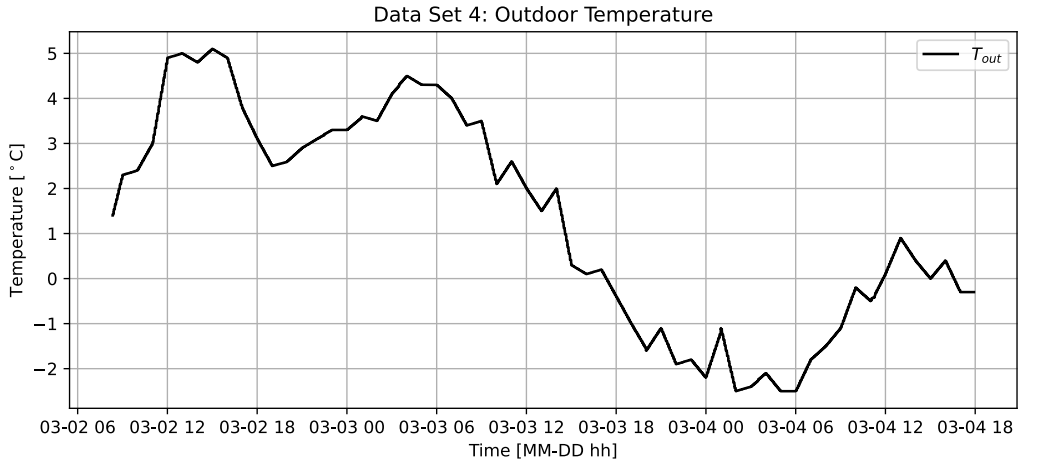

Figure A.19: *The outdoor temperature trajectory from Data Set 4.*

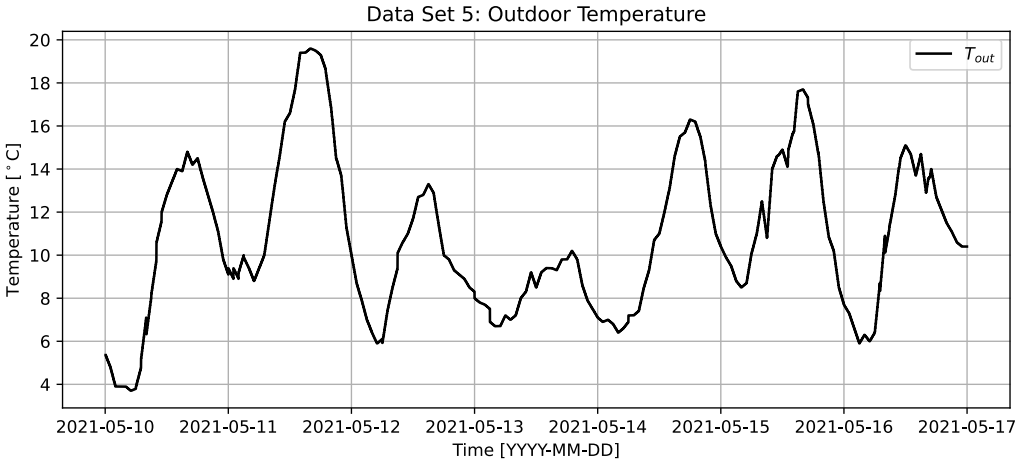

Figure A.20: *The outdoor temperature trajectory from Data Set 5.*

Appendix B: Parameter Estimation Results of the Power Models

This section presents the results of the model based parameter estimation of the Power Models. Each figure compares the measured values with the solution of the optimal model trajectory. In addition the distribution of the residual is presented.

B.1 Power Model 1

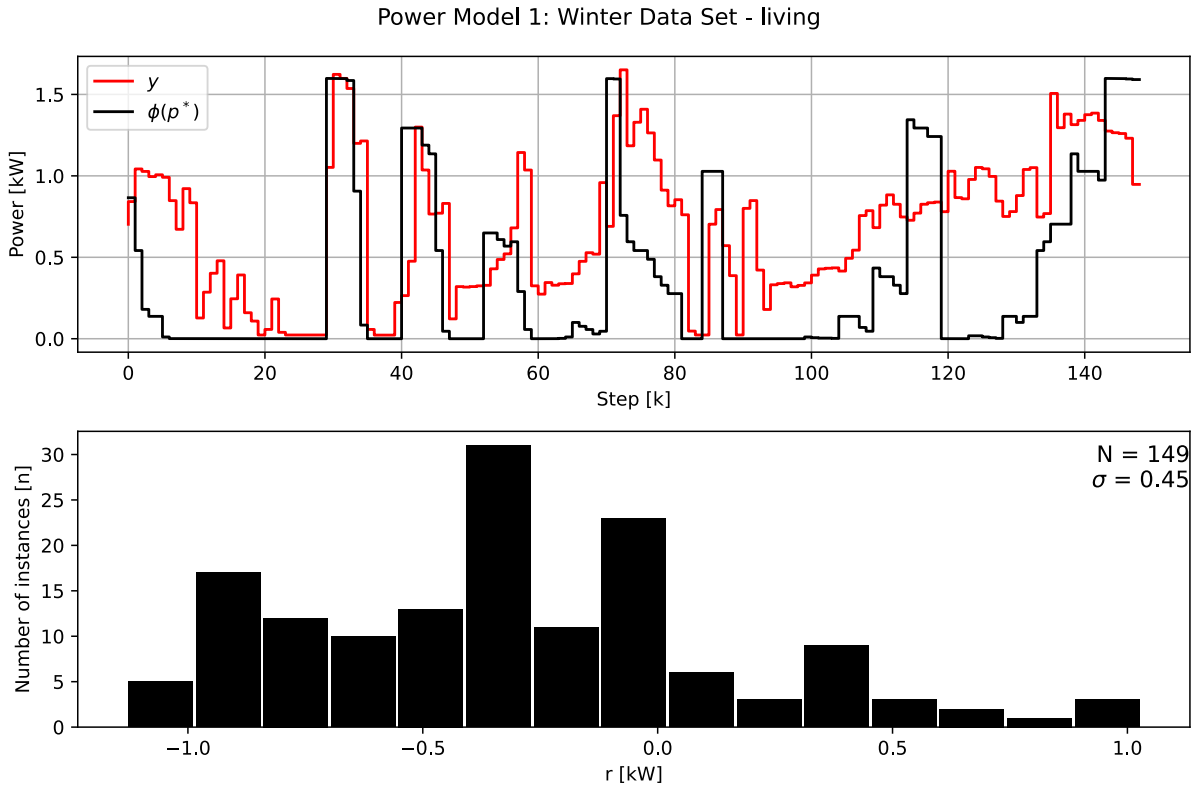

Figure B.1: *Upper plot compares the optimal model trajectory of Power Model 1 in black and the power measurements in red at time step k for Winter Data Set - living. The lower figure presents the distribution of the residual.*

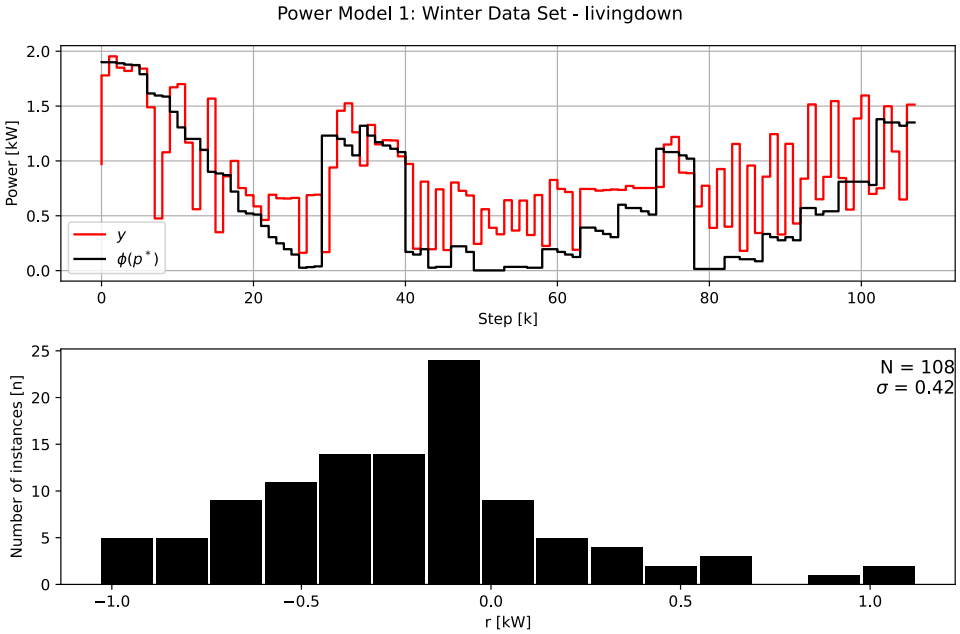

Figure B.2: *Upper plot compares the optimal model trajectory of Power Model 1 in black and the power measurements in red at time step k for Winter Data Set - livingdown. The lower figure presents the distribution of the residual.*

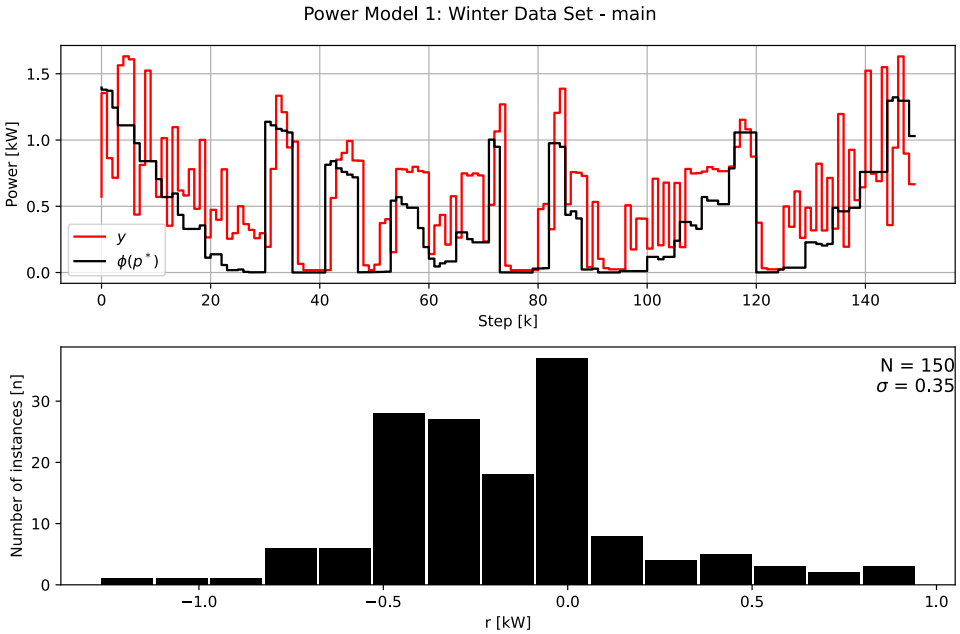

Figure B.3: *Upper plot compares the optimal model trajectory of Power Model 1 in black and the power measurements in red at time step k for Winter Data Set - main. The lower figure presents the distribution of the residual.*

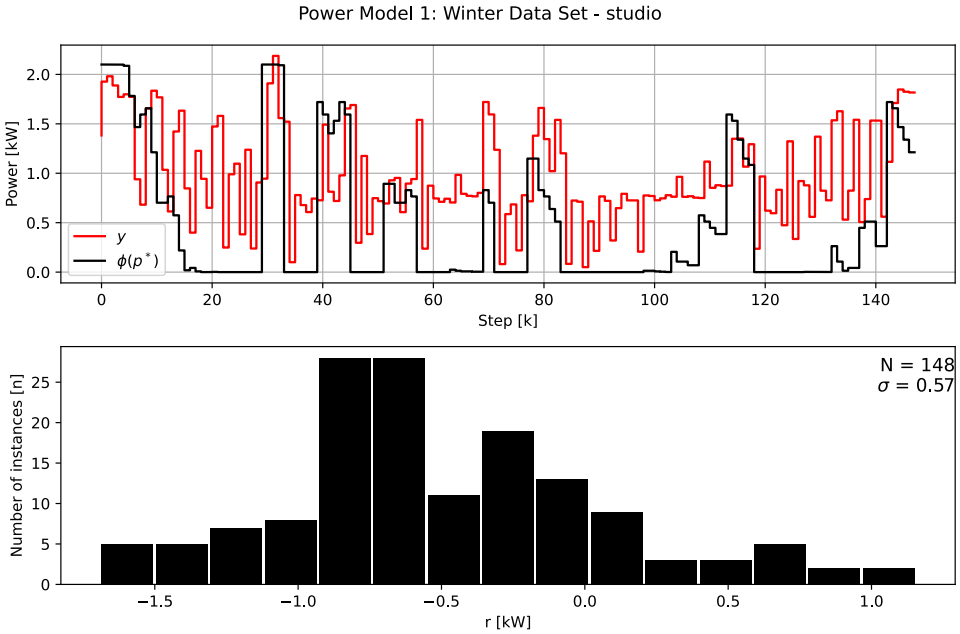

Figure B.4: *Upper plot compares the optimal model trajectory of Power Model 1 in black and the power measurements in red at time step k for Winter Data Set - studio. The lower figure presents the distribution of the residual.*

B.2 Power Model 2

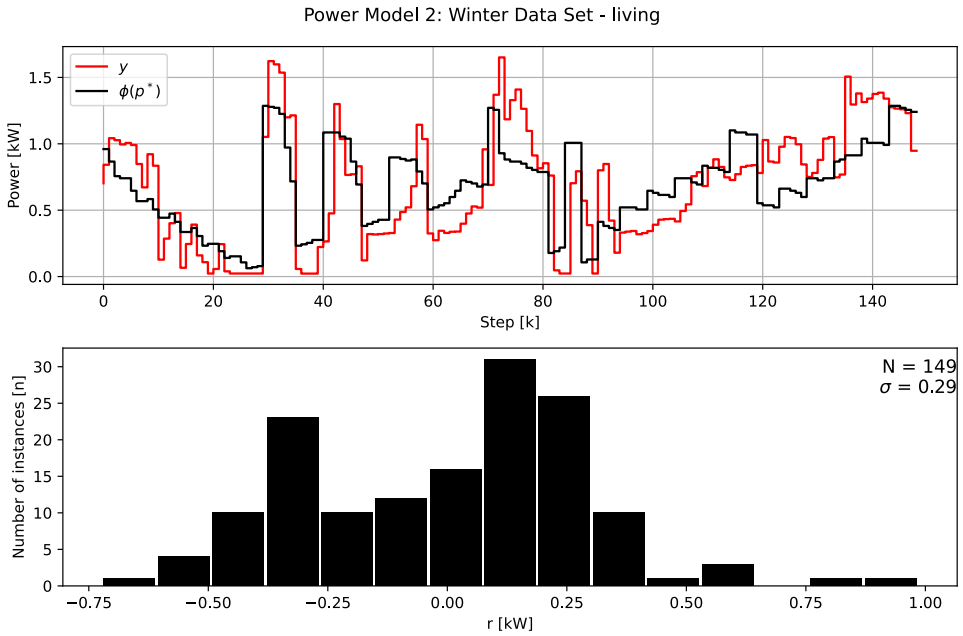

Figure B.5: *Upper plot compares the optimal model trajectory of Power Model 2 in black and the power measurements in red at time step k for Winter Data Set - living. The lower figure presents the distribution of the residual.*

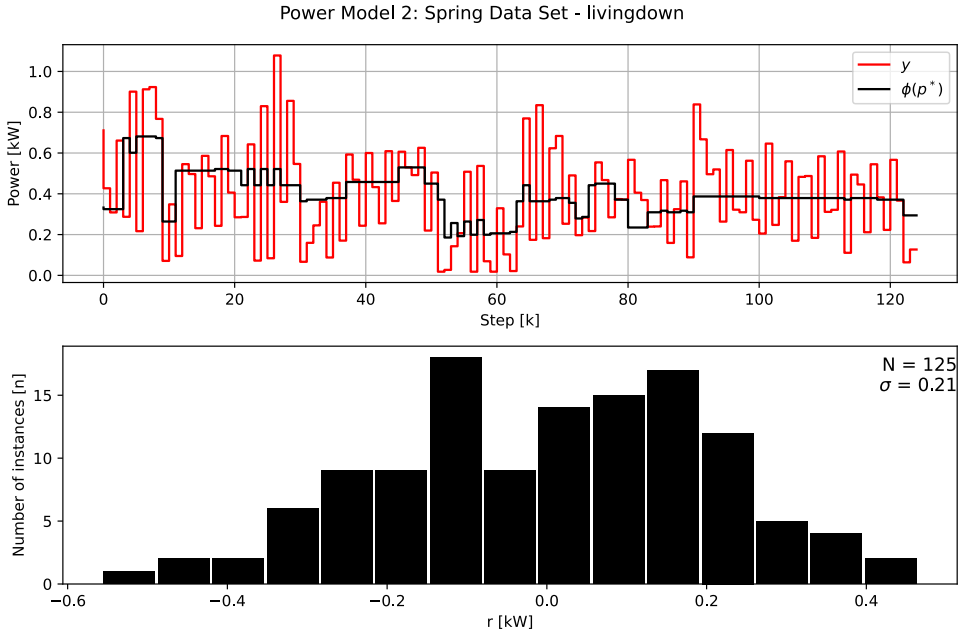

Figure B.6: *Upper plot compares the optimal model trajectory of Power Model 2 in black and the power measurements in red at time step k for Spring Data Set - livingdown. The lower figure presents the distribution of the residual.*

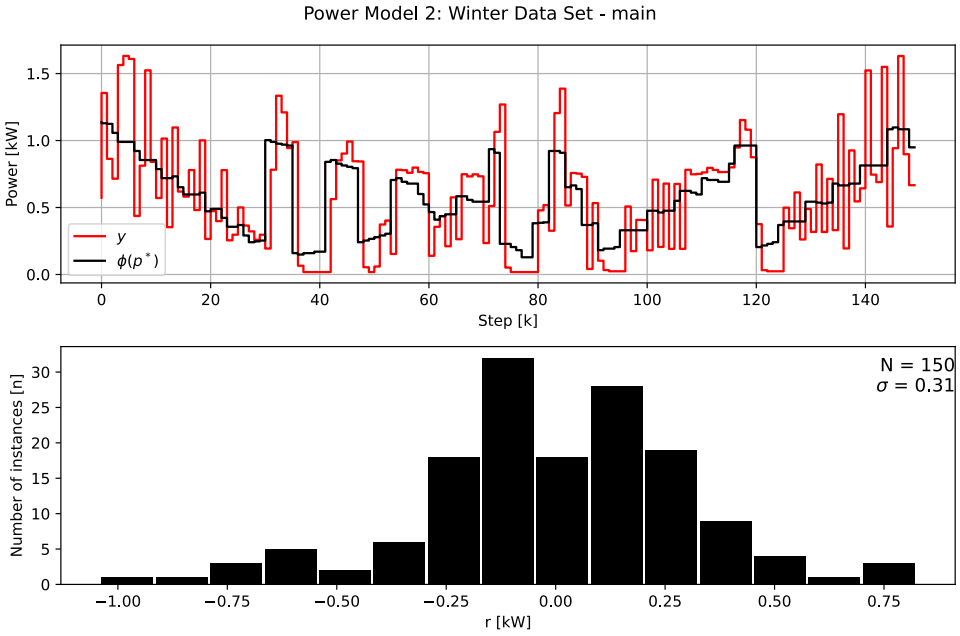

Figure B.7: *Upper plot compares the optimal model trajectory of Power Model 2 in black and the power measurements in red at time step k for Winter Data Set - main. The lower figure presents the distribution of the residual.*

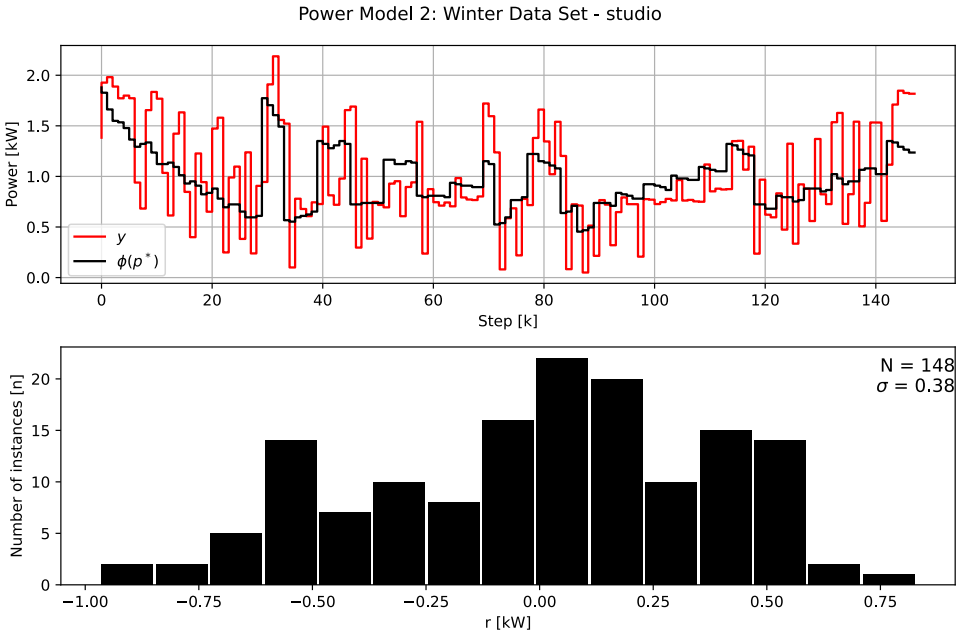

Figure B.8: *Upper plot compares the optimal model trajectory of Power Model 2 in black and the power measurements in red at time step k for Winter Data Set - studio. The lower figure presents the distribution of the residual.*

B.3 Power Model 3

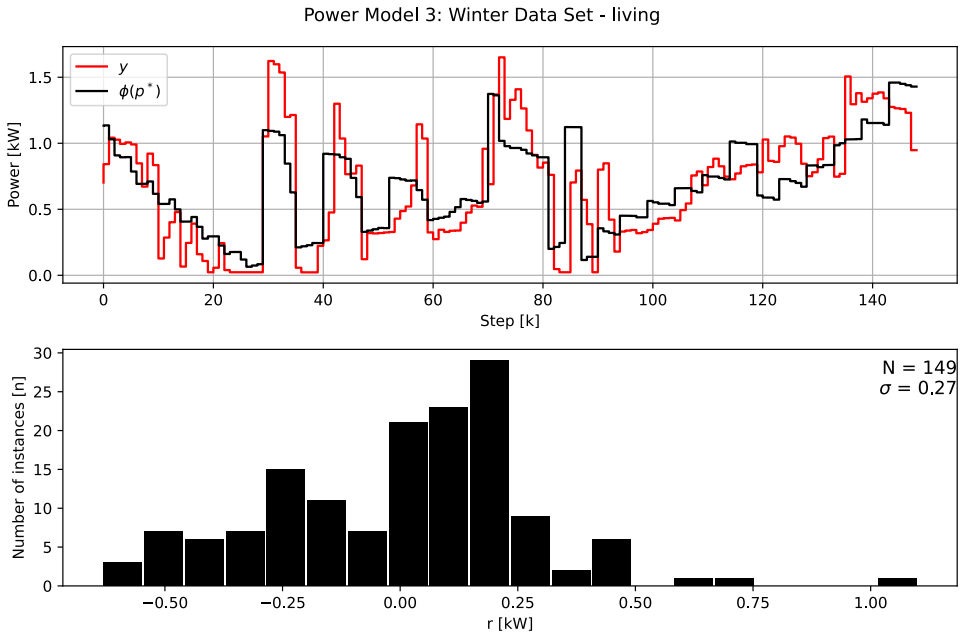

Figure B.9: *Upper plot compares the optimal model trajectory of Power Model 3 in black and the power measurements in red at time step k for Winter Data Set - living. The lower figure presents the distribution of the residual.*

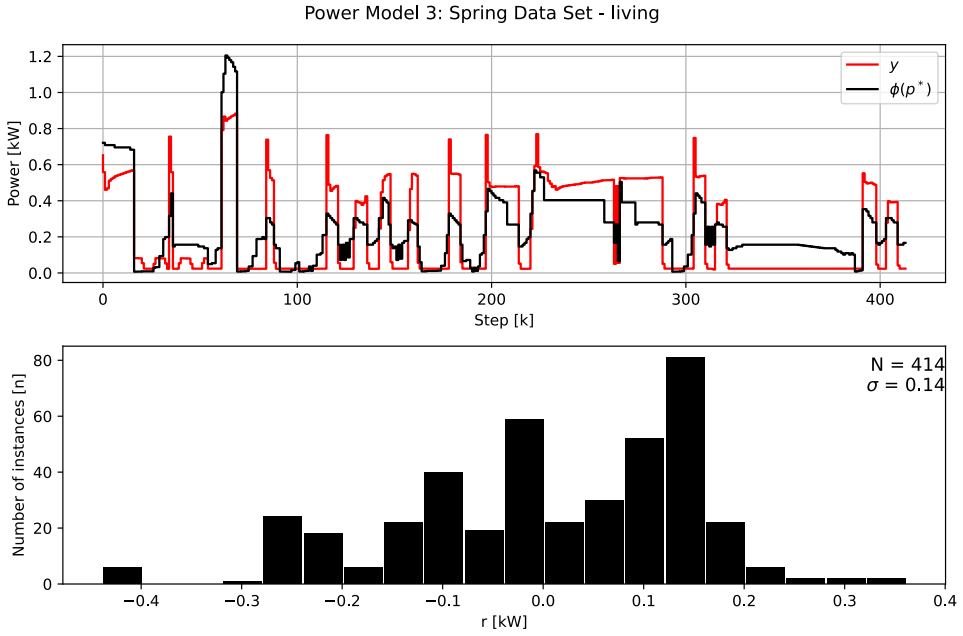

Figure B.10: *Upper plot compares the optimal model trajectory of Power Model 3 in black and the power measurements in red at time step k for Spring Data Set - living. The lower figure presents the distribution of the residual.*

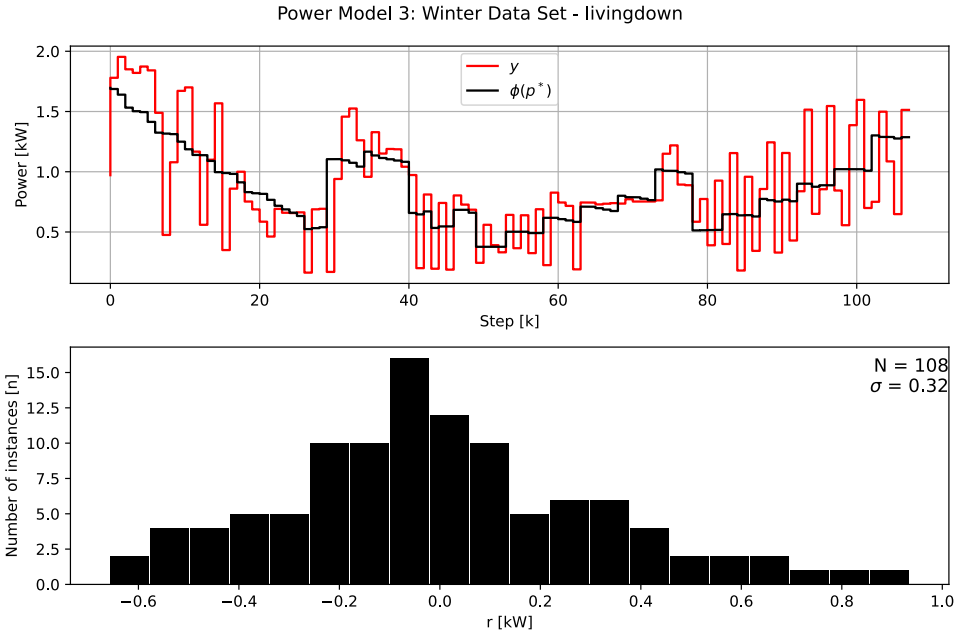

Figure B.11: *Upper plot compares the optimal model trajectory of Power Model 3 in black and the power measurements in red at time step k for Winter Data Set - livingdown. The lower figure presents the distribution of the residual.*

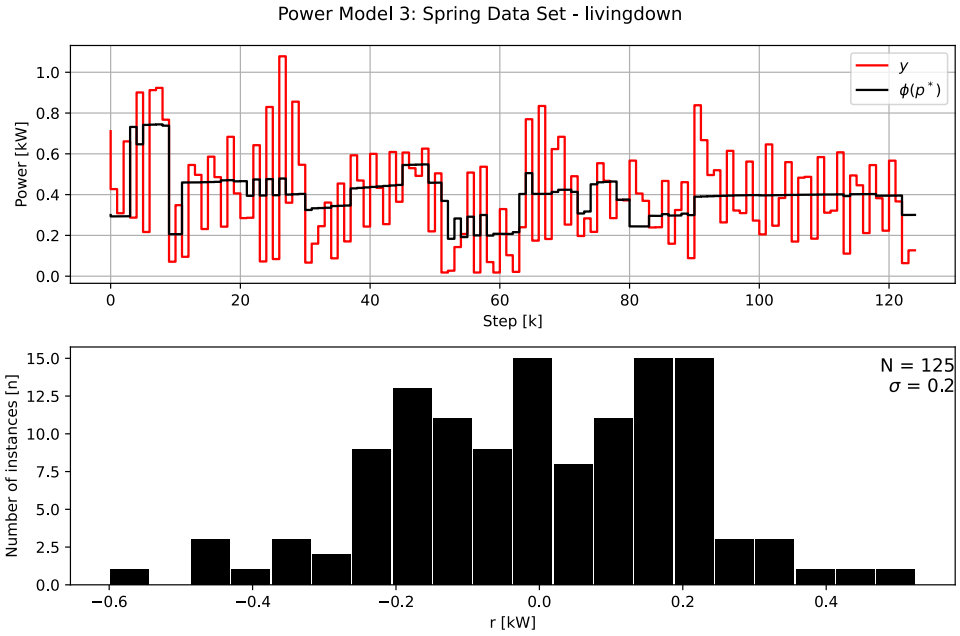

Figure B.12: *Upper plot compares the optimal model trajectory of Power Model 3 in black and the power measurements in red at time step k for Spring Data Set - livingdown. The lower figure presents the distribution of the residual.*

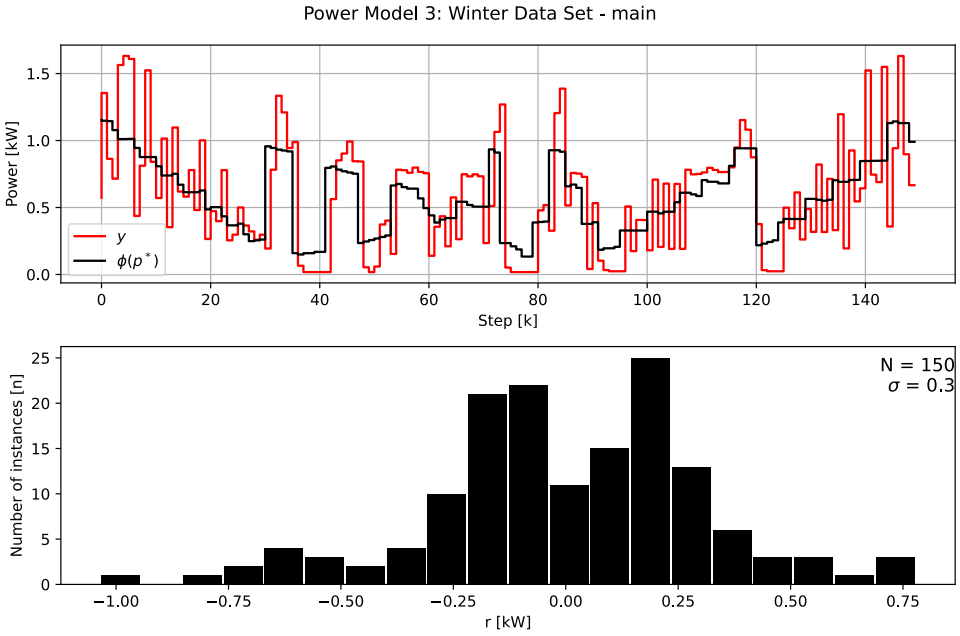

Figure B.13: *Upper plot compares the optimal model trajectory of Power Model 3 in black and the power measurements in red at time step k for Winter Data Set - main. The lower figure presents the distribution of the residual.*

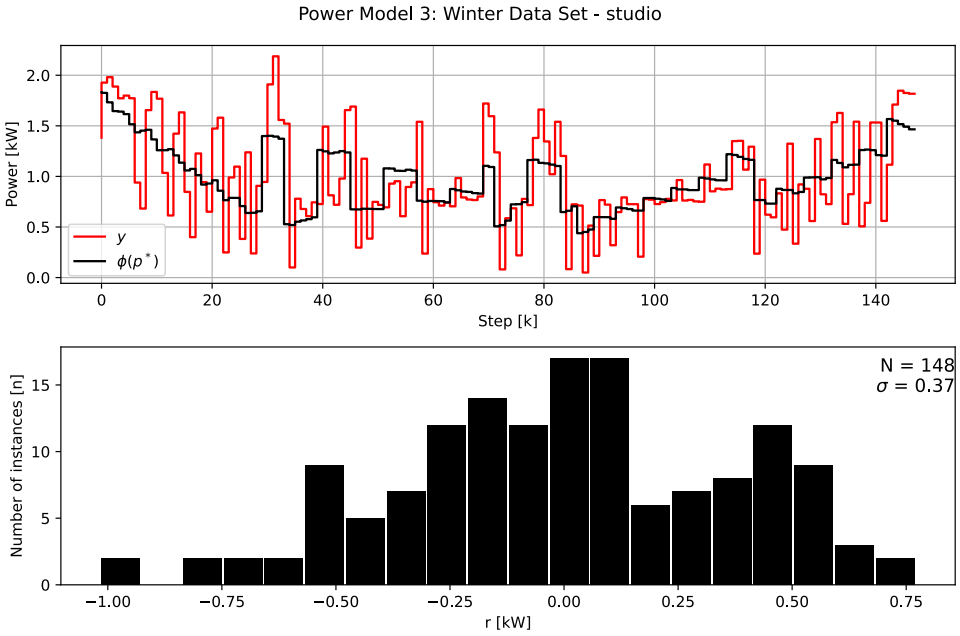

Figure B.14: *Upper plot compares the optimal model trajectory of Power Model 3 in black and the power measurements in red at time step k for Winter Data Set - studio. The lower figure presents the distribution of the residual.*

B.4 Power model 4

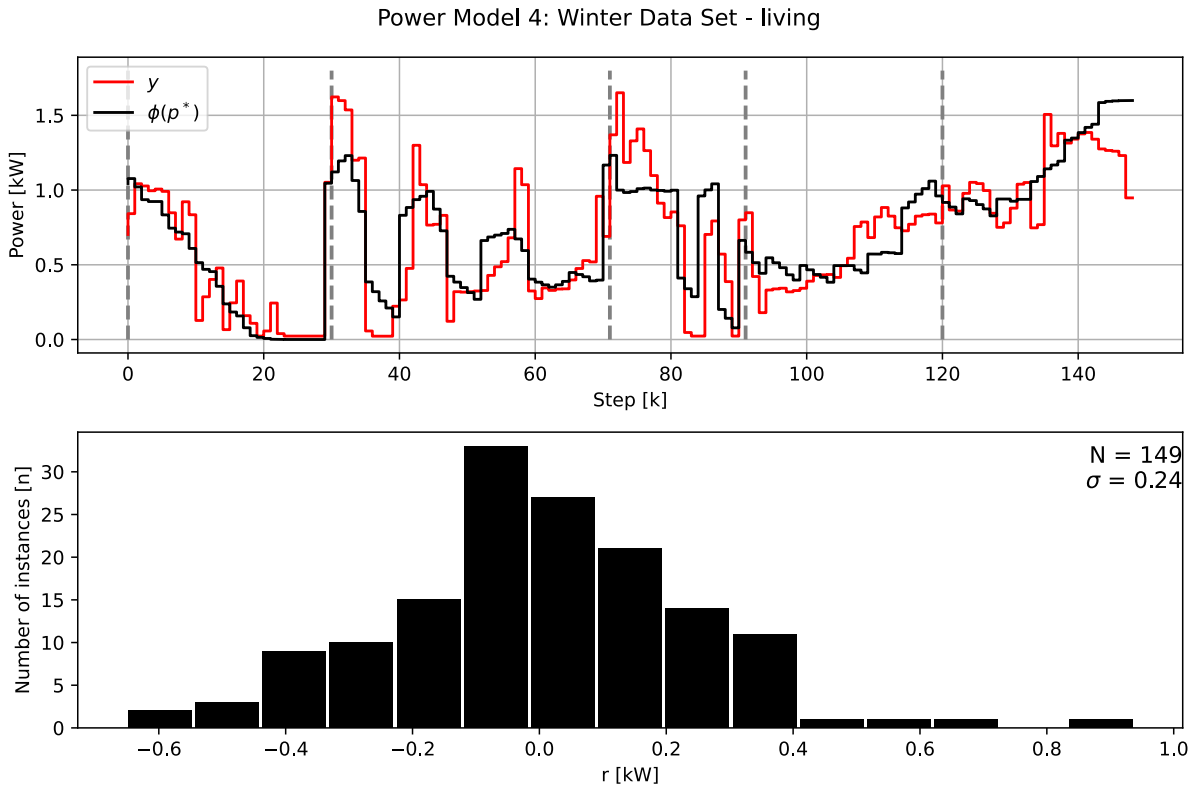

Figure B.15: *Upper plot compares the optimal model trajectory of Power Model 4 in black and the power measurements in red at time step k for Winter Data Set - living. The vertical grey dotted lines mark where it is a time gap of over 5 minutes in the time series. The lower figure presents the distribution of the residual.*

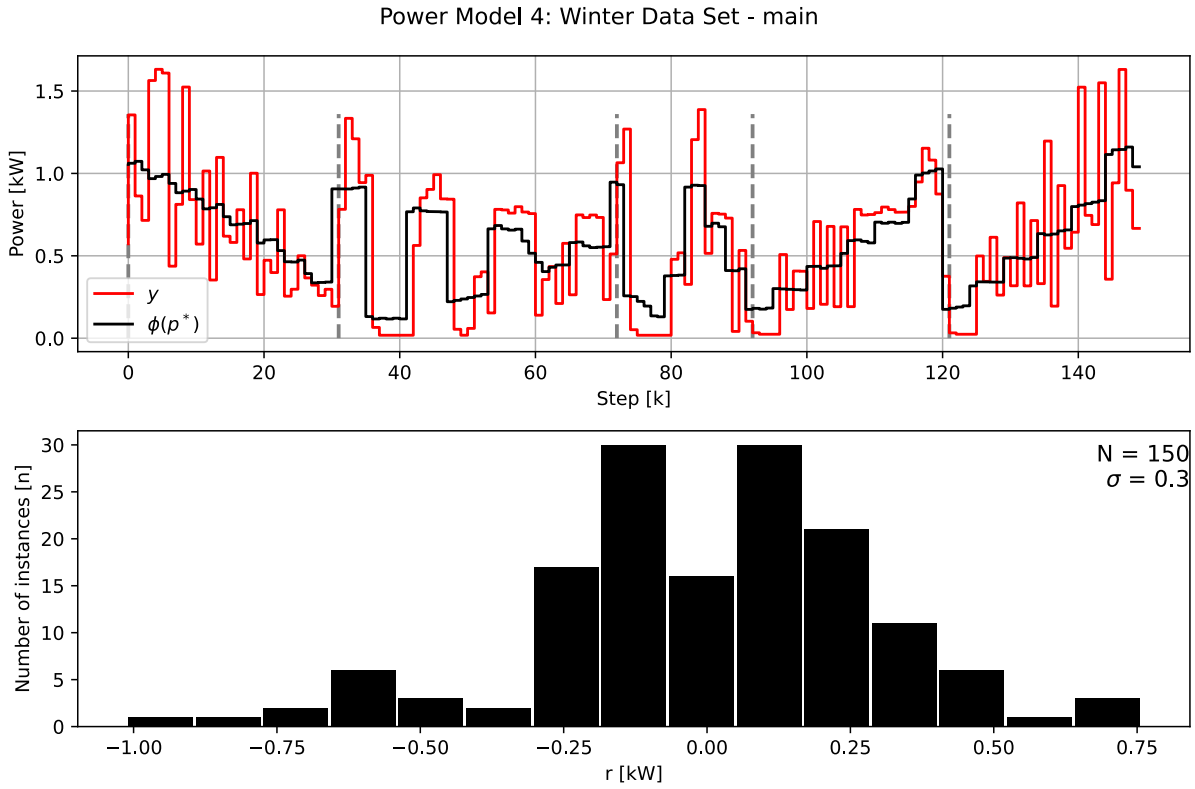

Figure B.16: *Upper plot compares the optimal model trajectory of Power Model 4 in black and the power measurements in red at time step k for Winter Data Set - main. The vertical grey dotted lines marks where it is a time gap of over 5 minutes in the time series. The lower figure presents the distribution of the residual.*

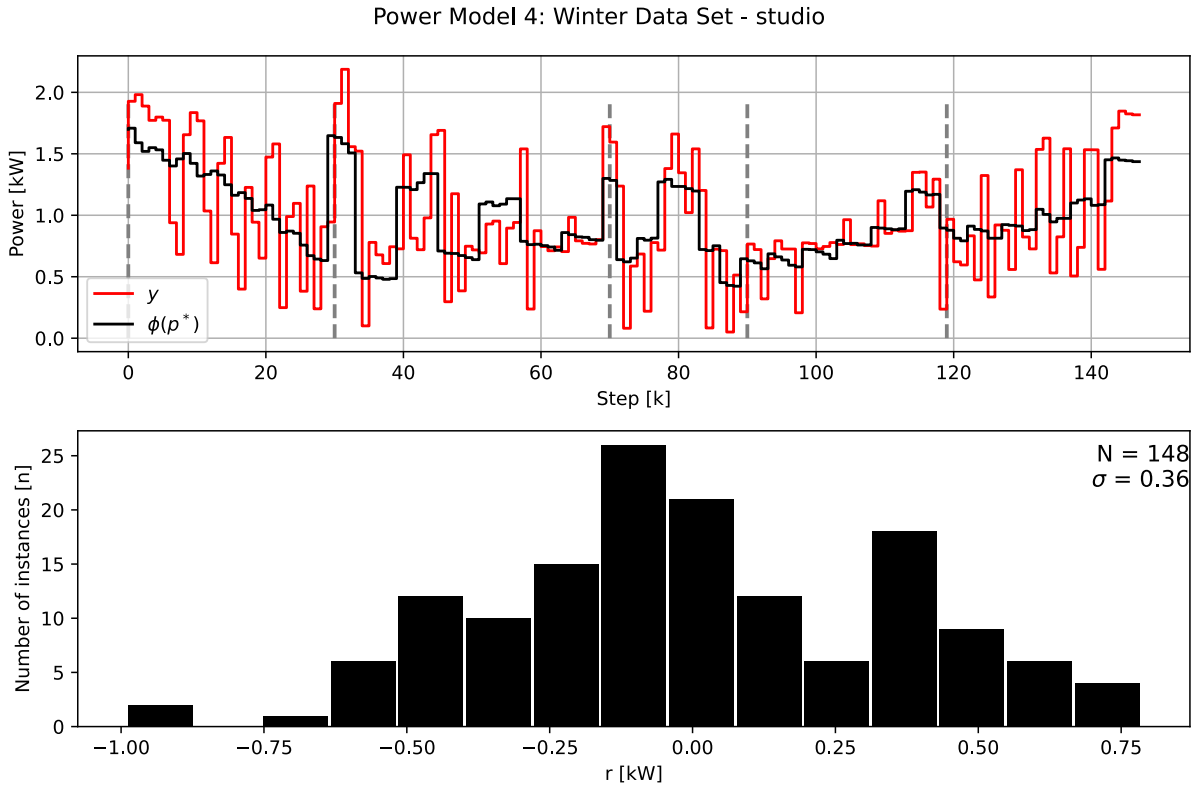

Figure B.17: *Upper plot compares the optimal model trajectory of Power Model 1 in black and the power measurements in red at time step k for Winter Data Set - studio. The vertical grey dotted lines mark where it is a time gap of over 5 minutes in the time series. The lower figure presents the distribution of the residual.*

Appendix C: Parameter Estimation Results of the Temperature Models

This section presents the results of the model based parameter estimation of the Temperature Models. Each figure compares the measured values with the solution of the optimal model trajectory. In addition the distribution of the residual is presented.

C.1 Temperature Model 1

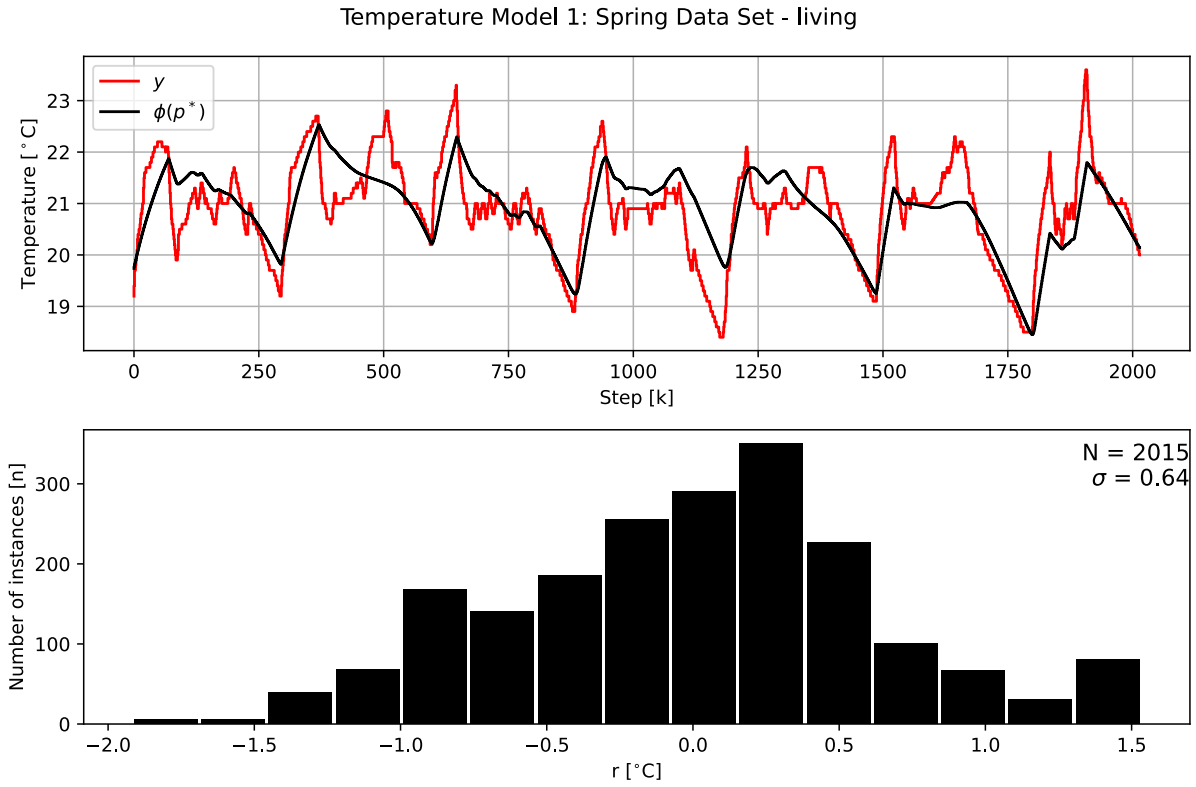

Figure C.1: *Upper plot compares the optimal model trajectory in black with the temperature measurements in red of Spring Data Set - living. The lower plot illustrates the distribution of the residual.*

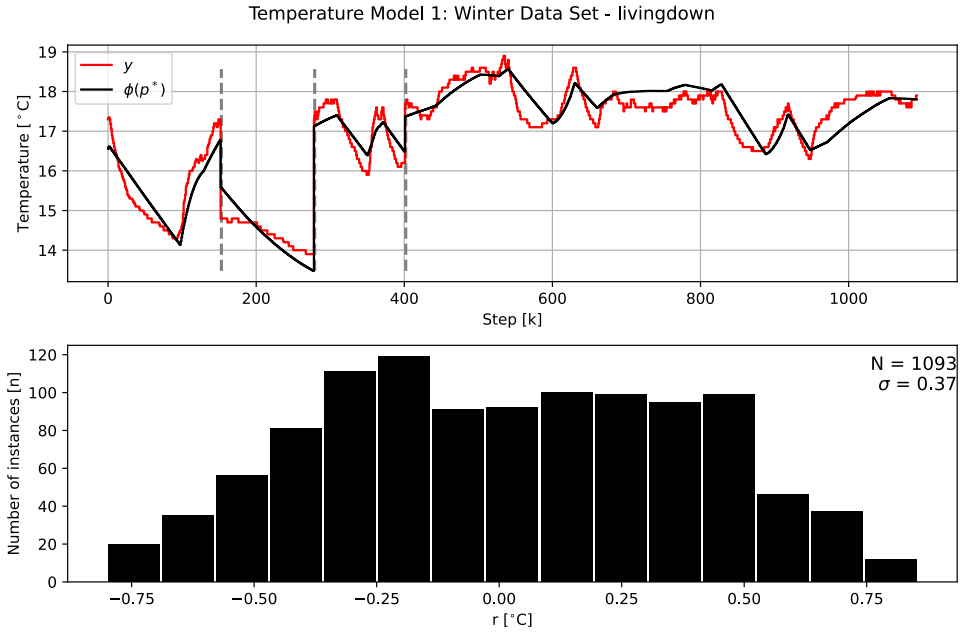

Figure C.2: *Upper plot compares the optimal model trajectory in black with the temperature measurements in red of Winter Data Set - livingdown. The grey vertical dotted lines mark where it is a gap in the time series of over five minutes. The lower plot illustrates the distribution of the residual.*

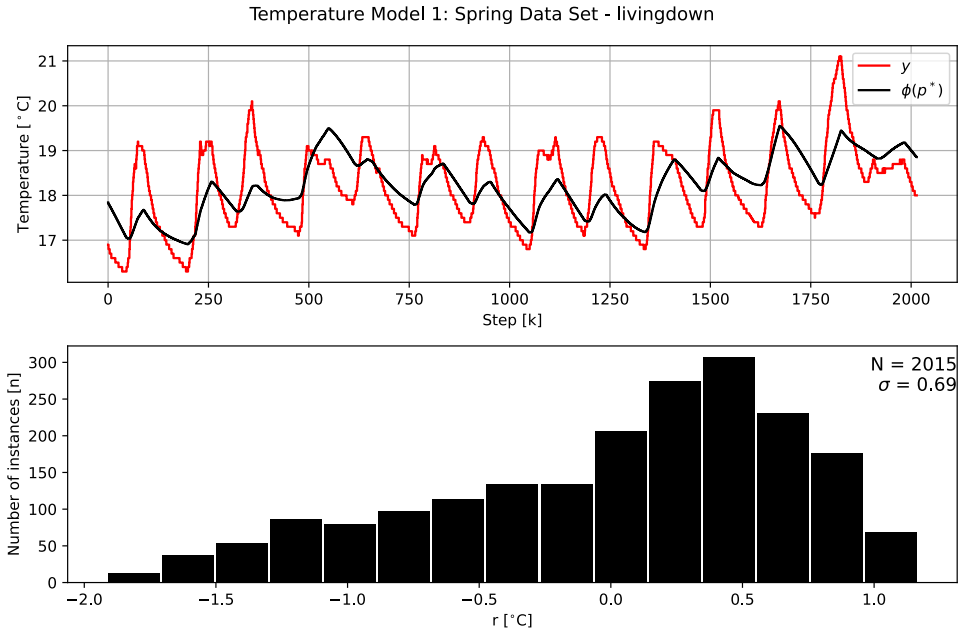

Figure C.3: *Upper plot compares the optimal model trajectory in black with the temperature measurements in red of Spring Data Set - livingdown. The lower plot illustrates the distribution of the residual.*

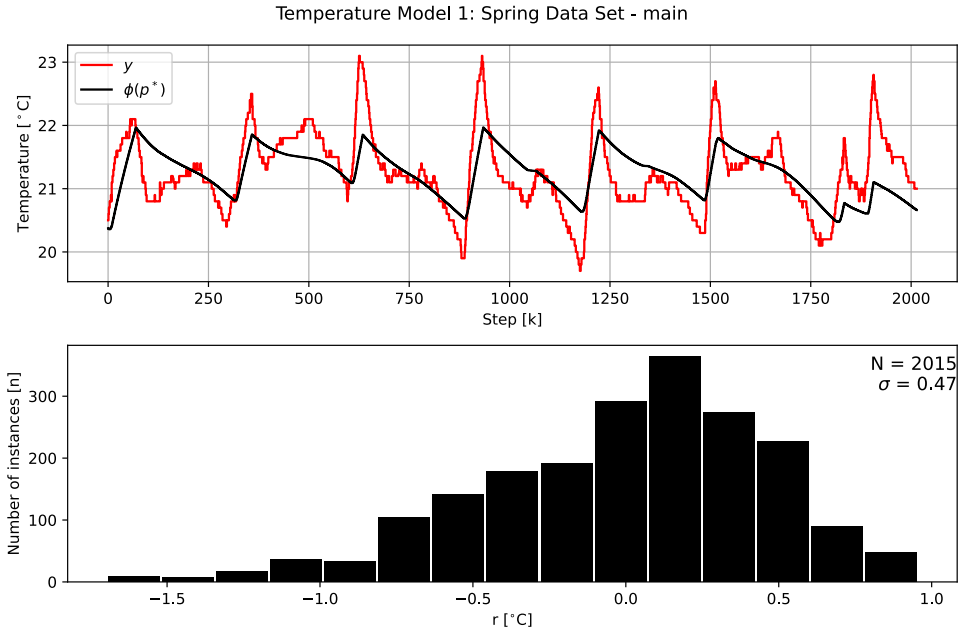

Figure C.4: *Upper plot compares the optimal model trajectory in black with the temperature measurements in red of Spring Data Set - main. The lower plot illustrates the distribution of the residual.*

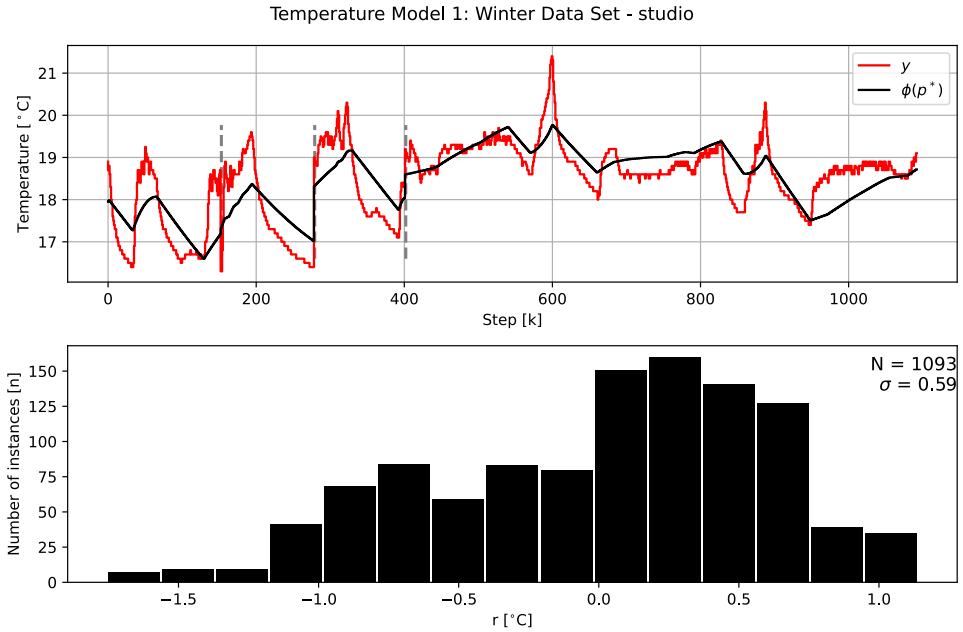

Figure C.5: *Upper plot compares the optimal model trajectory in black with the temperature measurements in red of Winter Data Set - studio. The grey vertical dotted lines mark where it is a gap in the time series of over five minutes. The lower plot illustrates the distribution of the residual.*

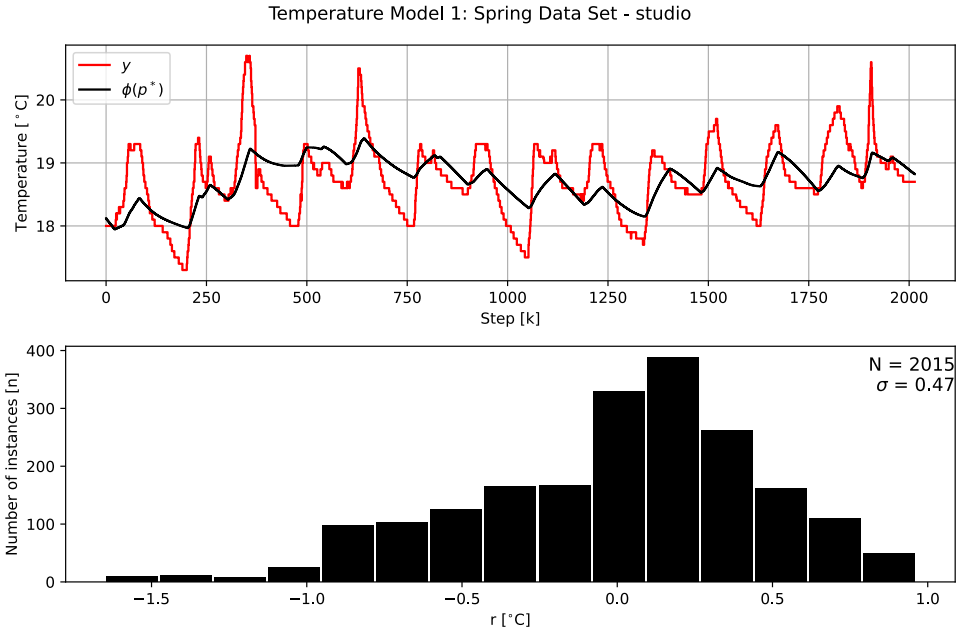

Figure C.6: *Upper plot compares the optimal model trajectory in black with the temperature measurements in red of Spring Data Set - living. The lower plot illustrates the distribution of the residual.*

C.2 Temperature Model 2

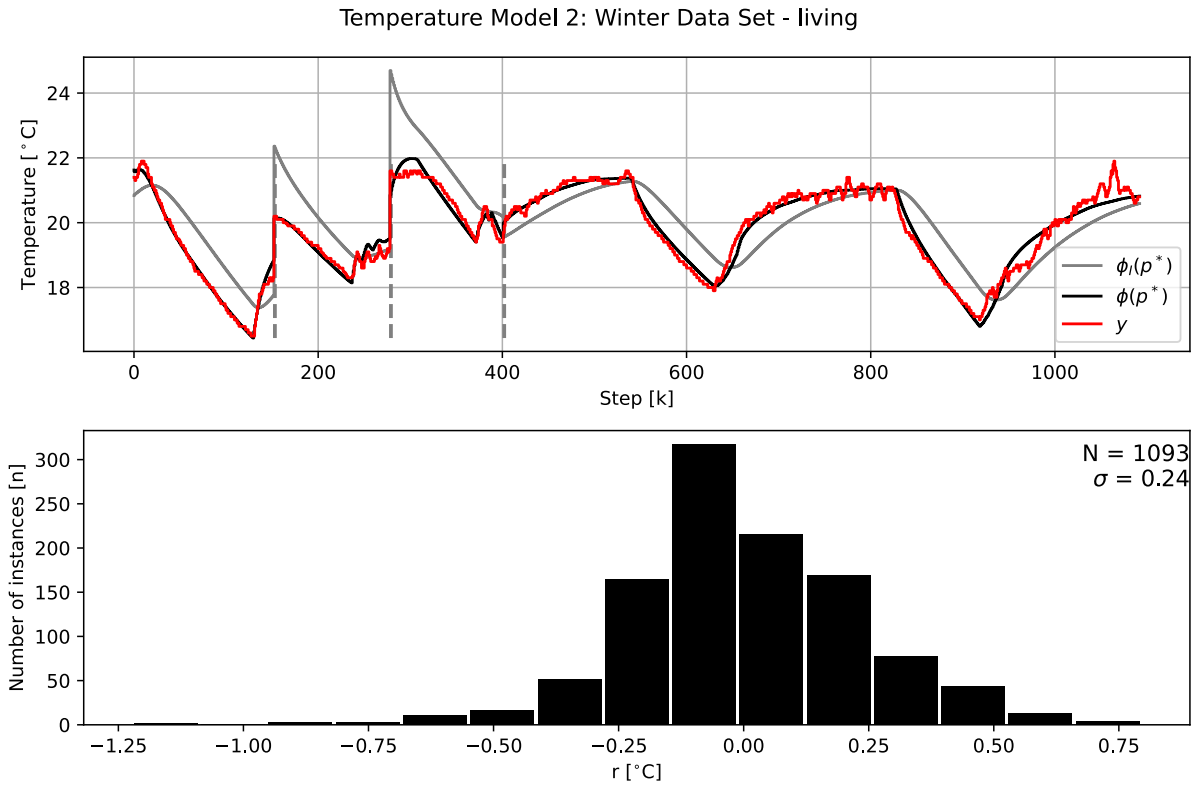

Figure C.7: *Upper plot compares the optimal model trajectory in black with the temperature measurements in red of Winter Data Set - living. The grey vertical dotted lines mark where it is a gap in the time series of over five minutes. The lower plot illustrates the distribution of the residual.*

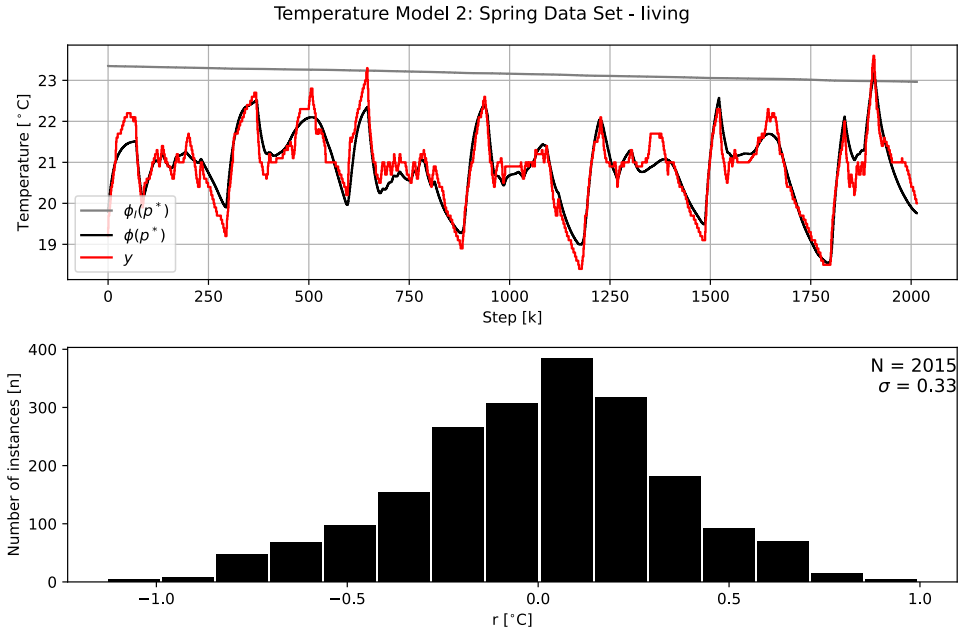

Figure C.8: *Upper plot compares the optimal model trajectory in black with the temperature measurements in red of Spring Data Set - living. The lower plot illustrates the distribution of the residual.*

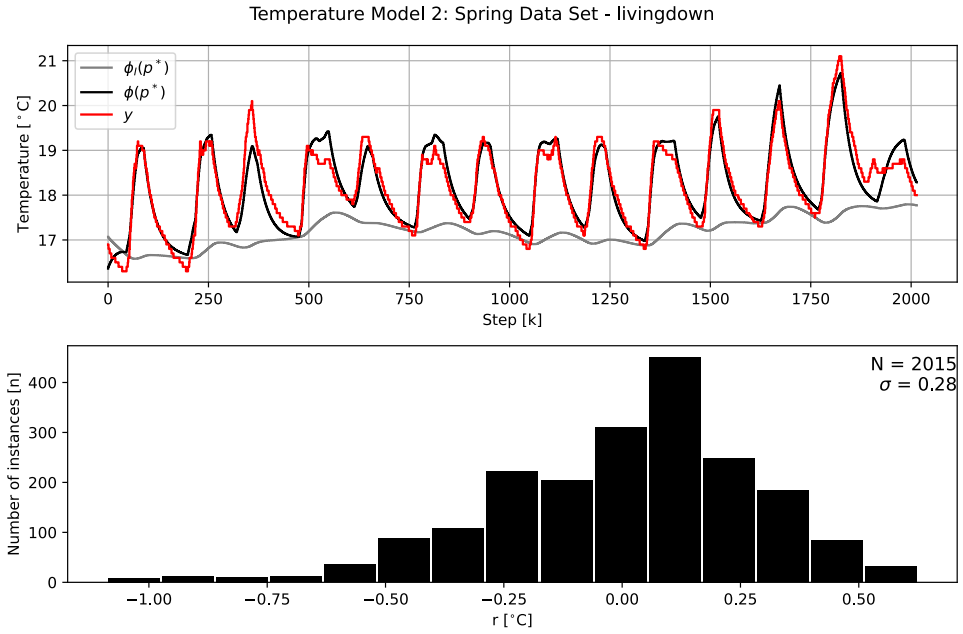

Figure C.9: *Upper plot compares the optimal model trajectory in black with the temperature measurements in red of Spring Data Set - livingdown. The lower plot illustrates the distribution of the residual.*

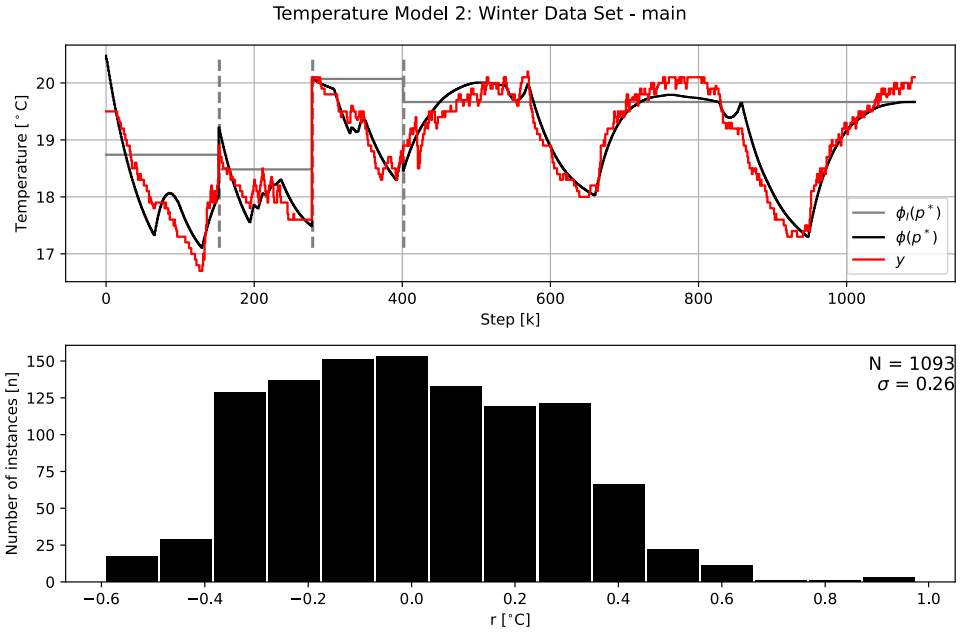

Figure C.10: *Upper plot compares the optimal model trajectory in black with the temperature measurements in red of Winter Data Set - main. The grey vertical dotted lines mark where it is a gap in the time series of over five minutes. The lower plot illustrates the distribution of the residual.*

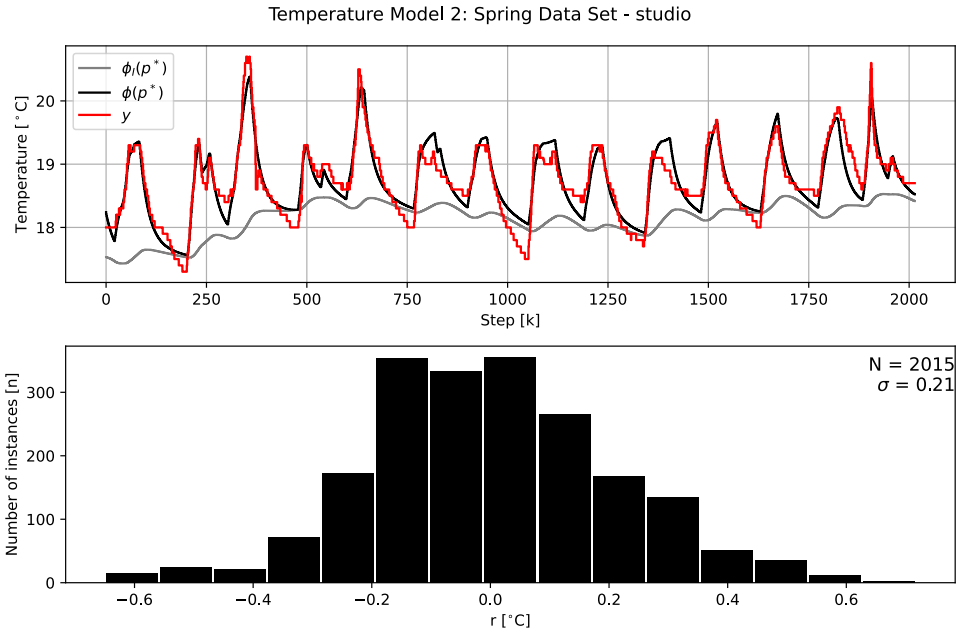

Figure C.11: *Upper plot compares the optimal model trajectory in black with the temperature measurements in red of Spring Data Set - studio. The lower plot illustrates the distribution of the residual.*

C.3 Temperature Model 3

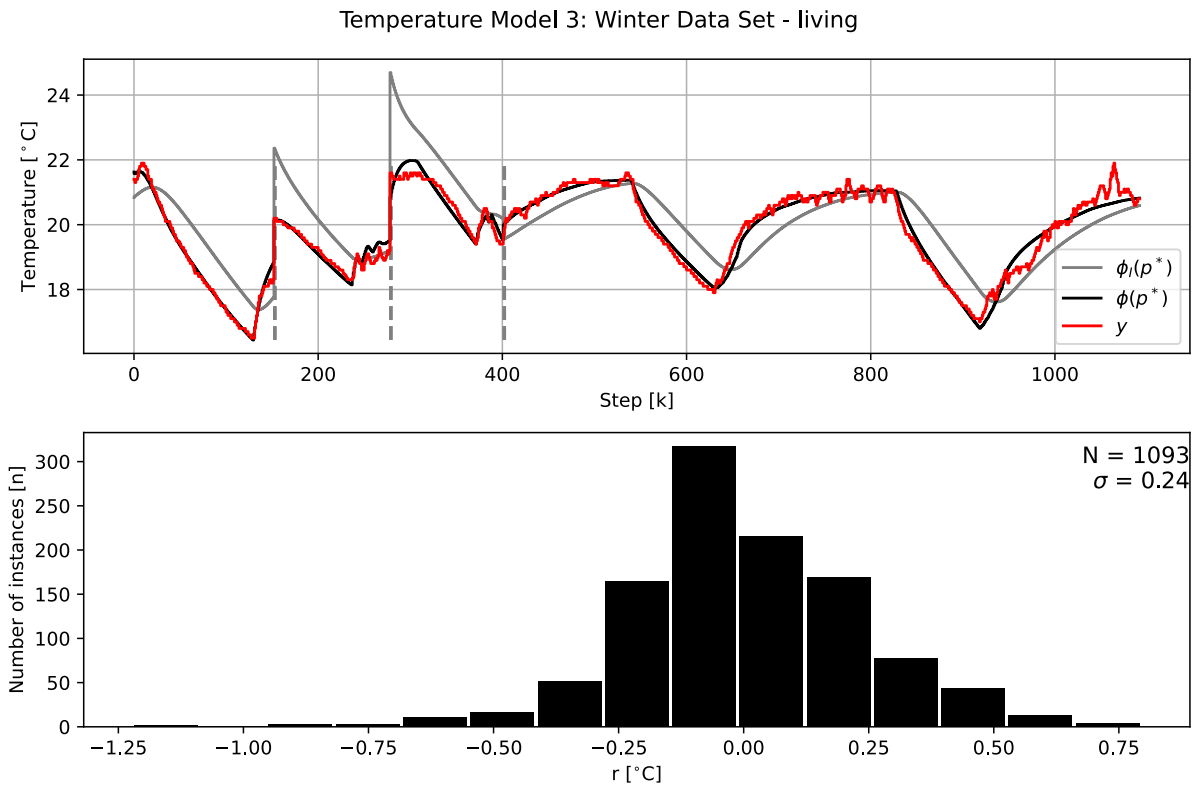

Figure C.12: *Upper plot compares the optimal model trajectory in black with the temperature measurements in red of Winter Data Set - living. The grey solid trajectory illustrates the temperature of the inertia thermal mass, while the grey vertical dotted lines mark where it is a gap in the time series of over five minutes. The lower plot illustrates the distribution of the residual.*

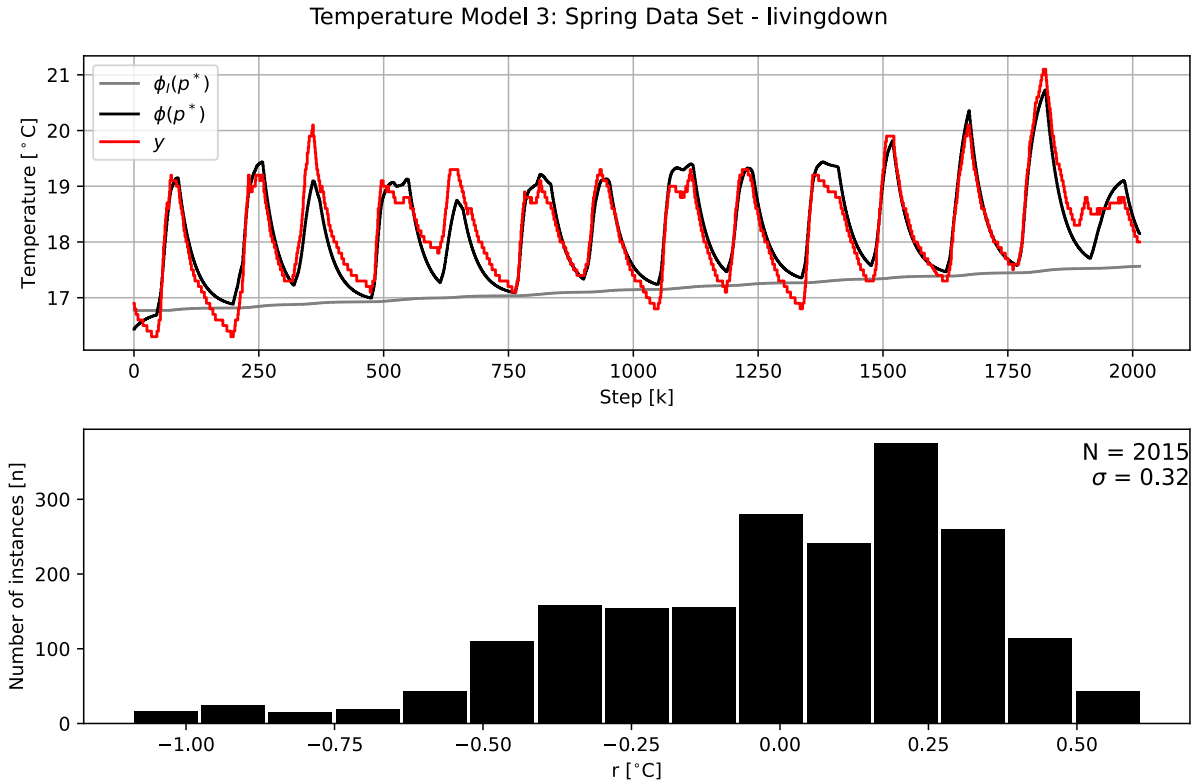

Figure C.13: *Upper plot compares the optimal model trajectory in black with the temperature measurements in red of Spring Data Set - livingdown. The grey solid trajectory illustrates the temperature of the inertia thermal mass. The lower plot illustrates the distribution of the residual.*

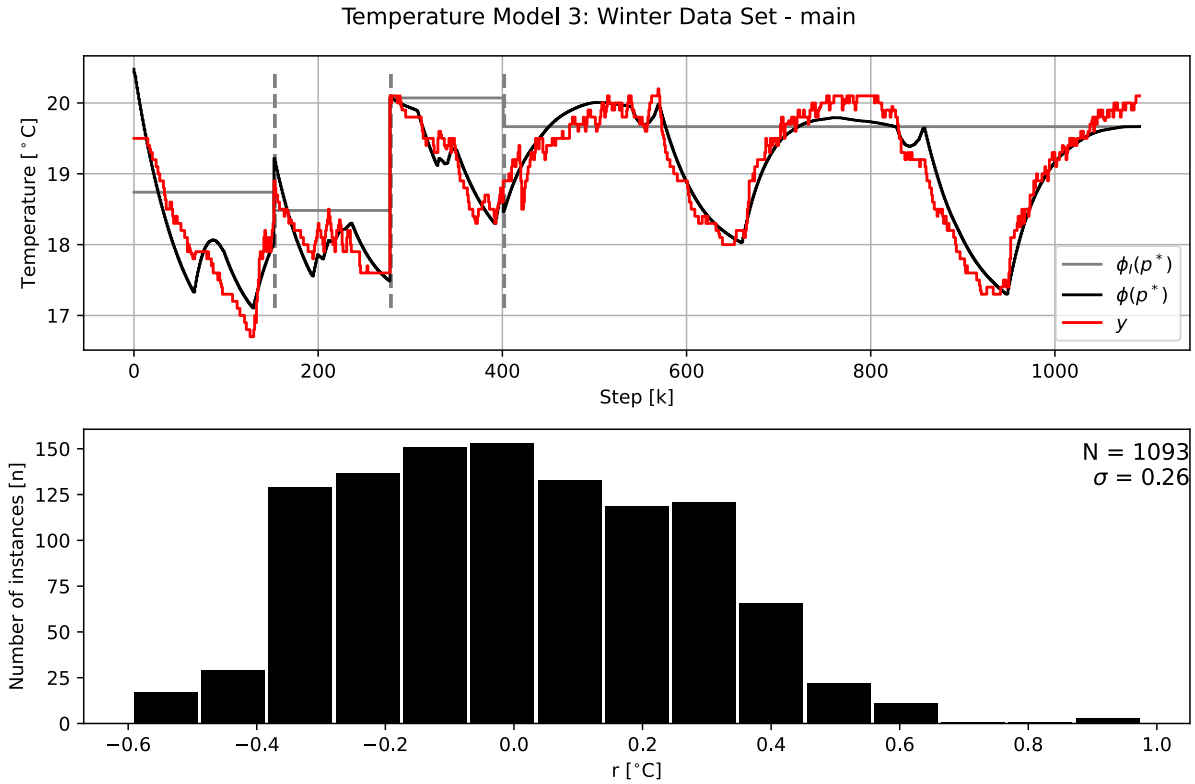

Figure C.14: *Upper plot compares the optimal model trajectory in black with the temperature measurements in red of Winter Data Set - main. The grey solid trajectory illustrates the temperature of the inertia thermal mass, while the grey vertical dotted lines mark where it is a gap in the time series of over five minutes. The lower plot illustrates the distribution of the residual.*

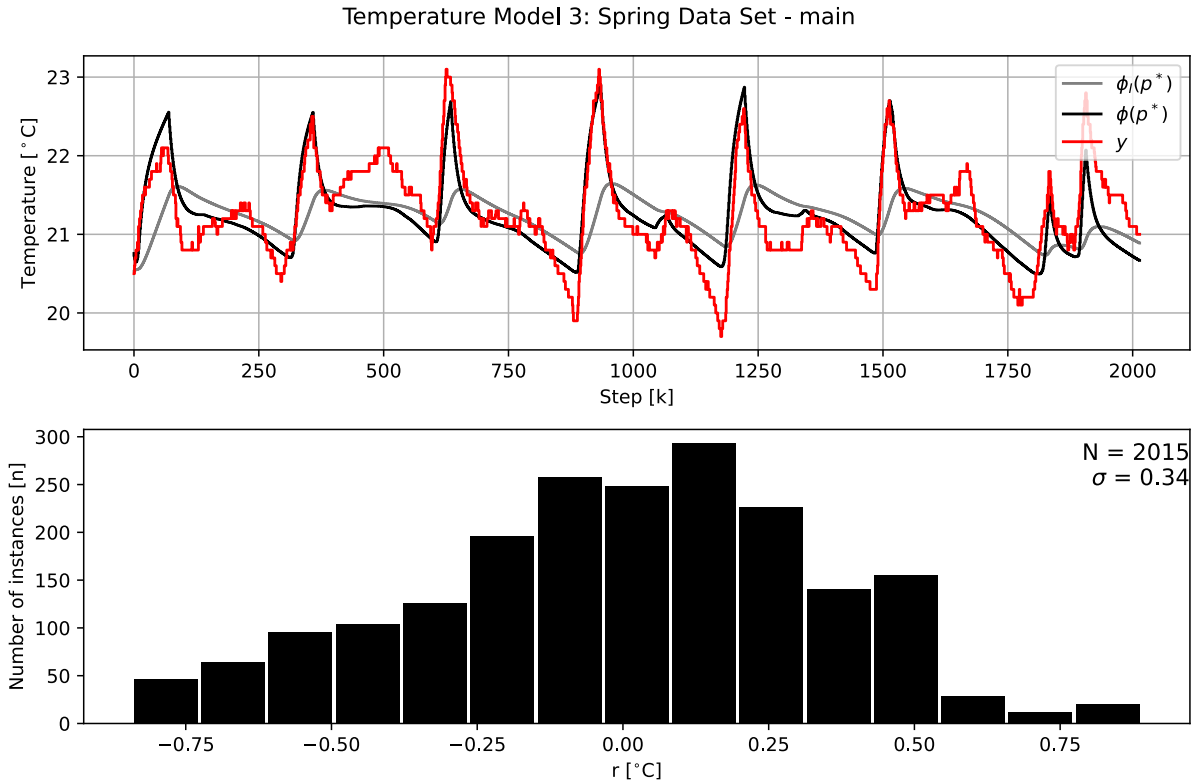

Figure C.15: *Upper plot compares the optimal model trajectory in black with the temperature measurements in red of Spring Data Set - main. The grey solid trajectory illustrated the temperature of the inertia thermal mass. The lower plot illustrates the distribution of the residual.*

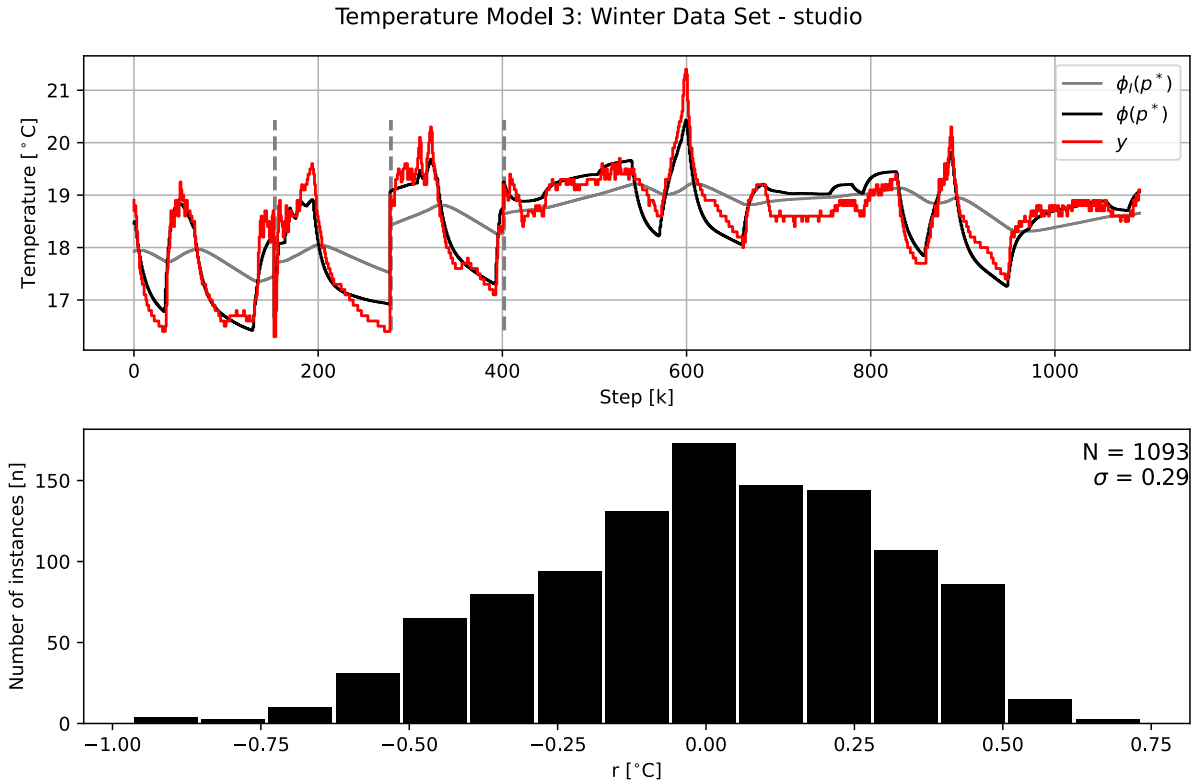

Figure C.16: *Upper plot compares the optimal model trajectory in black with the temperature measurements in red of Winter Data Set - studio. The grey solid trajectory illustrates the temperature of the inertia thermal mass, while the grey vertical dotted lines mark where it is a gap in the time series of over five minutes. The lower plot illustrates the distribution of the residual.*

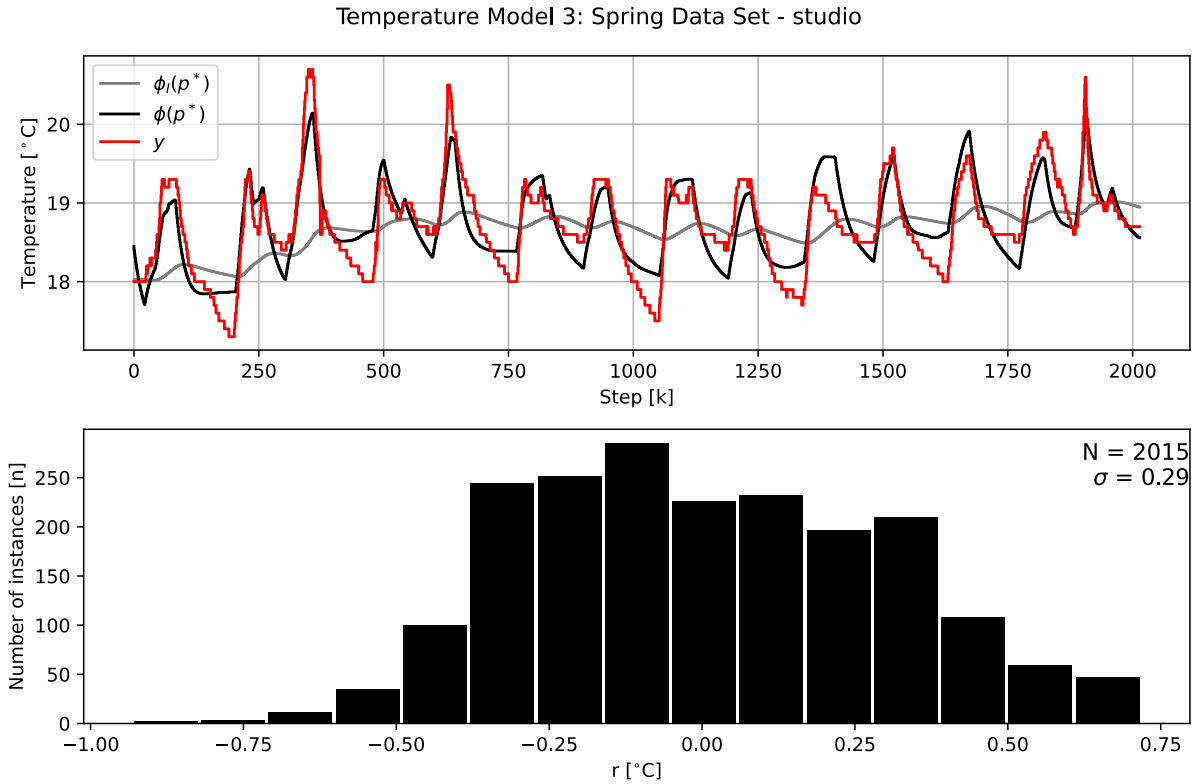

Figure C.17: *Upper plot compares the optimal model trajectory in black with the temperature measurements in red of Spring Data Set - studio. The grey solid trajectory illustrates the temperature of the inertia thermal mass. The lower plot illustrates the distribution of the residual.*